Spatial and Temporal Variations of Radon and their Applications:

A Case Study on Southern Thailand

Pattama Pisapak

A Thesis Submitted in Fulfillment of the Requirements for the Degree of

Doctor of Philosophy in Geophysics

Prince of Songkla University

2017

Spatial and Temporal Variations of Radon and their Applications:

A Case Study on Southern Thailand

Pattama Pisapak

A Thesis Submitted in Fulfillment of the Requirements for the Degree of

Doctor of Philosophy in Geophysics

Prince of Songkla University

2017

Thesis Title Spatial and temporal variations of radon and their applications:
A case study on Southern Thailand

Author Miss Pattama Pisapak

Major Program Geophysics

Major Advisor

…………………………………………

(Assoc. Prof. Dr. Tripob Bhongsuwan)

Examining Committee:

……………………….......Chairperson

(Assoc. Prof. Nares Chankow)

...…………………………….……...

(Assoc. Prof. Dr. Tripob Bhongsuwan)

...…………………….……………...

(Assoc. Prof. Dr. Thawat Chittrakarn)

...………………….……………...

(Dr. Kamhaeng Wattanasen)

The Graduate School, Prince of Songkla University, has approved this thesis as fulfillment of the requirements for the Doctor of Philosophy Degree in Geophysics

………………………….………….……….

(Assoc. Prof. Dr. Teerapol Srichana)

Dean of Graduate School

This is to certify that the work here submitted is the result of the candidate's own investigations. Due acknowledgement has been made of any assistance received.

....

(Assoc. Prof. Dr. Tripob Bhongsuwan)

Major Advisor

....

(Miss Pattama Pisapak)

Candidate

I hereby certify that this work has not been accepted in substance for any degree, and is not being currently submitted in candidature for any degree.

....
(Miss Pattama Pisapak)
 Candidate

ชื่อวิทยานิพนธ์	การศึกษาการเปลี่ยนแปลงเชิงตำแหน่งและเวลาของแก๊สเรดอนและการประยุกต์ใช้: กรณีศึกษาบริเวณภาคใต้ของประเทศไทย
ผู้เขียน	นางสาวปัทมา พิศภักดิ์
สาขาวิชา	ธรณีฟิสิกส์
ปีการศึกษา	2559

บทคัดย่อ

งานวิจัยนี้มีวัตถุประสงค์หลักเพื่อศึกษาการเปลี่ยนแปลงเชิงตำแหน่งและเวลาของแก๊สเรดอนและการประยุกต์ใช้: กรณีศึกษาบริเวณภาคใต้ของประเทศไทย การเปลี่ยนแปลงเชิงเวลาของแก๊สเรดอนได้ถูกตรวจวัดอย่างต่อเนื่องที่สถานีวัดที่เหมาะสม บริเวณรอยเลื่อนคลองมะรุ่ย ด้วยระบบหัววัดรอยนิวเคลียร์ชนิดของแข็ง (SSNTD) โดยได้ทำการตรวจวัดความเข้มของแก๊สเรดอนเฉลี่ยรายวัน ต่อเนื่องนาน 1 ปี ในระหว่างวันที่ 1 กรกฎาคม พ.ศ. 2552 ถึงวันที่ 30 มิถุนายน พ.ศ. 2553 ผลการตรวจวัดพบค่าความผิดปกติแก๊สเรดอนที่สัมพันธ์กับเหตุการณ์แผ่นดินไหว จากศูนย์ข้อมูลแผ่นดินไหว (ANSS: Advanced National Seismic System, of NCEDC; Northern California Earthquake Data Center) ประมาณ 67.3 % ของการเป็นตัวเตือนล่วงหน้าก่อนเกิดเหตุการณ์แผ่นดินไหวขนาด $M_w \geq 4$ ในช่วง 0-3 วัน การเปลี่ยนแปลงเชิงตำแหน่งของแก๊สเรดอนได้ถูกนำมาประยุกต์เพื่อใช้ประเมินผลความเสี่ยงต่อสุขภาพของประชาชนจากการได้รับสัมผัสแก๊สเรดอนในพื้นที่ศึกษาของ อ.นาหม่อม จ.สงขลา จากการตรวจวัดปริมาณความเข้มข้นแก๊สเรดอนและเรเดียมในดิน โดยทำการประเมินดัชนีความเสี่ยงจากรังสี พบว่ามีปริมาณสูงกว่าค่ากำหนดมาตรฐานโลก นอกจากนี้ได้ทำการตรวจวัดปริมาณความเข้มข้นแก๊สเรดอนในน้ำบ่อตื้นสำหรับการอุปโภคและบริโภค พบค่าเฉลี่ยเรดอนสูงกว่าเกณฑ์กำหนดมาตรฐานขององค์การพิทักษ์สิ่งแวดล้อมแห่งประเทศสหรัฐอเมริกา (USEPA, 1999; 11 Bq l^{-1}) และมีบางจุดสูงกว่าเกณฑ์กำหนดโดยคณะกรรมาธิการยุโรป (EU Council Directive, 2013; 100 Bq l^{-1}) ดังนั้นผลการศึกษาดังกล่าวแสดงให้เห็นถึงความน่าเป็นห่วงต่อความเสี่ยงสุขภาพของประชาชนอันเนื่องมาจากภาวะมลพิษรังสีในพื้นที่ อ.นาหม่อม จ.สงขลา และโดยเฉพาะอย่างยิ่งผู้ที่ใช้น้ำที่มีความเข้มข้นเรดอนสูงโดยตรง

Thesis Title   Spatial and Temporal Variations of Radon and their Applications: A Case Study on Southern Thailand

Author   Miss Pattama Pisapak

Major Program   Geophysics

Academic Year   2016

ABSTRACT

The main objective of this research was to study the spatial and temporal variation of radon concentration and their applications: a case study in south of Thailand. The temporal variation of radon in soil gas was observed continuously monitoring at a suitable sampling site at Khlong Marui Fault Zones, Phang Nga Province, using solid state nuclear track detector (SSNTD). The radon was monitored based on of a daily average radon concentration that covered a period year between July 1, 2009 and June 30, 2010. The results showed that the radon anomaly related to the observed earthquakes (data collected from ANSS; Advanced National Seismic System, of NCEDC; Northern California Earthquake Data Center) about 67 % of some precursory anomalous peaks can be correlated to the seismic events with $M \geq 4$ in order 0-3 days before the event occurred. The spatial variation of radon was applied to assess the health risks of exposure to radon in Namom district, Songkhla province. Investigations of radon and radium concentration in soil were used to estimate the radiological health hazard indices, it was found to exceed the world permissible limit. In addition, radon concentrations in well water samples were measured for human comsumption, found that the average radon levels exceed the limit of 11 Bq l $^{-1}$ (USEPA, 1999), and some settlements had radon levels higher than 100 Bq l $^{-1}$ (EU Council Dierective, 2013). These values show a significant health risk due to radiation pollution in study area. It is of concern that the results indicate health risks, especially to those consumers who directly use well water with high radon levels.

ACKNOWLEDGEMENTS

CONTENTS

CONTENTS (CONTINUED)

CONTENTS (CONTINUED)

CONTENTS (CONTINUED)

LIST OF TABLES

LIST OF TABLES (CONTINUED)

LIST OF FIGURES

LIST OF FIGURES (CONTINUED)

LIST OF FIGURES (CONTINUED)

LIST OF FIGURES (CONTINUED)

LIST OF FIGURES (CONTINUED)

CHAPTER 1

INTRODUCTION

1.1   General

Radon is an important terrestrial naturally occurring radioactive gas, which comes from the natural decay chain of ^{238}U. It can escape from the rock, soil and enters the surrounding air or water. Radon decays with a short half-life of 3.825 days and emits an alpha particle. Radon occurs as three isotopes; ^{219}Rn (Actinon), ^{220}Rn (Thoron) and ^{222}Rn (Radon), which are decay products of ^{223}Ra, ^{224}Ra and ^{226}Ra, respectively (Mullinger et al., 2007). Radon is present everywhere in the earth's crust, which can occur in widely varying concentrations. The levels of radon concentration are different depending on the geological structure of the area, including the underlying rock types, soil structure (porosity and permeability). Radon migration in soil gas is facilitated transport through by the rock fracture and fault zone, which it can be transported by diffusion or by flow in carrier fluids (soil air or water) (Etiope and Martinelli, 2002). In the atmosphere reaches by diffusion to the surface, this exhalation forming the radon flux of the earth's crust (Ristoiu et al., 1995). The ability of radon atoms to escape from soil or mineral grains is strongly dependent upon the physical properties of soil. The mobility of radon is mostly dependent on sizes and interconnection of pores. Highly fractured rock and rough, well-drained soil is likely to be highly permeable to radon, whereas clay and mud, particularly if wet, do not permit much radon movement. Radon originating from depths greater than a meter or two generally does not reach the surface because it decays before it can get there (Harris and Pearthree, 2002).

Radon concentration measurement is of great importance in researches related to weather, cancer and also of earthquake prediction. In fact, changes of radon concentration in air, groundwater and soil can be used for the possible correlation with a large seismic event, eventually associated with the highlighted radon anomalies (e.g. Ulomov and Mavashev, 1967; Chyi et al., 2001). Also, radon and its progeny

have been used as a tracer of the human health risk from radiation exposure (Duggal et al., 2013).

In this study was to apply the radon measurement methods in studies of environmental science, geology and geophysics (Papp et al., 2008), which are presented in the thesis. The first one based on the field of radon emission measurement that correlate to the earthquake. The correlation of radon anomalies and earthquakes can provide an important insight, e.g. stress changes in an active fault zone. The results of this study confirm earlier work of Dangmuan (2008); Pisapak (2009) that the fault zones in Southern Thailand are reactivated and presently active, but with lower magnitude seismicity. And the second one of the main issues in the radon concern to human health after long-term exposure, which the general public can be inhaled from air or ingested from water. Due to health effects pose by radon and its progeny to the general public, it is necessary to determine the present trace level of radon activity in the study area.

1.2   Problem identification

1.2.1   People were concerned that the big earthquake (and aftershocks) might have an effect on the faults in Southern Thailand.

1.2.2   Earthquake hazards still lack a warning system because the physical understanding of the occurrence not yet fully understood.

1.2.3   Other physical changes in the earth have been studied as a possible earthquake warning system, for example the radon emission in soil or natural waters.

1.2.4   Even though radon has often been discussed as a menace to human health, it shall also be mentioned here that it can be used as an ideal tracer for a considerable variety of applications in the fields of environmental science, geology, geophysics and hydrogeology.

1.3   Objectives of this study

The aim of this research is to study the spatial and temporal variation of radon concentration and their applications; a case study in southern Thailand. The

variations of radon concentration in soil gas were to investigate as a possible method for earthquake precursor from the monitoring site in Khlong Marui Fault Zones, Phang Nga Province, Southern Thailand. Which the variations of radon concentration as a function of time and related to the meteorological factors. Parallel work is to study the radon concentration in Namom district, Songkhla Province, Southern Thailand as a high background radiation area.

1.4   Thesis Outline

This thesis is structured in five chapters, as follows:

1.4.1   Chapter 1 (Introduction): General introduction is followed by problem identification, objectives of this study, and finally thesis outline.

1.4.2   Chapter 2 (Literature Review): Chapter two covers a general introduction about the background and literature review of radon information, a previous study in temporal variation of earthquake related signals in radon anomalies, radiation background in the study area, assessment of radon concentration.

1.4.3   Chapter 3 (Methodology): In this chapter, First contains the detail of the geology of the study area, describes of the applied measuring method of radon in soil relates to earthquake event, sample collection in different type of measurement techniques and calibration technique measurement of radon in soil and in water.

1.4.4   Chapter 4 (Result and discussion): The radon detections were done to get the result, which the percentage of radon anomalies were related to earthquake events. The second part presents an application of radon risk assessment from soil and water in the high background radiation area of Namom district.

1.4.5   Chapter 5 (Conclusion and Recommendation): In this chapter as a final part of the thesis that contains the conclusion and recommendation based on the results obtained from all presented studies in connection to radon.

CHAPTER 2

LITERATURE REVIEW

2.1   Introduction

One of the main members of natural radioactivity of the earth's crust is radon (^{222}Rn). Being a noble gas and having a relatively long lifetime, has a great mobility to reach considerable distances in different geological environments. Radon is present everywhere, in rocks and soil, in sub-surface and deep water, in atmosphere and indoor air, in different concentrations. Radon flux from soil are used as indicators for some applications such as radon risk assessment by the determination of radon potential of the soil, identifying the faults (Cosma et al., 2010), in applying migration models in soil and geological environments (Etiope and Martinelli, 2002) and for the transport to the atmosphere and inside homes.

Radon is one of many geophysical and geochemical phenomena that can be considered to be an earthquake precursor. Various studies have shown that an increase in the concentration of radon in groundwater is an earthquake precursor. Even though numerous examples of premonitory radon anomalies have been identified and described in the literature, statistical analysis of the relationship between radon and earthquakes has been difficult because of the lack of long-time series from a network of recording stations in active seismic or volcanic areas (Einarssóon et al., 2008). For this purpose many radon anomalies prior to earthquake observed and studied in soil gas as well as in groundwater or spring; a number of active and passive methods for getting radon signals have been developed and several models have been proposed as an explanation of the experimental field data.

2.2   Radon information

Radon is a natural radioactive gas discovered in the 1900s by Dorn, who called it radium emanation. Since 1923, the International Committee on Chemical Elements proposed the current name radon. It is produced continuously in

rocks, soil and minerals through α- decay of ^{226}Ra (Baykara and Doğru, 2006). Formed as a result of radioactive decay of the element uranium and thorium. Rock types, such as black shales and some igneous rocks, can have a higher content of uranium and thorium than the average values of the earth's crust. The occurrence of radon in ground water can be reasonably related to uranium contents of the bedrocks and it can easily enter into the interacting ground water by the effect of lithostatic pressure (Toscani et al., 2001). Radon is an important terrestrial gas whose presence and concentration is easy to detect. The concentration levels of radon are strongly affected by geological and geophysical conditions, as well as atmospheric influences, such as rainfall and barometric pressure rather than by chemical processes, as it is an inert gas. It is the only naturally radioactive gas and is the heaviest of all of the elements that occur a gas at room temperature and pressure conditions. Radon is one of a number of intermediate radioactive elements formed during the radioactive decay of ^{238}U, ^{235}U and ^{232}Th isotopes to form stable, non-radioactive isotopes of lead (Figure 2.1). ^{222}Rn is the radon isotope of most concern to public health because of its longer half-life, 3.8 days, than other radon isotopes, like ^{219}Rn, 4 seconds, or ^{220}Rn, 55.3 seconds, see Table 2.1.
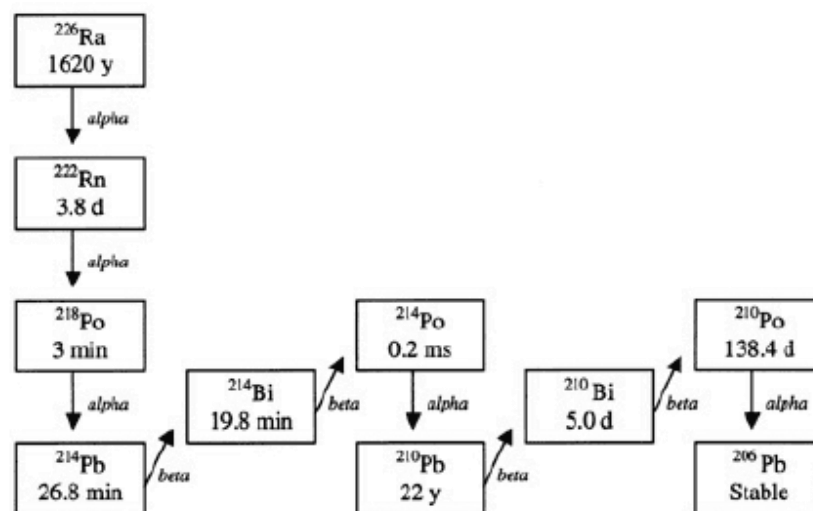
Figure 2.1   Products of radioactive decay of radon (CGS, 2008).

The ^{226}Ra sub-chain in Figure 2.1, it can be seen that the primary of very long lived ^{238}U decays to ^{234}U, and then, ^{234}U decays to ^{230}Th, which decays to ^{226}Ra. Radium (^{226}Ra) with a half-life of 1,620 years, decays to ^{222}Rn with a half-life of 3.8 days. Thus, ^{226}Ra is the immediate parent of ^{222}Rn, whereas ^{238}U is the ultimate parent. ^{222}Rn decays through intermediate steps until the longer lived ^{210}Pb is reached. The important feature is that the decay products, mainly alpha particles, down to ^{210}Pb pose a hazard to human health.

Table 2.1:   The three naturally occurring isotopes of radon with their half- lifves and radioactive decay series.

Isotope	Common name	Half-life	Decay chain series of
^{222}Rn	Radon	3.8235 days	U-238
^{220}Rn	Thoron	55.6 seconds	Th-232
^{219}Rn	Actinon	3.96 seconds	U-235

2.3   Source of radiation exposure

Radiation comes from both natural and human sources. Many elements exist in one or more radioactive form. The most common of these is an isotope known as potassium-40. Isotopes are forms of an element that differ from each other in the structure of their nuclei. Other radioactive isotopes found in nature include hydrogen-3, carbon-14, chlorine-39, lead-212, radium-226, and uranium-235 and 238. Humans and other organisms cannot escape exposure to radiation from these radioactive sources. They constitute a normal radiation, called background radiation that is simply part of existing on earth. Although some harmful effects can be produced by exposure to natural background radiation, those effects are relatively minor and, in most cases, not even measurable. Human activities have added to normal background radiation over the past half century. When nuclear weapons are exploded, for example, they release radioactive isotopes into the atmosphere. As these radioactive isotopes are spread around the world by prevailing winds, they come into contact with humans and

other organisms (HPS, 2008). Figure 2.2 shows the source of ionizing radiation exposure of the population of the United States. The main source for radiation exposure, with 55 %, comes from radon sources (NCRP, 1987).
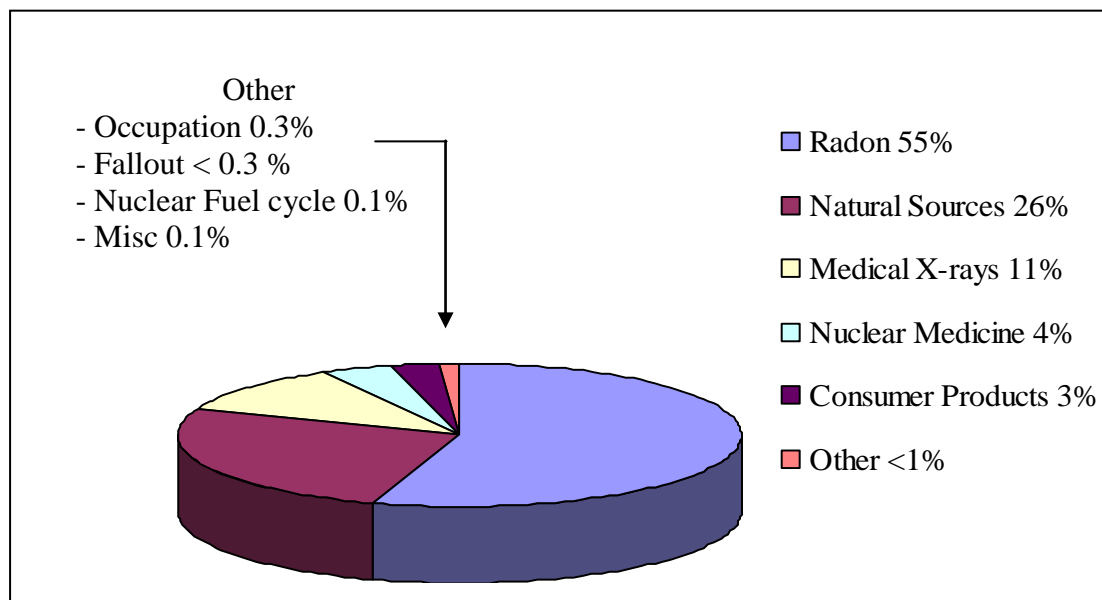
Figure 2.2   Source of radiation exposure in the United States (from NCRP, 1987).

2.4   Radon source

Uranium is present in the earth's crust and radon occurs in building materials, ground water and natural gas. Though, the ground is the major source of radon. Pores in the soil underground contain air with high radon concentrations. The lower air pressure indoors gives rise to a pressure-driven flow of radon-rich soil air into the indoor environment through cracks in the bottom slab and cellar walls. This under pressure is caused by temperature difference between outdoor and indoor and mechanical ventilation. Radon can more easily leave the rocks and soil by escaping into fractures and opening in rocks and into pore spaces between grains of soil as shown in Figure 2.3. Certain rocks and soil, such as some granites and shales, contain more uranium than others. However, ground with moderate contents of uranium and/or radium can also give high indoor radon concentrations. The influx depends largely on the building construction and permeability of the ground materials.

Building materials made from soil (e.g. clay bricks) or rock always contain uranium and radium. The content is usually low, but some types may have high concentration of radium, for example dark shales, concrete, granites, and building materials made of volcanic tuff, gypsum waste, etce. The radon concentration can reach several thousand becquerels per letre (Bq l^{-1}) in water from drilled wells in regions with granite rock,which contributes to indoor radon and to exposure via ingeston. Radon can therefore reach the air or water to which human has access, provided that transport is sufficiently rapid to be completed before the radon decays (Mose et al., 1990).
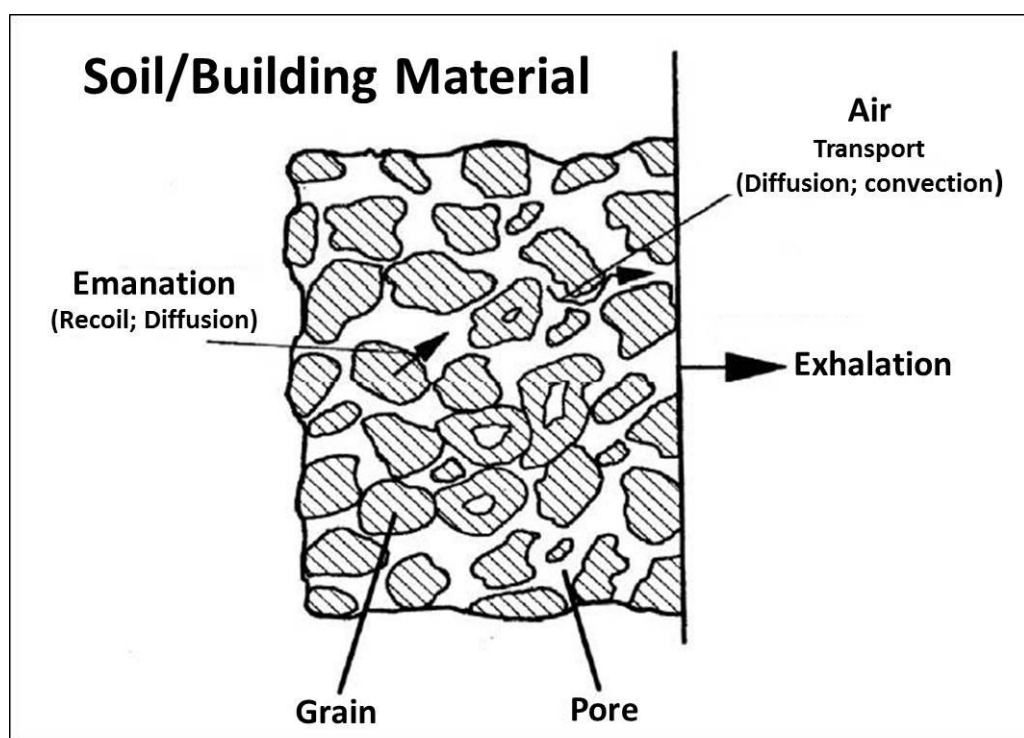
*Figure 2.*3   Mechanism of radon migration through pore space (Alharbi and Abbady, 2013).

2.5   Measurement techniques of radon

There are three classes of measurement techniques that are used today: (1) grab-sample technique, (2) continuous technique, and (3) integrating technique.

The choice between these classes will depend on the costs involved, the time over, which an instrument can be devoted to measurements at a single location, the kind of information require, and desired accuracy with which measurements can be related to an estimated of risk (Bodansky et al., 1987; Brill, 1994).

(1)   Grab-sample technique

Grab-sample technique involves measurement of ^{222}Rn in a discrete sample of water (or air) collected over a very short time (on the order of minutes) compared to the mean-life of ^{222}Rn. Examples include measurements of radon in groundwater, freshwater and marine water, and air samples. Radon measurement equipment such as RAD7 can be used to measure ^{222}Rn in air at any time when it is used in "sniffer" mode in which case radon is typically present with minimal ingrowth of its progeny and large number of measurements can be taken in a relatively short period of time.

(2)   Continuous technique

Continuous technique provides time-series concentrations of ^{222}Rn in samples (soil gas, air, water) and counting are done simultaneously. The automatic taking of measurements at closely spaced time intervals over a long period of time. Recently developed instruments such as Smart Radon Due and Scintillation Radon Mornitors can also be used for continuous monitoring of ^{222}Rn as well as ^{220}Rn in air, soil gas or water.

(3)   Integrating technique

Integrating technique provides the integrated concentration over a certain period of time. Such measurements are useful to determine monthly or annual average ^{222}Rn concentration of a specific building. The passive detectors, which are quite inexpensive, are examples of integrating techniques. Such devices are useful to assess the effectiveness of remedial techniques to alleviate indoor radon problems. Additionally, integrated results can also be determined from continuous long-term measurement records (Cothern and Smith, 1987).

2.6   Radon entry into home

Radon gas enters homes from the ground through cracks or openings in the foundation. The difference in air pressure between the inside of a building and soil around it has also played an important role in radon entry. If the air pressure of home is higher than beneath the soil, radon will remain outside. Though, if the air pressure of the home is lower than the surrounding soil (which is usually the case), the home will act as a vacuum, sucking radon gas inside. Once radon entry into the home, its concentration in indoor air is influenced by the amount of household ventilation. Opening windows and doors, operating bathroom and kitchen fans, and operating clothes dryers all tend to change the radon concentrations by increasing ventilation and/or by pulling more radon in from soil through the lower parts of the home, as shown in Figure 2.4.
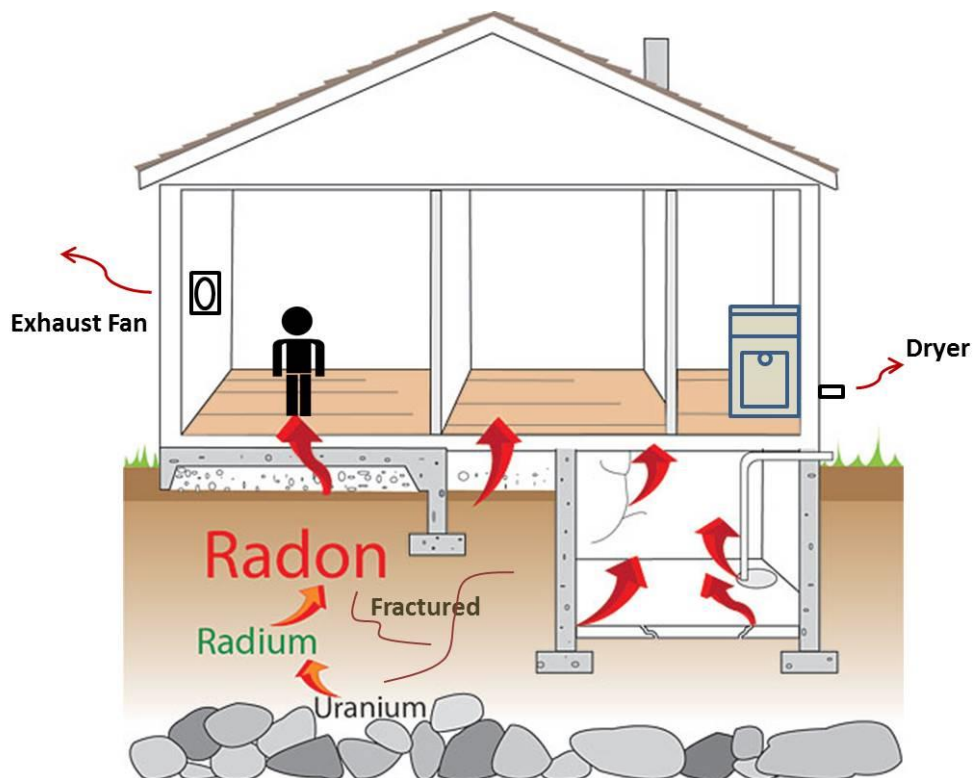
*Figure 2.*4   How radon enters a home (from:https://www.unce.unr.edu/programs/ sites/radon/homes/).

2.7   Health effect and risk of radon

Many studies looking at the health effects of radon have been conducted throughout the years. These studies have helped understand the importance of controlling radon. Their main finding is that long-term exposure to above-background levels of radon increases the risk of developing lung cancer. The health risk of radon is caused by exposure to its progeny, which are produced when radon decays. If radon gas is present, the decay products will become suspended in the air. Because they are electrically charged, most will attach to dust particles, aerosols or smoke, and readily deposit in the airways of lung after being breathed in. While lodged there, the progeny emit alpha radiation, which can damage the cell lining the airways of the lung. The report confirms that radon is the second leading cause of lung cancer in the U.S. and that is a serious public health problem. The study fully supports EPA estimates that radon causes about 21,000 lung cancer deaths per year. About 2009 of these deaths occur among people who have never smoked (BEIR VI, 1999), meaning radon is number one cause of lung cancer among non-smokers. It is well established that there are synergistic effects between radon exposure and smoking, so that the risk of lung cancer due to radon exposure increase at a much higher rate for smokers and ex-smokers than for non- smokers. However, it has been suggested that other effects of radon exposure include increased risk of non- malignant respiratory diseases, but this is much less clearly established than the lung cancer risk.
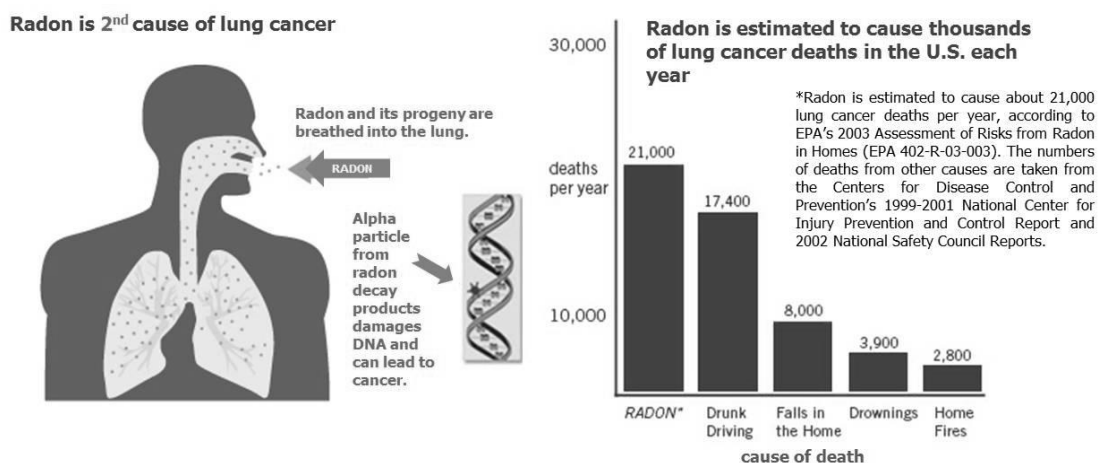
*Figure 2.*5   Health effects of radon (BEIR VI, 1999)

2.8   Guidelines for concentrations of radon

Many countries have defined the action level of radon concentration to guide their program to control domestic exposure to radon. The action level is not a boundary between safe and unsafe, but rather a level at which action on reduction of radon level will usually be justified. Since 1990, the European Commission had recommended and "action level" of 400 Bq m^{-3} for existing dwellings and 200 Bq m^{-3} for new construction, which had been approved by many European countries; in Australia, the action level was 200 Bq m^{-3}; in the United States the action level was 150 Bq m^{-3} (David Suzuki Foundation, 2015). Regulatory guidelines and international recommendations for radon in drinking water have been issued. In 1999, The United States Environmental Protection Agency (USEPA) has proposed that the allowed maximum contamination level (MCL) for radon concentration in drinking water is 11 Bq l^{-1}. The current Directive lays down requirements for protection of health of the general public with regards to radioactive substances in water intended for human consumption. The European Union Directive EC2013/51/EURATOM was adopted in 2013 a recommendation of radon in drinking water that set at 100 Bq l^{-1} (EU Council Directive, 2013), while concentrations above this level permit the consideration of possible remedial actions. In the United States, many people receive their water from private wells. EPA regulations that protect public drinking water systems do not apply to privately owned wells. As a result, owners of private wells are responsible for ensuring that their water is safe from radon and contaminants. In addition, the recommendation that EPA's newly proposed an alternative standard active level of radon in water of 150 Bq l^{-1}.

The Namom district of Songkhla province has the highest radon concentrations in air and in groundwater within the province (Bhongsuwan et al., 2001), and the Songkhla granite is known to contain uranium at the high level of 18 ppm eU (Ishihara et al., 1980; Sirijarukul, 1994). Radium also has been observed in shallow well waters, in the area with granitic rock. The radium concentrations are found to vary from 3.51 to 292.1 mBq l^{-1} (Wutthisasna et al., 2006). The highest radium concentration obtained in this study area exceeds the maximum allowable concentration levels for radium limit in drinking water of 185 mBq l^{-1}, recommended

by the USEPA (2001) (USEPA, 2001; Hirunwatthanakul et al., 2006). High radon levels in groundwater tend to directly correlate with high levels of uranium or radium in the rocks. This is probably because fractured and weathered granitic rock is highly permeable and allows for the escape of radon and radium in the rock. Radon in water is responsible for the whole body internal radiation dose that may be more harmful than radon in air. Thus, determination of radon in water has also been of major interest in this study, because of its harmful health, which causes lung cancer.

Guideline values (action levels) of radon vary among countries, and have been measured and estimated in different countries. Table 2.2 shows the domestic radon concentration and the action level in different countries.

Table 2.2:   Radon guideline values (action levels) in different countries.

Country	Average radon concentration in dwelling (Bq m^{-3})	Action level (Bq m^{-3})
Finland	123	400
Germany	50	100
Ireland	60	200
Israel	*	200
Lithuania	37	100
Luxembourg	*	150
Norway	51-60	200
Poland	*	400
Russia	19-250	*
Sweden	108	400
Switzerland	75	400
United Kingdom	20	200
Canada	*	200
USA	46	150
European community	*	400

* Not available (David Suzuki Foundation, Report, 2015)

2.9   Earthquakes

Earthquakes in Thailand

Thailand is situated close to an active seismic region, the Sunda Subduction Zone, which is about 500 km west of Thailand in the Andaman Sea. The earthquake epicenters are mainly located along the north-south trending Burma-Andaman Sumatra subduction and fault zone along Thailand's westernmost frontier. Over 450 historical earthquakes have been recorded in Thailand (Nutalaya and Sodsir, 1984). Further earthquakes epicenters have been located mainly in western and northern regions of Thailand. In 1963 the Meteorological Department set up the first seismic station in Chiang Mai. Since then the monitoring of earthquakes in Thailand has become more systematic. Seismic events recorded on February 17, 1975 at Tak Provinces (M = 5.6) and on April 22, 1983 at Kanchanaburi Provinces (M = 5.9) (Poobrasert, 1987). Frequently strong and very strong earthquakes occur, sometimes very big ones, like the M_w 9.3 on December 26, 2004. However, these earthquakes have only less direct rather than more an indirect impact on Thailand, like shaking of high-rise building (USGS, 2005).

Shortly after the devastating M_w 9.3 Sumatra-Andaman Earthquake on December 26, 2004, the Geophysics Group in the Department of Physics at the Faculty of Science, Prince of Songkla University established in collaboration with the Department of Mineral Resources a seismic network in Southern Thailand in order to monitor possible local earthquakes along the Ranong and Khlong Marui Fault Zone (Dangmuan, 2008).

2.10   Seismicity associated with Andaman-Sumatra Arc

Though the seismicity associated with this arc is moderate and does not raise any concern so far, the scenario has significantly changed after the December 26, 2004, Sumatra Andaman Earthquake with a magnitude of M_w 9.3. The rupture of this earthquake propagated northwards towards the Nicobar-Andaman Island arc, and to this date as many as few thousand aftershocks were reported after

the main event. Apart from the main shock of December 26, 2004, the aftershocks of March 28, 2005 (M_w 8.4) and July 24, 2005 (M_w 7.3) were felt along the coastal area of Andhra Pradesh and Tamilnadu margin, India. The frequency and amplitude of earthquakes in the Andaman and Nicobar belt show a significant rise since December, 2004 and thus pose a new seismic hazard for the coastal region of India, Myanmar, Thailand and Indonesia, though fortunately none of these aftershocks were associated with a tsunami.

The great Sumatra Andaman Earthquake of December 26, 2004 occurred at a depth of about 30 km beneath the Sunda Trench off the north-west coast of Sumatra, Indonesia (3.244° N; 95.825° E) at 00:59 UTC time (Stein and Okal, 2005). The rupture propagated upwards on a shallowly (8°) dipping fault plane with a strike of 329°. The 2004 earthquakes ruptured the boundary between the Indian-Australian plate and the southern portion of the Eurasian plate, which moves generally northward along the Nicobar and Andaman Islands (Bilham, 2005; Ni et al,. 2005) (Figure 2.6 and Figure 2.7). Up to 15 meters of thrust displacement was accommodated at the plate interface within a few minutes, offshore from Bada Ache, Sumatra where the strongest excitation of the tsunami occurred (Figure 2.7) (Ley et al., 2005). Farther north, the rupture slowed considerably and for the last five of its eleven minutes duration, no further tsunami waves were produced. During the following hour, however, this northern section of rupture accumulated many meters of slip, which contributed perhaps a third of total energy released. This slow slip accounted for a three-fold upward revision of magnitude from 9.0 to 9.3 (Bilham, 2005). Later analysis of continuously recording GPS station revealed that co-seismic horizontal displacements had occurred over a vast region. From decimeter scale shifts at the nearest stations (e.g. 270 mm at Phuket, Thailand, to the west to several millimeters measured at points in southern China, the Philippines and India (Vigny et al., 2005).

The total length of rupture is comparable to the distribution of aftershocks, which is more than 1200 km for the December, 26 event. This increases to more than 1600 km when the contiguous Nias earthquake (moment magnitude M_w 8.7) of March 28, 2005 is included (Figure 2.7). The March 28 earthquake indicated

further rupture of the plate interface to the southeast and raised concern about the altered state of stress and possibly heightened tsunami hazard on adjoining sections of the plate boundary.
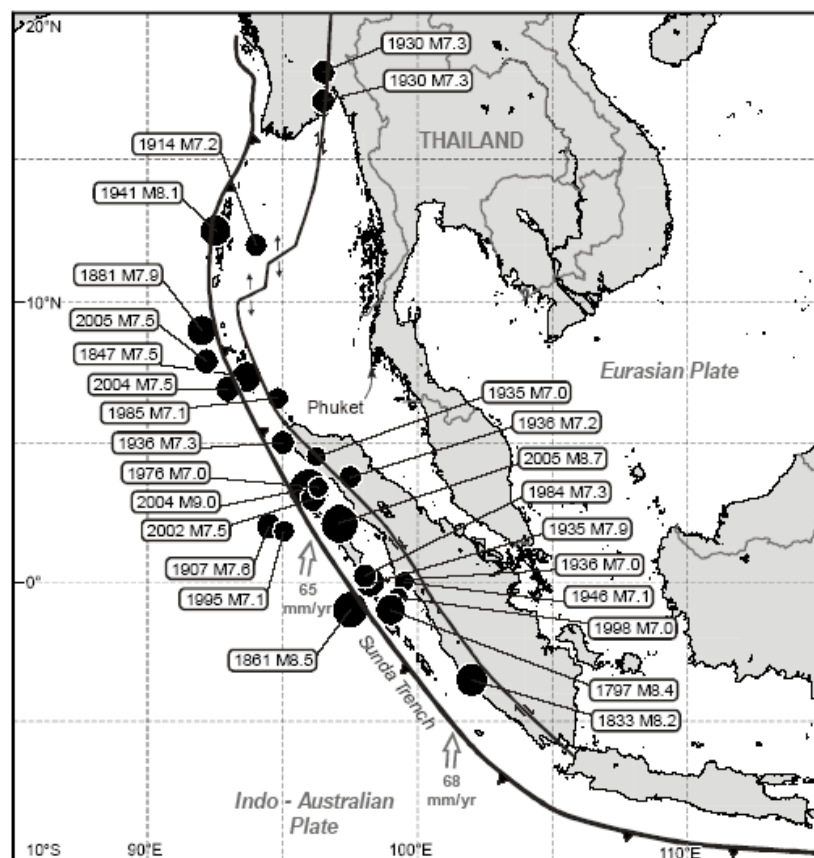
Figure 2.6   The previous large and great earthquake ruptures along the Sunda-Andaman trench and region adjacent to the December 26, 2004 and March 28, 2005 earthquakes. Event of magnitude ≥ 7.0, depth < 100 km. (Bell et al., 2005).
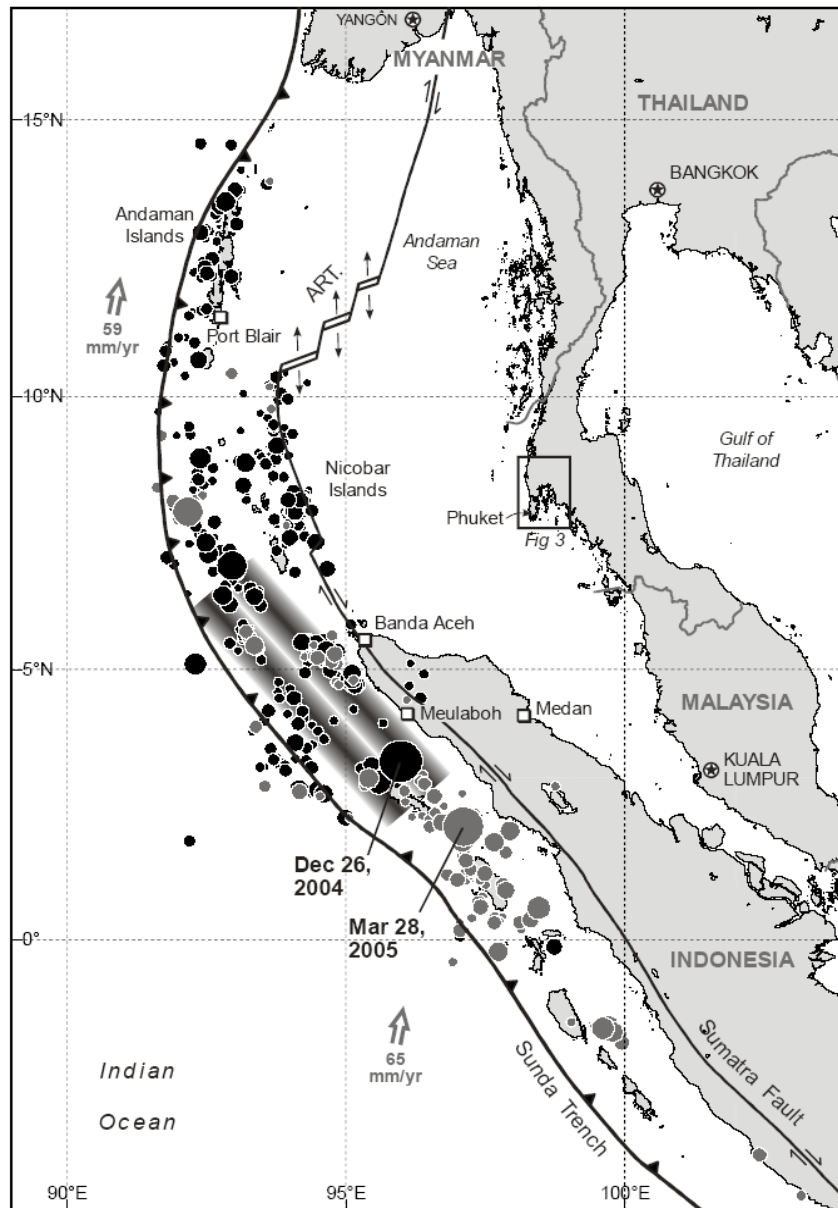
Figure 2.7   The major structural elements of the Indian-Australian and Eurasian plate boundary, with the mainshock M_w 9.3 and aftershocks for the December 26, 2004. Great Sumastra-Andaman earthquake (black circles), and contiguous Nias earthquake of March 28, 2005 and combined aftershock earthquake (M_w 8.6) of thereafter (gray circles). The earthquake sequence covers a rupture zone 1,600 km long and 200 km wide (Lay et al., 2005).

Large earthquakes are known to have ruptured the Andaman section of over-trust plate boundary in 1847 (M_w 7.5), 1881 (M_w 7.9), 1941 (M_w 7.7), and in the northern Andaman Sea, a section of the Andaman ridge-transform boundary near the coast of Myanmar, in 1930 (M_w 7.3) (Nutalaya et al., 1985; Ortiz and Bilham, 2003; Bilham et al., 2005, Figure 2.6). Those historical events produced the tsunami that, while locally destructive slip on deeper parts on the plate interface than occurred on Dec. 26, 2004. The earthquakes of 1930, centered in the far north of the Andaman Sea on section of the plate boundary characterized by right-lateral strike-slip faulting, destroyed the ancient seaport of Pegu. Tsunami associated with those events caused severe flooding and fatalities in Myanmar (Nutalaya et al., 1985).

Historic great earthquakes along this plate boundary occurred farther south, offshore from Sumatra in 1797 (M_w 8.4), 1833 (M_w 9), and 1861 (M_w 8.5), providing the basis for the long recognized potential for great earthquake events with an estimated magnitude larger than those mentioned above (Newcomb and McCann, 1987). The waves of the 1833 event probably made landfall nearby with heights in the range 5-10 m (Cummins and Leonard, 2004). A smaller (M_w 7.8) event in 1907 just south of the 2004 rupture zone produced seismic and tsunami damage in northern Sumatra (Newcomb and McCann, 1987). The 28 March 2005 earthquake ruptured the same region as the 1861 and 1907 events (Figure 2.6). The inferred rupture area of that and adjoining 1861 event was broken again by the recent of the 2005 Nias earthquake. Smaller events in the Andaman trench, also presumed to involve thrusting motions, occurred beneath the Nicobar Islands in 1881 (M_w 7.9) and near the Andaman Islands in 1941 (M_w 7.9). However, there is no historical record of a previous tsunamigenic earthquake in the Bay of Bengal compared to the 2004 event (Bilham et al., 2005).

2.11 Relationship between radon and earthquake

The identification techniques of proposed earthquake related signals of radon anomalies has been difficult because of several other influences, like the earth's tides, barometric pressure, temperature, rainfall, tectonic processes. The effect of tectonic activities on the permeability of aquifers or crack patterns of the earth's crust

are difficult to correct or to estimate and therefore it is also difficult to find significance in the temporal variation of earthquake related signals in radon anomalies. However, many researchers interested in relation between concentration of radon and earthquakes.

The relationship between radon and earthquakes has been studied in South Iceland since 1977, when the first equipment for this purpose was installed. The instruments were operated until 1993. The radon monitoring network consisted of up to 9 stations. Samples of geothermal water were collected from drill holes every few weeks and sent to the laboratory for radon analysis. The resulting time series varied in length from 3 to 16 years. Many earthquake-related radon anomalies were identified (Jónsson and Einarsson, 1996).

Environmental research, the mapping of fault zones, the prediction of earthquakes, and geological trace analysis has been developed mainly using uranium. There have been various researches dealing with the measurements of radon concentration in soil, gas emanating from the ground along active faults, which may provide useful signals before seismic events. Radon tends to migrate from its source mainly upwards. This rate of migration is affected by many factors, such as distribution of uranium (especially ^{226}Ra in the same series) in the soil and bedrock, soil porosity and humidity, micro-cracks of bedrock, rainfall, air temperature, barometric pressure, surface winds (Planiníc et al., 2001). Durrani and Ilíc (1997) discussed the subject of the radon emanation from fractures and fault zones in the bedrock. They have also discussed the radon concentration changes with earthquakes in fault zones and the radon transportation by diffusion or groundwater movement in fracture zones. Radon activities are clearly higher in some areas such as geological fault systems, geothermal sources, uranium deposit and volcano areas (Al-Tamimi and Abumurad, 2001).

Measurement of radon in soil gas and in ground water has been carried out all over the world and the results seem to indicate the radon as a good indicator of earthquake prediction. However, the current literature describing the possible correlation between radon anomalies and earthquake events uses such qualifying and caution words as possible, apparent, could, may be, and so on. It is clear that in some case there are precursor changes in radon levels, but that the causal relationship or

mechanism relating these to earthquake activity is not yet well understood. Thus, even if some results seem to suggest that geodynamical events could influence radon concentrations, however, because of the complexity of its transport mechanism, the correlation needs more investigation in order to clearly and firmly established it.

CHAPTER 3

RESEARCH METHODOLOGY

This chapter describes the location of the study area and the research methods. The applied radon measuring in soil gas relates to earthquake located in Maung district, Phang Nga Province. Radon in soil gas was measured continuously monitoring at one station based on a major of Khlong Marui Fault Zone (KMFZ), using a solid state nuclear track detector (SSNTDs). The site was suitable for the radon monitoring on the basis of high average radon concentration and detected for a daily coverage the period of year between July 1, 2009 to June 30, 2010. In addition, the radon exposure to the general population health risk was to investigate in Namom district, Songkhla province. The investigation of the radon risk in this work has 2 main objectives, 1) To observe the correlation between concentrations of radon (^{222}Rn) and radium (^{226}Ra) in soil and to estimate the potential natural radiation hazard in Namom district, Songkhla province, and 2) To investigate the radon levels in the water supplies to households, and to determine the health hazards due to radon gas that can accumulate and reach high concentration levels indoors.

3.1   Radon observations in soil gas as a possible earthquake precursor

This study is based on a field of a temporal variation of radon emission and earthquake events, which shows that the correlation of radon anomalies with earthquake can provide an important insight e.g. stress changes in active fault zones in Southern Thailand. The role of radon in the performance of prediction tools, it is necessary to give an overview on the geophysical development of an earthquake and the effects which can be expected. It is also important to clarify what prediction of earthquake really means and what is necessary to make a prediction meaningful and when should an earthquake warning be issued.

3.1.1 The location of study area

Site selection

Considering site selection for radon continuous monitoring have been selected as follow. Pisapak (2009) have recorded radon in soil gas atten track detector stations (ST-1 to ST-10) that are located along the Khlong Marui Fault Zone, mainly in Thap Put district, Phang Nga Province, (Figure 3.1). In this study, the measurement of the radon concentration in soil gas was conducted at one station (ST-10) which is the best site of all stations for radon continuous monitoring. Further, the radon concentration at station ST-10 is in general much higher than at other stations for the measurement every week as reported by Pisapak (2009). It is possible, that the radon anomaly is related to the karst characteristic of the Permian limestone (see Figure 3.1). As radon is a gas that can move easily through underground cavities or fractures in the limestone created by the karst weathering, even from much deeper regions of the subsurface.

Geologic setting

The Khlong Marui Fault (KMF) is of strike-slip nature, aligned parallel to Ranong Fault (RF). It initially moved 150 km sinistral, and then moved right lateral at the transition of Jurassic and Cretaceous. In the middle of Tertiary, the fault is similar to the Ranong Fault Zone (Tapponnier et al., 1986) (see Figure 3.2).

The structural geology of the N–S trending Thai Peninsula is dominated by the KMF and RF, both broadly linear NNE-trending strike-slip fault zones centered around elongated slivers of ductile fault rocks. These are bounded and overprinted by brittle strands, which are part of a population of parallel and branching sinistral faults, which are localized into the two similar but discrete fault zones. The smaller KMF passes from Kho Phuket (Phuket island) in the south towards Surat Thani in the north, while strands of the RF can be traced from Takua Pa in the south to Pran Buri in the north, crossing the peninsula entirely. A relatively undeformed block with a strike-normal width of no more than 50 km lies between the two faults

(Watkinson et al., 2008). Thailand is situated close to an active seismic region, the Sunda Subduction Zone (Petersen et al., 2004). Thus, earthquake epicenter is mainly located along Andaman Sumatra subduction and fault zone along the western side coast of Thailand, which is about 500 km west of Thailand in the Andaman Sea (Nutalaya and Sodsir, 1984). In history over 450 seismic events were recorded in Thailand, mainly located in western and northern regions of Thailand. However, very strong seismic events, like the M_w 9.3 that occurred on December 26, 2004 Sumatra-Andaman Earthquake can be used as possible monitors of the local earthquakes along KMFZ.
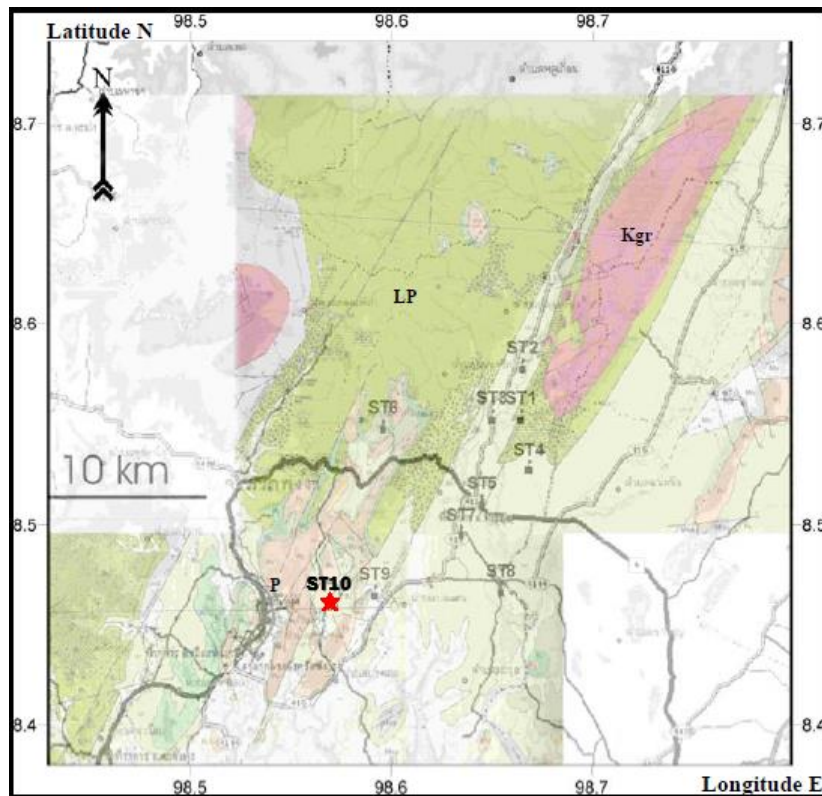
Figure 3.1   The locations of radon monitoring site at ST-10; ★, is the best site from 10 stations of track detector stations (ST-1 to ST-10) for radon in soil gas in Phang Nga Province (Pisapak, 2009) with geological base map (from Garson et al., 1975); P = Permian limestone, LP = Lower Permian and Kgr = Cretaceous granite.
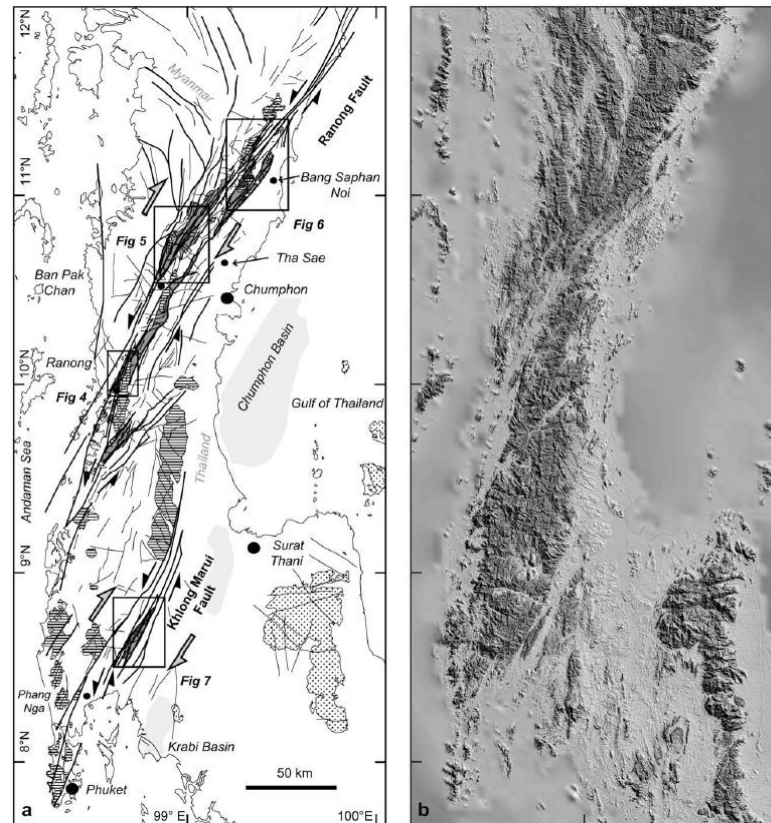
Figure 3.2   The Thai Peninsula showing the Ranong and Khlong Marui fault zones (KMFZ). (a) Fault map. (b) SRTM digital elevation model of the same area (Watkinson et al., 2008).

3.1.2 Radon measurement as a passive technique detector

Solid State Nuclear Track Detector (SSNTDs)

The principle of radon detection by solid state nuclear track detectors (SSNTDs) is based on the production of alpha particle tracks in solid state materials. Allyl diglycol carbonate plastic films (CR-39) was used as detectors during the soil gas radon measurement in this study (Pershore Mouldings Ltd, Worcestershire WR10 2DH, UK) (Alter and Fleischer, 1981).

SSNTD is the passive technique which has several advantages; low cost, unaffected by humidity, low temperature, moderate heating and light, and can be

easily obtained long term method. It is technique most widely used for measuring the radon and can be used for site assessment both indoors and outdoors (Durrani and Ilíc, 1997).

Before applying the SSNTDs system in the field, testing in the laboratory has to be carried out. The temperature and time for the etchants are varied so that later the suitable etching condition can be used for producing tracks as earlier shown by Pisapak (2009). The procedure has the following steps:

Steps in using the CR-39 nuclear track-etched detector:

1. Prepare the NaOH solution with a concentration of 6.25 N, 1,000 cm^3
2. Take a beaker with NaOH solution in the water-bath (Grant-W14), etching can be accelerated by increasing the temperature to 85°C and keep it constant (see Figure A1.1 in appendix A).
3. Put the CR-39 plastic film for etching treatment 100 minutes in the NaOH solution at 85° C, by this enlarging the etched tracks to sizes which can be viewed with an ordinary optical microscope.
4. After 100 minutes, take out the CR-39 plastic film and wash it thoroughly.
5. Waiting for the CR-39 plastic film to be dry and put it on a microscope slide.
6. The tracks were counted using an optical microscope (OLYMPUS-BHC) (x 100 magnifications).
7. Adjust the focus of the optical microscope (OLYMPUS-BHC) at a magnifications 10x10 (x100) with the tracks appeared in a raster frame box (100 windows per 1 frame), as shown in Figure A1.2 in appendix A.
8. Counting the tracks on the CR-39 plastic film within 25 frames (1 frame = 1 mm^2) with a total area of 25 mm^2 or 0.25 cm^2. The track density is measured on the CR-39 plastic film in tracks mm^{-2}.
9. Changing from tracks mm^{-2} in tracks cm^{-2} as 25 mm^2 x 4 = 1cm^2

On the CR-39 plastic film a large number of tracks appear as shown in Figure 3.3. The number to be counted can be decreased by using the frame with the

counting track and randomly cover the CR-39 plastic film and then using statistical analysis of the data for determination of the track density.

<table>
<tr><td>(a)</td><td>(b)</td></tr>
</table>
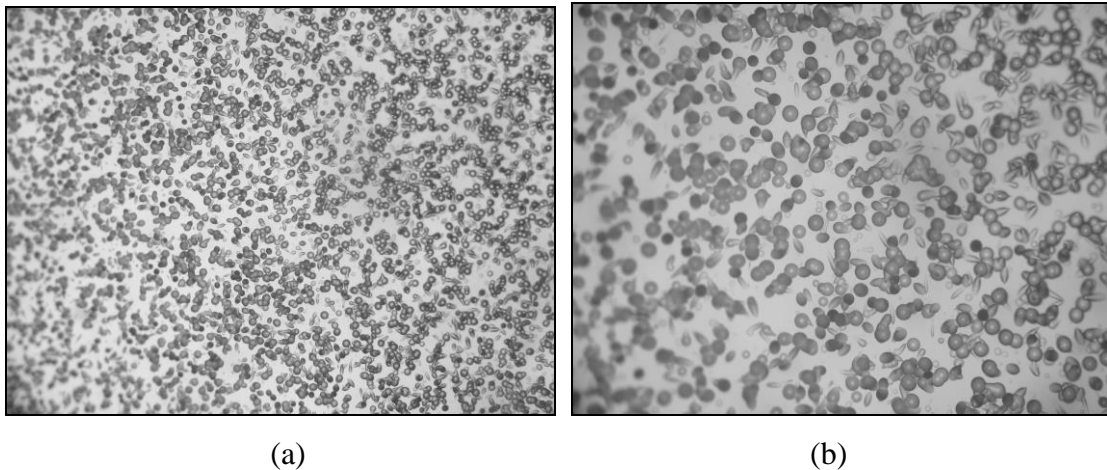
Figure 3.3   After chemical etching particle tracks can be viewed under an optical microscope at (a) x100 magnification and (b) x200 magnification.

3.1.3   Radon tack measurement setup

In this study, a solid state nuclear track detector (SSNTDs; CR-39) is used for measurements of soil gas radon in the cumulative alpha track for daily. The track was placed inside a cylindrical tube of 2 inch diameter, and 1 m in length, and then put in a dug hole of 1 m depth in soil. The detectors are on the top of the tube and sealed airtight against the outside environment by a common electrical tape. The changes of radon concentrations in the soil gas were determined by using solid state track detectors in monitoring profiles. The CR-39 plastic film, 2x2 cm^2, was mounted inside at the top of the cylindrical plastic lid can. Before the cans were put on the top of the tube, the opening of the tube was covered with thin polyethylene film to filter ^{220}Rn (Thoron) emission and humidity coming through the bottom opening of the tube as shown in Figure 3.4 and 3.5.

The detectors were put into holes of 1 m depth that were dug at ST-10 as the best site for monitoring in Muang District, Phang Nga Province (see in Figure

3.1). The detectors at the top of each tube were changed every day cover a period year from July 1, 2009 to June 30, 2010.
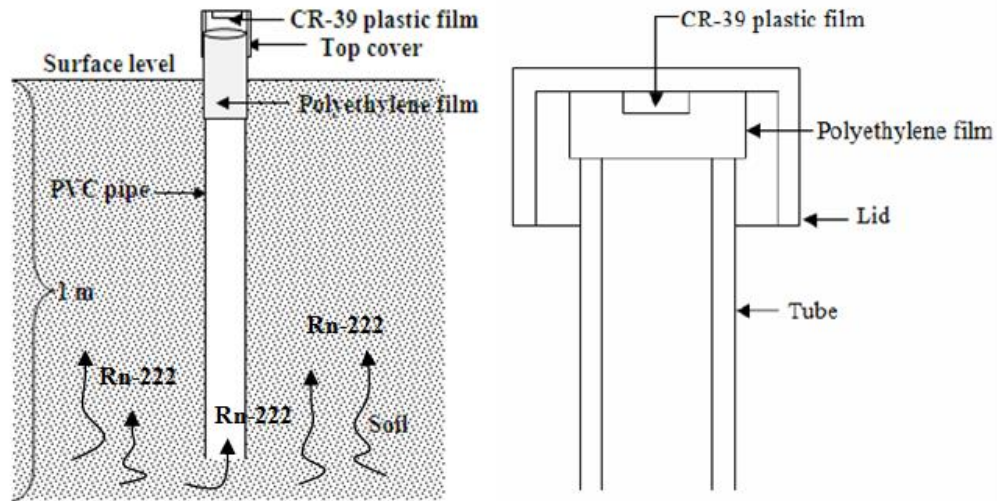
Figure 3.4   Schematic sketch of a track measurement method using a plastic pipe of about 1 m length puts into the soil and a CR-39 plastic film as the detector. The polyethylene film filters ^{220}Rn (Thoron) emission and humidity coming through the bottom opening of the tube.

Further the standard radon concentration has been calibrated using a known activity radium solution. The calibration procedure to find the relationship between the alpha track density on the detector after etching and the standard radon concentration of known activity. In this study radon concentration was then calculated using the following this calibration equation (Pisapak, 2009):

$$Rn\,Conc.(Bq\,m^{-3}) = \frac{106.524 \times Corr.TD\,(T\,cm^{-2})}{ExposureTime\,(day)} \quad , \qquad (3.1)$$

where *Rn Conc* (Radon concentration) is the concentration of radon in soil gas in Bq m^{-3} unit. *Corr.TD* (corrected track density) is the alpha track density that corrected in Track cm^{-2} unit. *Exposure Time* is the exposure time in days of soil gas radon exposure to the SSNTDs detector.

Figure 3.5   The measurement method of track detector for radon in soil gas: (a) a hole of 1 m depth, (b) a plastic tube put into the hole, (c) the tube was covered with thin polyethylene film and sealed airtight by a standard electrical tape, (d) the CR-39 film in a lid, (e) cover tube lid down and sealed airtight by a standard electrical tape, and (f) CR-39 film was changed every week.

The meteorological parameters including air pressure, temperature and rainfall were obtained daily from the Thai Meteorological Department (TMD), and were used for investigating their effect on the temporal radon variations is taken into consideration by statistical tests.

3.1.4   Seismic event data

Several studies regarding radon anomaly release to earthquake occurrence have been developed in earthquake prediction (Ghosh et al., 2007; Planinic et al., 2004; Inceoz et al., 2006). The relationship concludes that radon anomalies have been observed at a large distance from the earthquake epicenter, resulting from changes in the sudden vicinity of the monitoring station, rather than in the distant focal region. This is accomplished if it is assumed that changes in stress or strain is propagated from the rupture zone to the radon station, leading to variations also in porosity, emanating power or flow rate of the local groundwater, near the radon monitoring station.

The empirical relationship was obtained on the basis between the earthquake magnitude and the radius of the effect precursory manifestation zone. According to the formulation of Hauksson and Goddard (1981), experimental observations prove that earthquake is correlatable with radon anomalies which occur at distances calculated by the given empirical relationship as:

$$M = 2.4 \log D - 0.43, \tag{3.2}$$

Friedman (1991) proposed modified the above relationship as:

$$M = 2.4 \log D - 0.43 - 0.4, \tag{3.3}$$

where M is the magnitude and D is the distance to a radon monitoring station. However, all the above empirical relations have shown a relationship between epicentral distance and magnitude of the seismic events, but no relationship has been proposed, which has a correlation of radon anomalies with a seismic event. The data analyzed for the constants of the equation provides a range of uncertainties.

The earthquake data 210 events were collected from ANSS; Advanced National Seismic System of NCEDC (Northern California Earthquake Data Center) databases for the period from July 1, 2009 to June 30, 2010. The distribution of the seismic events region along Andaman Sumatra subduction and fault zone along the western of Thailand.

For data to be used in seismic analysis, all of data on body-wave magnitude (m_b) were converted to the moment magnitude (M_W) using the empirical relation defined by Scordilis (2006), is given below:

$$M_w = 0.85\,m_b + 1.03. \tag{3.4}$$

And then compute moment magnitude to seismic moment is given by Hanks and Kanamori (1979). The moment magnitude is defined as:

$$M_w = \frac{2}{3}\log(M_o) - 10.73, \tag{3.4}$$

where the logarithm is taken in base 10, and M_w is the Richter magnitude and M_o is measured in dyne cm.

Calculation the angular distance on the earth's surface between the epicenter of earthquake and the radon measurement station is defined as:

$$Angular\,Distance = cos^{-1}\left[sin\lambda_{EQ}sin\lambda_{SITE} + cos\lambda_{EQ}cos\lambda_{SITE}cos\left(\varphi_{EQ} - \varphi_{SITE}\right)\right], \tag{3.5}$$

where λ_{EQ}, ϕ_{EQ} is latitude and longitude of the epicenter of earthquake, and λ_{SITE}, ϕ_{SITE} is latitude and longitude of the radon measurement station.

So degrees of arc along the earth's surface can be used to find an epicentral distance (D) of the earthquake in kilometers when 1 degree of arc is approximately 110 km. The epicentral distance (D) is defined as:

$$D\,(km) = 110{\times}Angular\,distance. \tag{3.6}$$

Before that, the data determined the extent of the area. A shading in the Figure 3.6 is a result of a circular area with radon gas station; ST-10 in the center, at the latitude 8.46° N and longitude 98.57 ° E, situated in the Khlong Marui Faults. The distance far from the radon monitoring station to the west approximately 4-8 degree (angular distance). The innermost circle has a radius of 2 degrees or about 220 km. Circle next to a radius of 4 degrees about 440 km and circular hoop next to a radius of 6 degrees or 660 km outer circle with a radius of 8 degrees or 880 km, covering a radius of 135° bounded by latitude 0.7-10.9 °N and by longitude 91.6-100.0 °E with a moment magnitude ranging from M_w 4.4 to 7.8 (distance from the radon monitoring

station; ST-10 with duration 430-855 km) show that the distribution of 210 events in Figure 3.7, but different data was determined from equation (3.3), the earthquake magnitude is the smallest (M_{min}) to influence radon at a distance (D) = 440 - 880 km to the earthquake must have a minimum (M_{min}) = 5.6 - 6.3 means that a magnitude of 5.6, it will cause changes in radon measurement range up to a maximum of 440 km and a 6.3 earthquake magnitude has triggered a change in radon measurement at a distance of not more than 880 km.
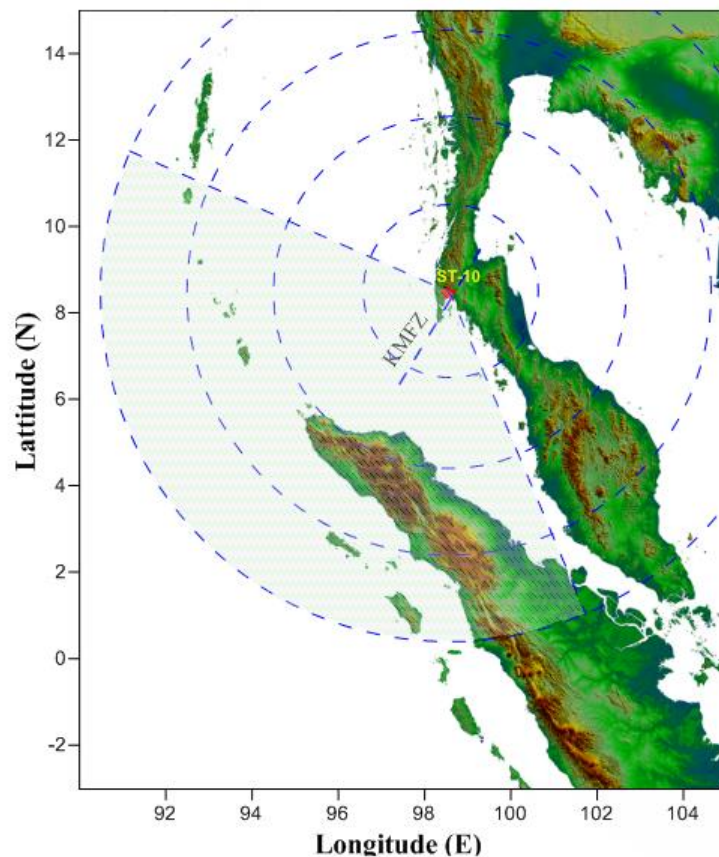
Figure 3.6   The location of radon in soil gas measuring station (ST-10; ★), KMFZ is a vertical sliding downward to against in the Andaman Sea and the shaded bar area for earthquakes is expected the effect of a change in soil gas radon anomaly.

However, several causes, including the geophysical properties of the crust involved, the way from the epicenter to the station measured radon (epicentral

distance; *D*) as well as the orientation of the faults that are around; there may be a way to make the link to any such faults (KMF, RF) and earthquakes smaller than M_{min} may be able to influence the radon concentration at a distance; *D* is far more than usual than the contrary. Thus 210 independent seismic events were selected, is shown in Figure 3.7.
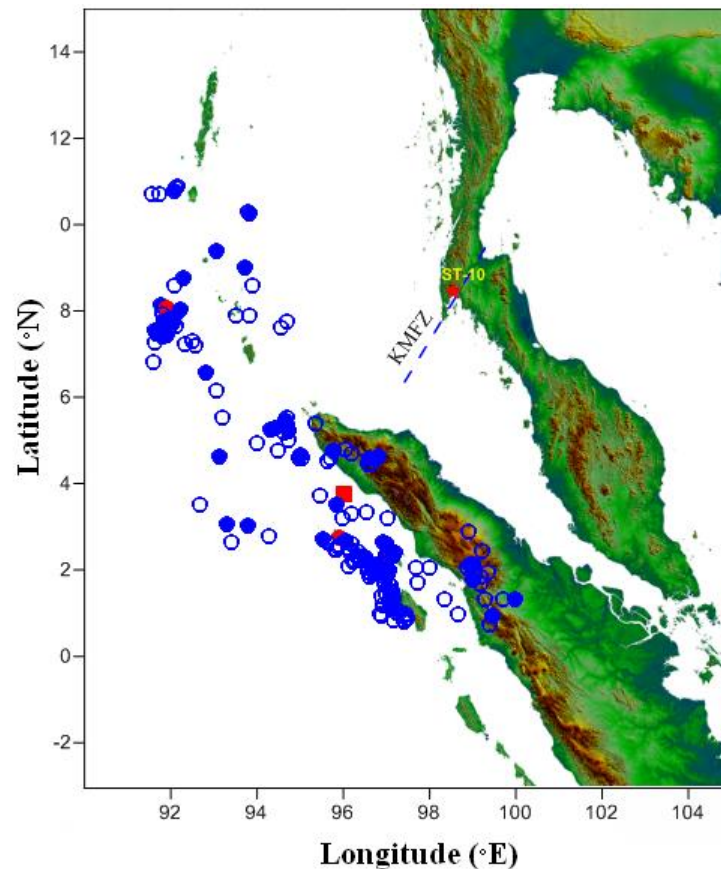
Figure 3.7   Locations of all seismic events detected by the ANSS databases for the period from July 1, 2009 to June 30, 2010.

3.2   The health effect of radon exposure in Namom district

In this work was to observe the correlation between concentrations of radon (^{222}Rn) and radium (^{226}Ra) in soil and to investigate the radon in water supplies to households and to estimate the potential natural radiation hazard in Namom district.

If well water is the major source of radon in this area, it could affect human health by exposure to radon, from the well water, via both ingestion and inhalation.

3.2.1   The location of study area

The study area, Namom district, is a district of the Songkhla province in Southern Thailand. Location map of the study area, geologic units, and sampling sites are shown in Figure 3.8. Namom district comprises 92.47 square kilometers with four sub-districts, namely (1) Pijit, (2) Tungkamin, (3) Klongrang, and (4) Namom. Namom district covers a flat terrain surrounded by mountains and hills. The main geologic units here include Triassic granite (Trgr), Carboniferous shale (Cy), and Quaternary sediment (Q). The Triassic granite named Songkhla granite prevails to north, east and south of the study area. Two main stream systems deliver water and sediments from the eastern and southern granitic highlands. Unconsolidated sediment exposed in this area was of Quaternary age (DMR, 2005). Namom district has higher uranium concentrations in the granite bedrock than other nearby districts (DMR, 1989). This granite and the country rocks are intruded by aplite dike and quartz veins caused by pneumatolytic and hydrothermal activities (Pungrassami, 1984). Subsequently there has been dissemination of cassiterite in leucogranite, together with columbium-tantalum minerals, and other ore minerals such as pyrite, arsenopyrite, wolframite, zircon, ilmenite, monazite, xenotime, and rutile. Moreover, torbernite, a highly radioactive mineral was discovered in tin mines (Thung Pho-Thung Khamin mining district) in this area (Pungrassami, 1984). That mineral has a uranium content of 48%. It was found in dikes and joints, or along fractures of granite, and in quartz, quartzite and decomposed granite (Pungrassami, 1984). Faults in the rocks cause solubilization of radium, with released and dissolved radionuclides and various heavy metals entering underground soil and water. In addition affecting of the true level of radon exposure for human was also observed in the surroundings of the environment via ingestion and inhalation.
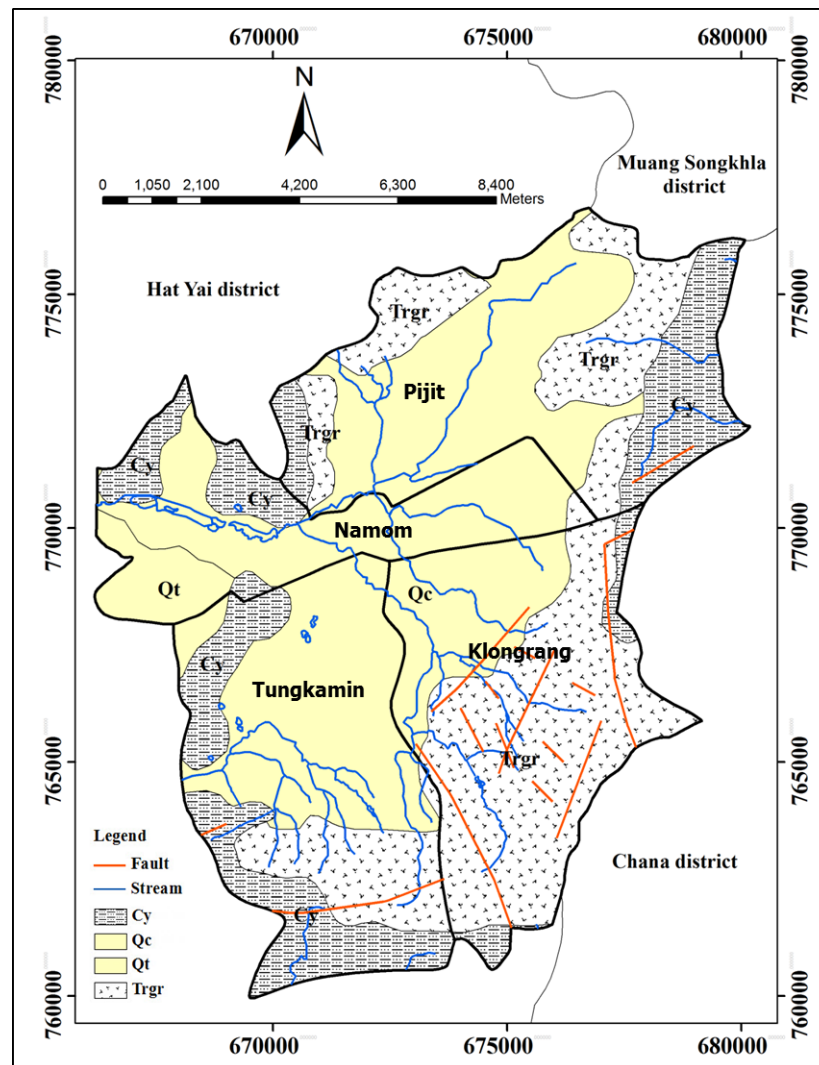
Figure 3.8   The location on a simplified geologic map of Namom District, Songkhla province. Rock units include Trgr: Triassic Granite; Cy: Carboniferous shale; and Q: Quaternary sediment.

3.2.2   Radon measurement by using an active measurement method

An active measurement method which has several advantages; electrical power required, can be easily measured in short time method, direct data reading, storing the time distribution of radon concentration, and continuous measurement was very helpful in identifying the cause of the problem. The devices involve pumping of gas into or through the detecting area of the instrument, such as;

silicon detector with HV- attachment and alpha spectroscopy, ionization chamber and scintillation chamber (Lucas cell). This study, then measured using the device RTM1688-2 for measuring radon in soil and the RAD7-RAD-H$_2$O for measuring radon in well water.

Radon measurements in soil gas

Radon in the soil gas measurements were performed by using the devices RTM1688-2 (SARAD Dresden, Germany), an electronic radon portable continuous monitor system with a silicon-surface barrier-type detector (dimensions 232x135x135 mm and weight 3.5 kg). In the study, a stainless steel probe with a length of 100.0 cm and 0.5 cm in a diameter was sunk into the ground to a depth of 70 cm at each measuring site, to avoid the major influence of meteorological variables (e.g., Hinkle, 1994; Sciarra et al., 2012). If the ground is firm it may be difficult to insert the probe to a sufficient depth. The probe was penetrated into the soil with a rotating handle or immersed with gentle strokes of a hammer. Soil air measuring assembly consists of a stainless steel probe connected to the devices RTM1688-2. Radon monitor by silicone pipes and valves to close on the top soil hole followed. The glass microfiber filter at the inlet prevents dust particles and radon progenies entering the detector chamber (Sumesh et al., 2011). The valve is opened so that soil gas can be collected in the detector chamber by air pump at a constant flow rate of 0.30 l min^{-1}. Radon concentration was measured by the device RTM1688-2 for 30 min in the every sampling site. Therefore, radon concentration inside the chamber with an internal volume of 130 ml is determined using an alpha spectrometric analysis with the concentration measurement range 0 - 10 MBq m^{-3}. The short living daughter products generated by the radon decay inside a measurement chamber. Positively charged ions of ^{218}Po accumulate under the influence of electric field on the surface of a semiconductor detector. The number of ^{218}Po ions collected is proportional to the concentration of radon present in the air inside the enclosure. ^{218}Po is an unstable isotope with a half-life of 3.05 min, and the detector can record only about half of the particles emitted from its decay, which are directed towards the detector surface. The

equilibrium between the radon decay rate and ^{218}Po detector activity is given after about 5 half-life times, i.e. after about 15 min, which is a minimum measurement time interval for radon concentration. The devices RTM1688-2, used for the measurements, has two modes of ^{222}Rn concentration measuring: "Slow", taking into account not only the disintegration of ^{218}Po, but also ^{214}Po, and "Fast", which provides only ^{218}Po decay calculation. But in this case, the measurements based on the "Fast" mode for application of the device which had been calibrated by the manufacturer. A schematic diagram of experimental arrangement for radon measurement in soil gas and the radon chamber operation are presented in Figure. 3.9.
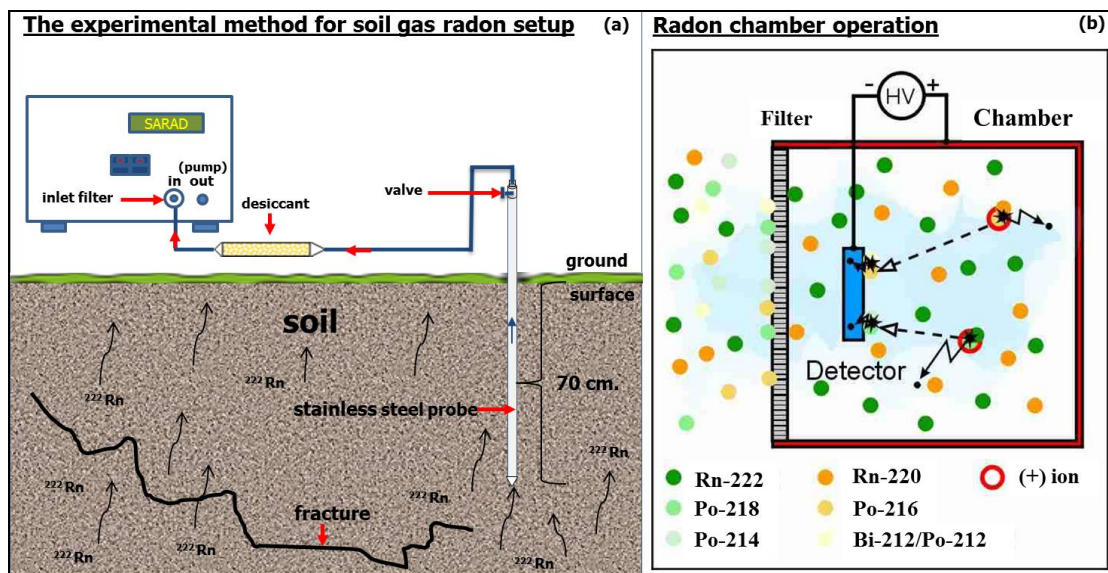
Figure 3.9 Schematic diagram of experimental arrangement for radon measurement in soil gas: (a) the experimental method for soil gas radon setup; (b) a schematic diagram of radon chamber operation. (Filter prevents progeny inlet from ambient air Radon/Thoron decay generates positive charged ^{218}Po/^{216}Po ions, ions are collected on detector by electrical field forces, alpha particle emitted by the decay of ^{218}Po/^{216}Po and their daughters are detected with high probability, equilibrium state between collection and decay process after about 5 half-life times of each nuclide, progeny activity on detector surface is proportional to the Radon/Thoron air concentration)

Radon measurements in well water

On the measurement of the radon concentration in well water samples is based on detection of the RAD7-RAD-H_2O system in a closed air loop, as shown in Figure 3.10 (Durridge CO.). The measurement of radon concentration in water is performed after aeration by air bubbling in the water sample, in a closed loop system. The system pulls samples of air containing radon and its progeny through a fine glass microfiber inlet filter, which allows only radon to pass through into a chamber for detection by an ion implanted Silicon alpha detector. In the RAD7 chamber, radon decays, producing detectable alpha emitting progeny, particularly polonium isotopes. Though the RAD7 detects progeny radiation internally, the only measurement it makes is of radon gas concentration. One can measure radon in water at concentrations from about 0.37 Bq l^{-1} to more than 1.5 x 10^5 Bq l^{-1} (Durridge CO.). This method is very efficient as the radon discharge from water to the air loop is 94% for a 250 ml sample. The efficiency depends on ambient temperature, but is typically above 90% (Durridge CO.). Since the extraction efficiency is always high, only very small temperature effects can be seen overall. However, relative humidity has the greatest impact on the measurement. The humidity of the measuring chamber inside the RAD7-RAD-H_2O is controlled by a calcium sulphate column at the air inlet of the instrument. The relative humidity inside the instrument will be kept at under 10% for the whole 30 min duration of measurement. High humidity would reduce the efficiency of ^{218}Po ions, formed as radon decays inside the chamber. However, the humidity reaching over 10 % during the last 10 min of the counting period will not much affect the measurement result (Durridge CO.).

The RAD7-RAD-H_2O system reaches equilibrium in about 5 min, so no more radon is taken from the water. The process is based on the following steps. 1. ^{222}Rn gas is removed from water sample by using a bubbling kit. 2. Expelled radons enter the chamber by air circulation. 3. ^{218}Po decayed from ^{222}Rn is collected into a silicon solid-state detector by an electric field. 4. ^{222}Rn concentration is calculated from the count rate of ^{218}Po at the end of the test which runs for 30 min after start (Figure 3.10). The RAD7-RAD H_2O prints out a summary, showing the average radon reading from the 4 cycles counted, a bar chart, and a cumulative spectrum. The

radon content in the water sample is calculated automatically by the RAD7-RAD H$_2$O (Durridge CO.).
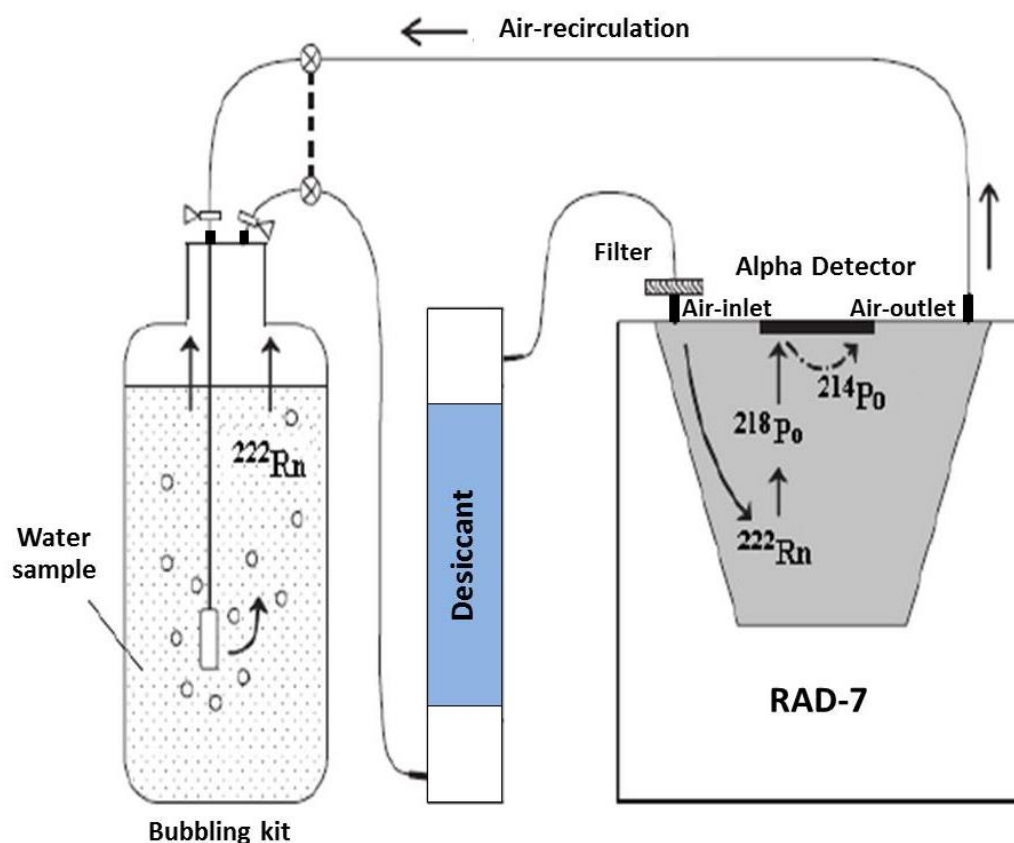
Figure 3.10   Schematic   diagram   of   experimental   arrangement   for   radon measurement in water of the RAD7-RAD- H$_2$O assembly.

Measurements of radium content in soil sample

Radium content in the collected soil samples of the study area was measured using "Sealed Can Technique" (e.g., Sharma et al. 2003; Khan et al. 2012). The soil samples were dried in an oven at 110 ℃ for 24 h and then grounded and sieved in a 200 mesh sive (see in Figure 3.11). A 100 g of soil samples was then packed and sealed in an impermeable airtight polyethylene container (diameter 7 cm and height 5.5 cm) to prevent the escape of ^{222}Rn and ^{220}Rn. Before measurements, the containers were kept sealed hermetically for about four weeks in order to reach secular equilibrium of the ^{226}Ra and ^{222}Rn and their decay products (Sharma et al.

2003; Mahur et al. 2008; Khan et al. 2012). After attainment of secular equilibrium, the samples were subjected to high resolution gamma spectrometric analysis. The experimental setup for measurements of radium content using "Sealed Can Technique" is shown in Figure 3.12.

| Dried at 110 ºC, 24 hrs. | Sieved in a 200 mesh sieve. | Weighed 100 g. |

Figure 3.11   The soil sample sample preparation for measurements of effective radium content.
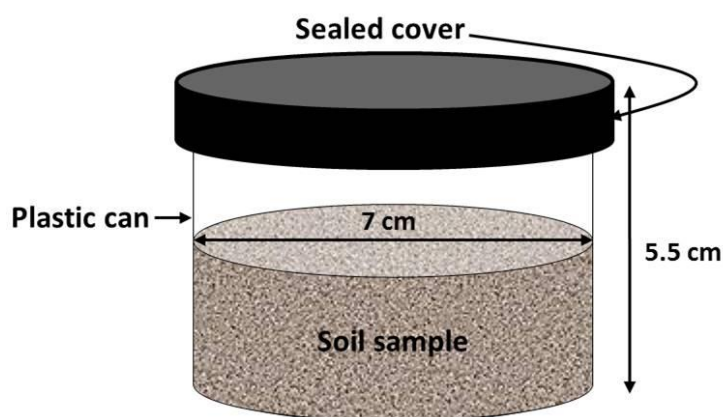
Figure 3.12   The experimental method for radium content setup using Sealed Can Technique.

A gamma-ray spectrometric system with a coaxial high purity germanium detector (HPGe, GC7020, Canberra, USA) with endcap size 3.75 in. (1 in. = 2.54 cm) of 83.7 % relative efficiency and energy resolution of 1.77 keV at the 1332 keV gamma-ray line of ^{60}Co. A low background lead shield with thickness of 4

in. (Canberra model 747, USA) was used to reduce the background gamma-ray in detector chamber and has 0.040 in. tin and 0.062 in. copper graded liner to prevent interference by lead X-ray. The IAEA-CU-2010-04 sample soil-06 with known activity of ^{226}Ra was used for efficiency calibration of the gamma spectrometric system is shown in Figure 3.13.
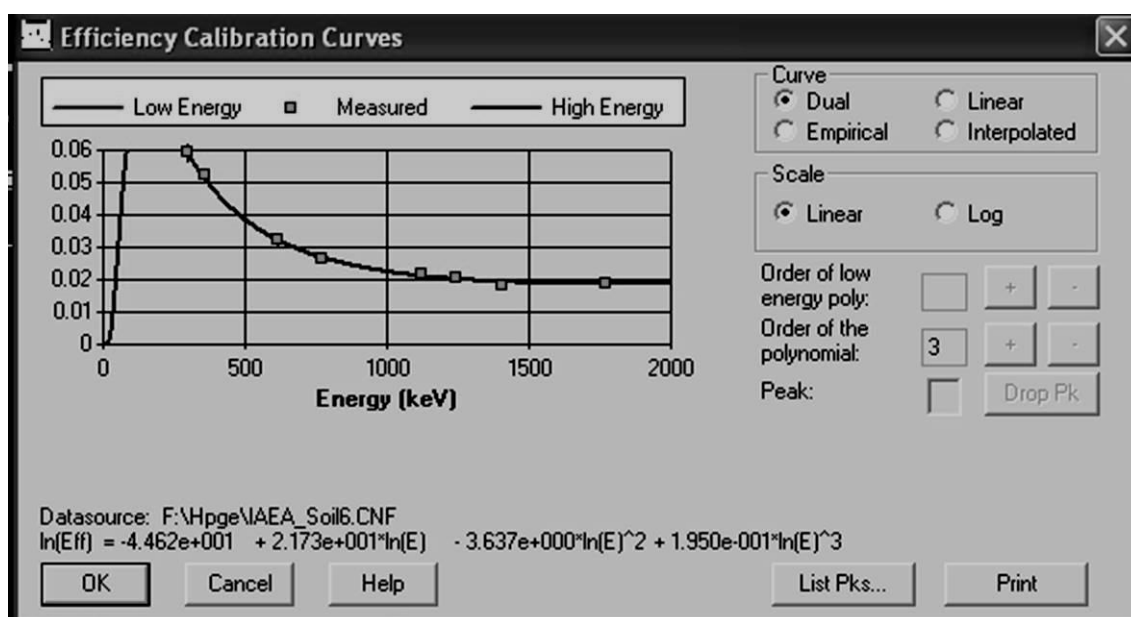
Figure 3.13   The efficiency calibration curve of the gamma spectrometric system.

After attaining secular equilibrium, each of the prepared samples was analyzed for the ^{226}Ra, ^{232}Th and ^{40}K activities. All the samples were counted for a period of 7200 s to obtain the γ-spectrum. The gamma-ray photo peaks at several energies of ^{214}Pb (at 295.2 keV and 351.9 keV) and ^{214}Bi (at 609.3 keV, 1120.3 keV and 1764.3 keV) were used to determine the concentration of ^{226}Ra (also known as ^{238}U equivalent). Gamma-ray emitted from ^{228}Ac (at 911.2 keV) and ^{212}Pb (at 238.6 keV) were used to determine the concentration of ^{232}Th. The 1460.3 keV gamma-ray radiating was used to determine the concentration of ^{40}K in different samples. The spectra were analyzed using the Genie2k computer software (Canberra, USA), which Figure 3.14 shows a partial γ-ray spectra for the highest concentration of the soil sample L1-10.
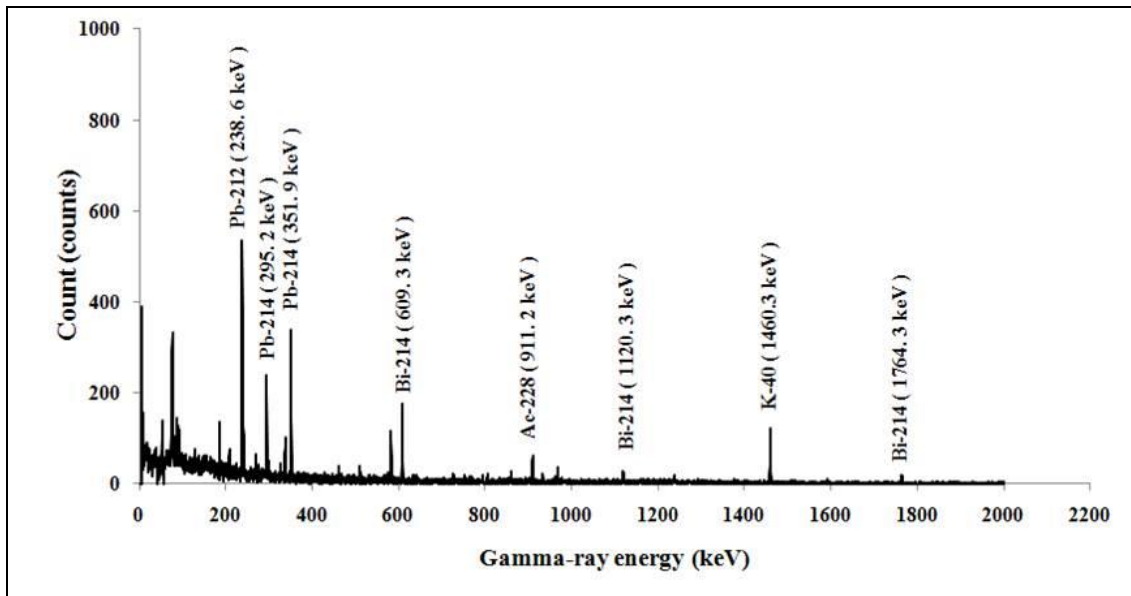
Figure 3.14   A partial γ-ray spectra for the soil sample L1-10 of the highest concentration.

CHAPTER 4

RESULTS AND DISCUSSIONS

This chapter aims to evaluate the overall significant results that obtain throughout the present work. In the virtual a period year from July 1, 2009 to June 30, 2010 the radon concentration in soil gas and earthquake measurements were carried out. In the meanwhile, the health effect of radon exposure to the general population risk was observed in Namom district, Songkhla province. The results obtained are presented in this chapter.

4.1   Radon observations in soil gas as a possible tool for earthquake prediction

4.1.1   The radon concentration in soil gas at ST-10

At station ST10 at 8.46^o N and 98.57^o E, the radon concentrations in soil gas measurements were conducted in Muang district, Phang Nga Province. Soil gas radon was distributed from the Khlong Marui Fault Zone within the study area. The results of radon concentration were present as the variation of cumulative alpha track for daily, which was then separated in the average radon concentration for monthly. The radon emission data cover 12 months in a period year from July 1, 2009 to June 30, 2010. The data for each day all of 12 months show in Figure 4.1 to Figure 4.4. The results of radon concentration for daily indicated that the difference between the minimum 6 ± 1 kBq m^{-3} was measured on June 21, 2010 and June 27, 2010 and the maximum value of 16837 ± 53 kBq m^{-3} was measured on November 10, 2009 (see also Table 4.1). The data in Table 4.1 show that the monthly average values of radon concentration for all of 12 months in a period year ranged from $854 - 3651$ kBq m^{-3}, which the total average radon concentration value is 1945 ± 111 kBq m^{-3}. To identify soil gas radon anomalies was observed in during a period of monitoring by comparing radon concentration with neighboring days. Due to the high values relative to neighboring days are referred to as radon peak or radon anomaly. The comparison of the anomalies with all data 98 peak as shown in Figure 4.5.
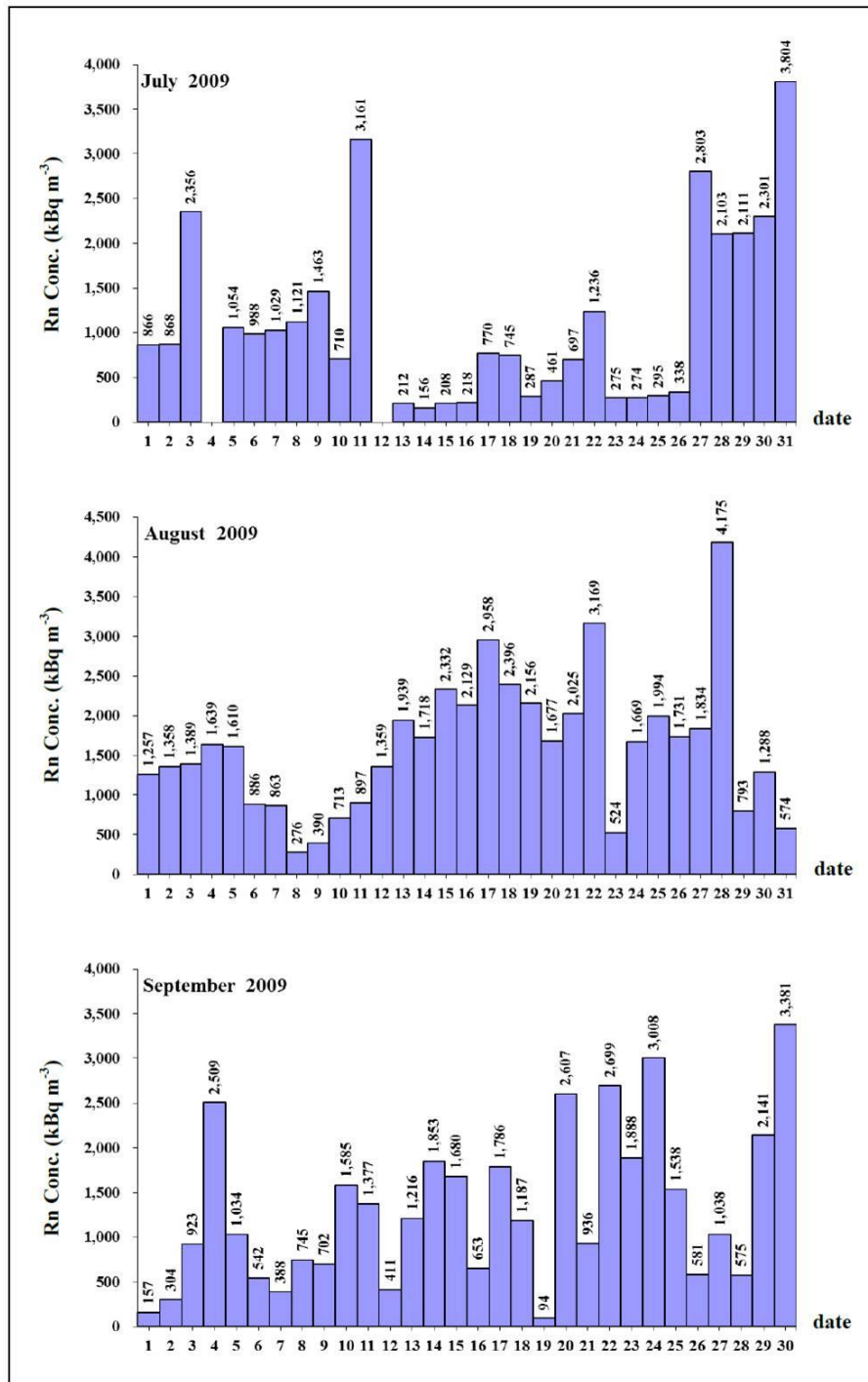
Figure 4.1   The cumulative alpha track radon concentrations (kBq m^{-3}) for daily at station ST-10 was observed in Phang Nga Province over a three months from July 1 to September 30, 2009.
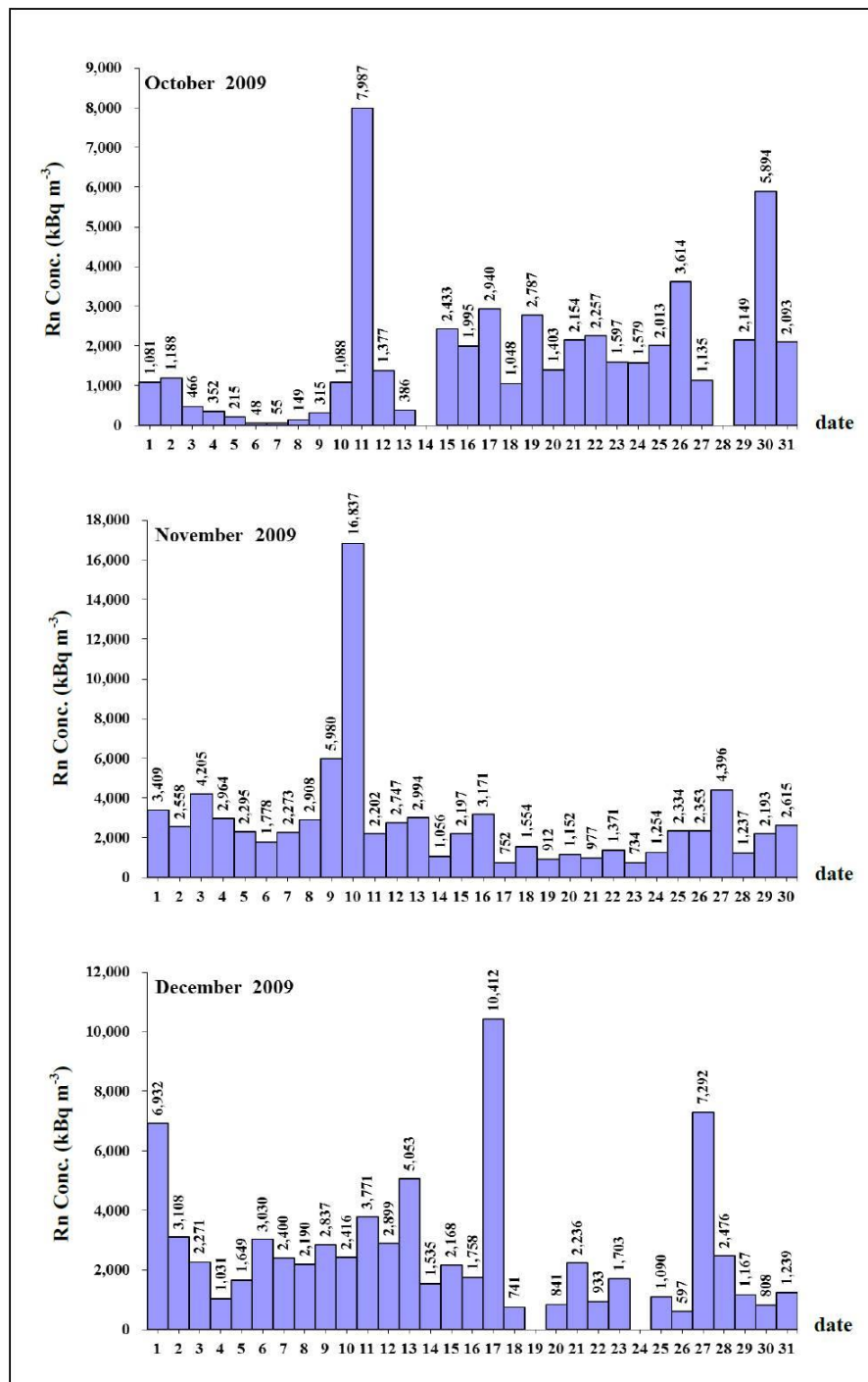
Figure 4.2   The cumulative alpha track radon concentrations (kBq m^{-3}) for daily at station ST-10 was observed in Phang Nga Province over a three months from October 1 to December 31, 2009.
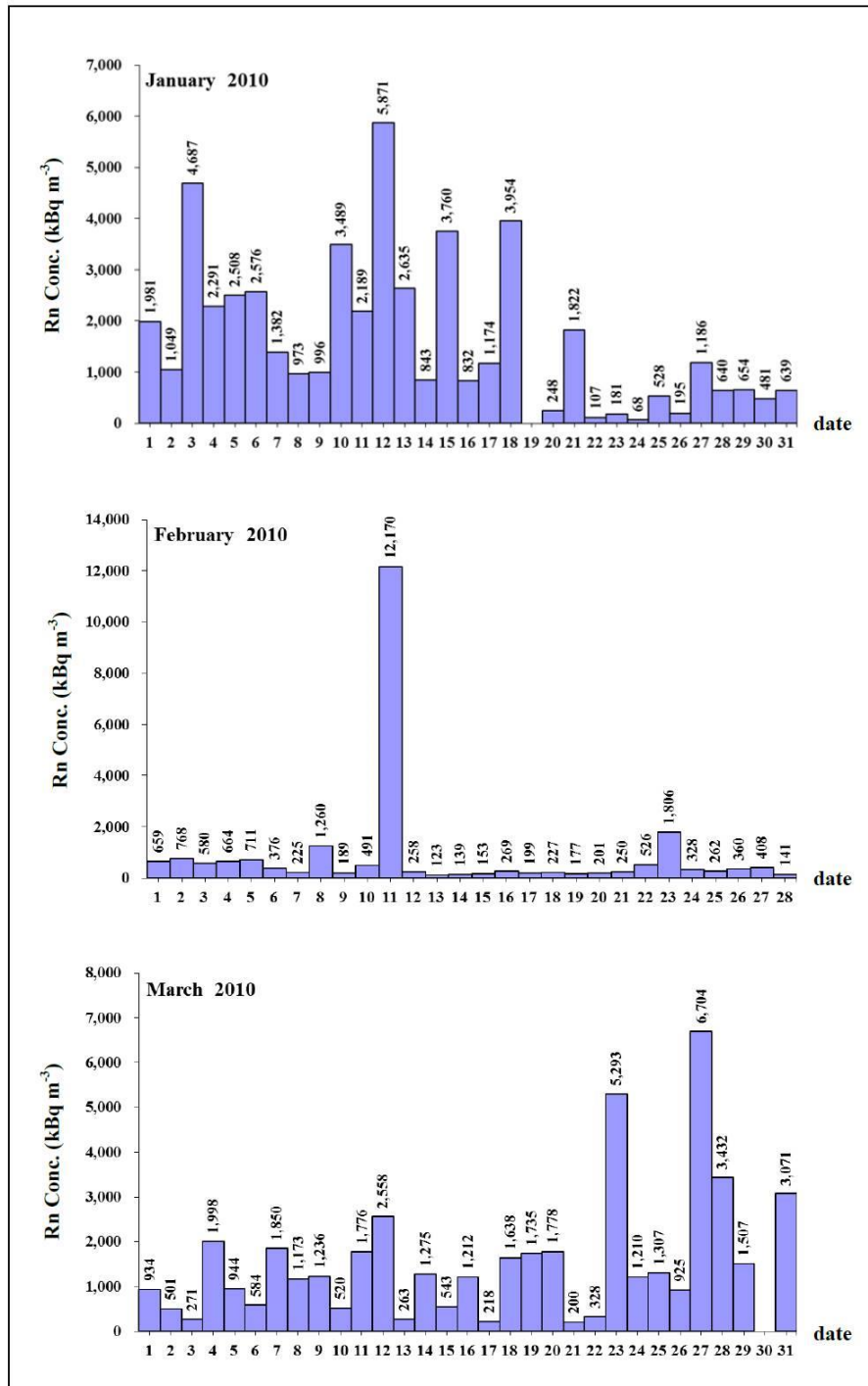
Figure 4.3   The cumulative alpha track radon concentrations (kBq m^{-3}) for daily at station ST-10 was observed in Phang Nga Province over a three months from January 1 to March 31, 2010.
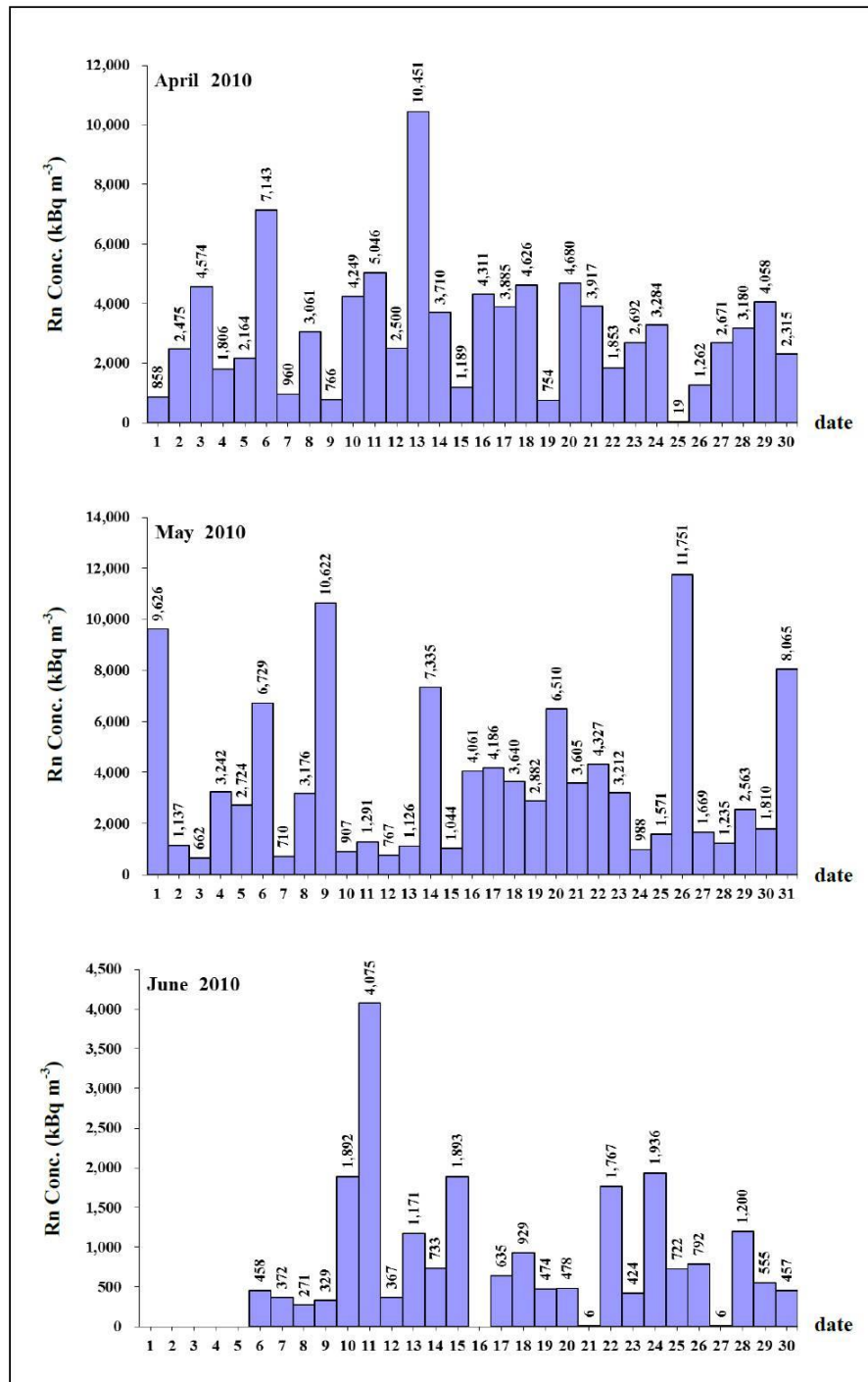
Figure 4.4   The cumulative alpha track radon concentrations (kBq m^{-3}) for daily at station ST-10 was observed in Phang Nga Province over a three months from April 1 to June 30, 2010.

Table 4.1:   Summary data of the average radon concentrations for monthly over a period year from July 1, 2009 to June 30, 2010 was observed in Phang Nga Province with maximum, minimum and standard error.

Month	Radon concentration (kBq m^{-3})			
	Mean	SE	Max	Min
Jul-09	1135	183	3804	156
Aug-09	1604	154	4175	276
Sep-09	1318	162	3381	94
Oct-09	1786	321	7987	48
Nov-09	2780	531	16837	734
Dec-09	2641	414	10412	597
Jan-10	1665	266	5871	68
Feb-10	854	425	12170	123
Mar-10	1566	267	6704	200
Apr-10	3149	386	10451	19
May-10	3651	556	11751	662
Jun-10	914	181	4075	6
Total	1950	111	16837	6
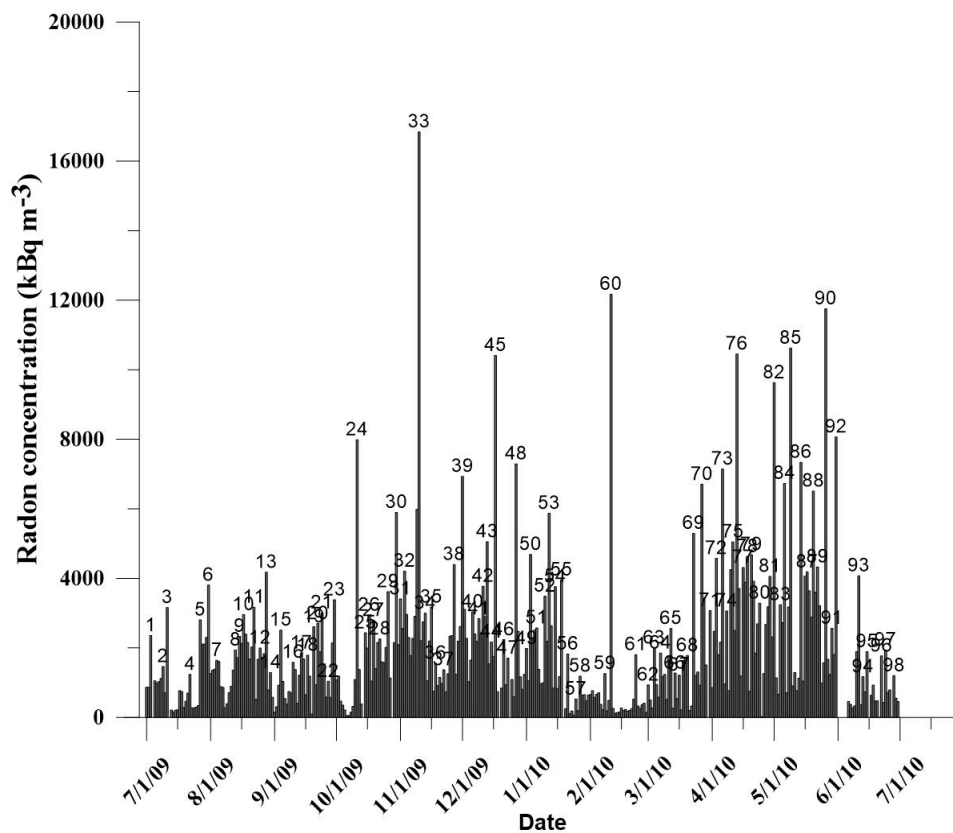
Figure 4.5   The anomaly of radon concentration in soil gas with 98 peaks.

4.1.2   Radon and meteorological measurements

The effect of meteorological variables of radon concentration in soil gas was provided by the TMD (Thai Meteorological Department) for a mean values daily period from July 1, 2009 to June 30, 2010, which were used for investigating their effect on the temporal radon variations at ST-10 and which is taken into consideration in the statistical tests. As already established, air pressure (P), Temperature (T) and rainfall (H) have a positive correlation with radon concentration. Correlation coefficients of radon concentration in soil with different meteorological parameters are summarized in Table 4.2. It shows the observed correlation between the radon concentrations of investigation and their effect on the other factors.

Interpreting the value of the correlation coefficient shows that the variables of radon concentration in soil gas with parameter P, T and H have less effect with the r value -0.15 0.13, and -0.03, respectively. There is a random, nonlinear relationship between the two variables. When the coefficient of correlation is a positive amount, such as 0.13, it means a direct relationship between two variables. If the coefficient of correlation is a negative, such as -0.15 and -0.03 it means a inverse relationship between two variables.

Table 4.2:   Correlation coefficient of radon concentration in soil gas with a different meteorological parameter at ST-10.

Parameter	Average	Standard Deviation	% Coefficient of variation	Coefficient of correlation
	(Avg)	(Std)	(CV; Std/Avg)	(r)
Radon concentration ($kBq\ m^{-3}$)	1,950	2,075	106	-
Air pressure (mbar)	1,010	2	0	-0.15
Temperature (℃)	28	1	4	0.13
Rainfall (mm)	10	22	214	-0.03

However, the maximum value (3651 kBq m^{-3}) of radon concentration is related to the minimum air pressure value (1008 mbar) found in the May 2010 of the summer season with the relative values shown in Figure 4.6. Air pressure is important influence to radon in soil gas, wherein a decrease in air pressure causes an increase in radon emission from the ground. With the maximum value (1012 mbar), air pressure found in the January 2010 is forced into the ground, thus diluting radon, but no correlation with the minimum value (854 kBq m^{-3}) and radon concentration found in the February 2010. The investigation of the influence of other meteorological parameters (e.g., rainfall, temperature) and related fluctuations of soil gas radon concentration can be used in a procedure of examining radon maximum as a possible radon anomaly (caused by an earthquake).
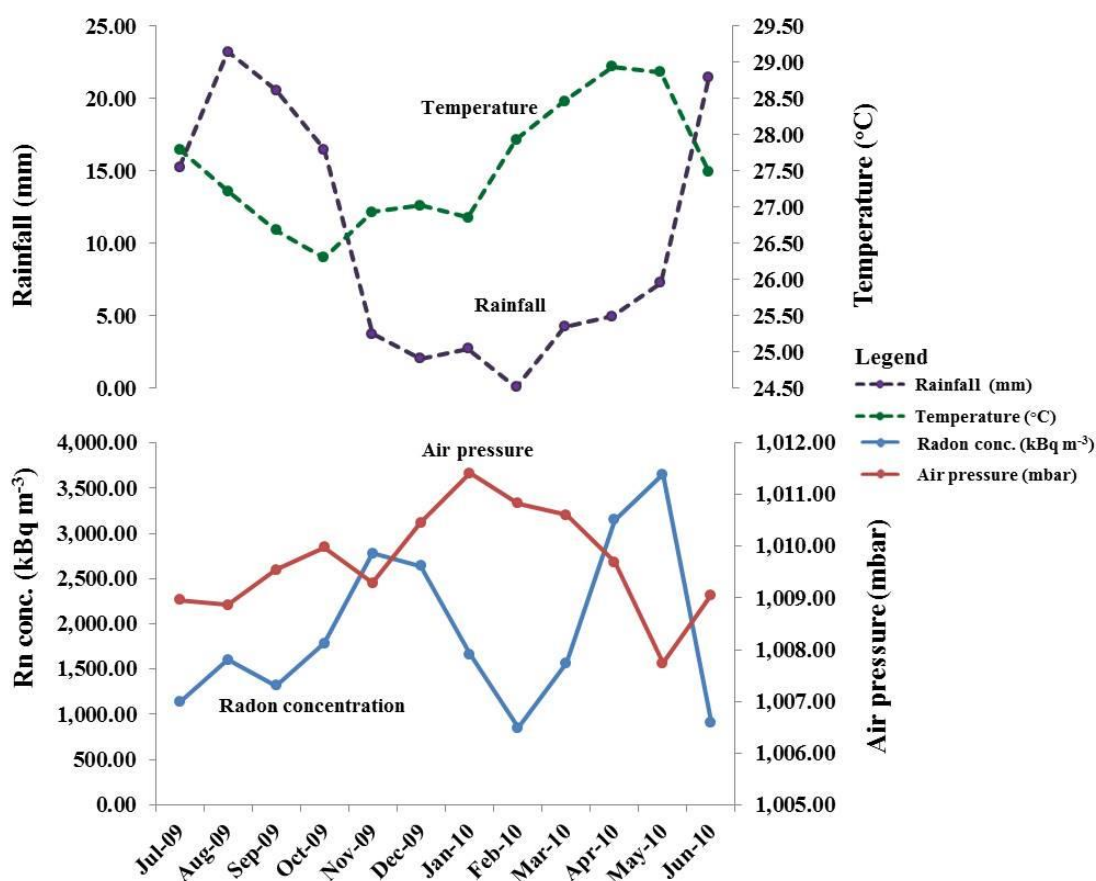
Figure 4.6   The seasonal variation of radon concentration with meteorological parameters, air pressure (P), temperature (T) and rainfall (H) in an average for the monthly coverage during the period of July 1, 2009 to June 30, 2010.

From the comparison of the anomalies with the P, T and H data, it can be seen that the meteorological parameters have less effect on the peaks of the soil gas radon concentration, because the measurements were taken at 1 m depth as suggested by Wattananikorn et al. (1998).

4.1.3   Correlation of radon peak with seismic events

From the analysis of the relationship between epicentral distance (D) and earthquake magnitudes (M) (Hauksson and Goddard, 1981; Friedmann, 1991), the earthquake magnitude ($M_w \geq 5$) was able to detect changes in the soil gas radon that is valid for interpretation of radon data. However, the Khlong Marui fault continues into the Andaman Sea. Thus, the ST-10 station can measure the change of radon concentration caused by an earthquake of magnitude $M_w < 5$. A large distribution of earthquakes with magnitudes 4.2–7.8 recorded in the ANSS database set at the same time of the radon measurement shows that there were 210 events up to the outermost epicentral distance of 855 km. Local geology of the Khlong Marui fault, has a significant effect on the seismic events in the Andaman Sea influencing the effect relationship to radon emanation encountered at the monitoring site. In this study, it is interesting to observe the earthquake magnitude $M_w \geq 4$ indicating earthquake prediction studies after radon changes a specific spike anomaly in the observation area (Crockett et al., 2005).

When analyzing the data value of earthquake magnitude $M_w \geq 4$ and epicentral distance that are related to a radon peak occurred during the measurement interval of 365 days during the time of July 1, 2009 to June 30, 2010, with a total result of 98 radon peaks, (Figure 4.5 and Figure 4.7). The magnitude was separated with 3 ranges of them at $M_w \geq 4$, $M_w \geq 5$ and $4 \leq M_w < 5$ and precursor time was separated in the order are 0-1, 0-3, 0-5, and 0-10 days, as can be seen in Table 4.3.

Further, as a possible earthquake precursor using the change of radon that occurred during the period time of measurement relative to the radon peak results showed 98 peaks (Figure 4.7). The earthquake $M_w \geq 4$ of precursor time 0-3, 0-5, and 0-10 occurred after 66 of 98 radon spike-like anomalies is the best signal, 67.3 % and

no earthquakes $M_w \geq 4$ after a total of 32 peaks, 32.7% behavior is not a precursor. As well as, in the case of $M_w \geq 5$ and $4 \leq M_w < 5$ of precursor time 0-1, 0-3, 0-5, and 0-10 shown the signal of radon anomalies that occurred lower than $M_w \geq 4$.
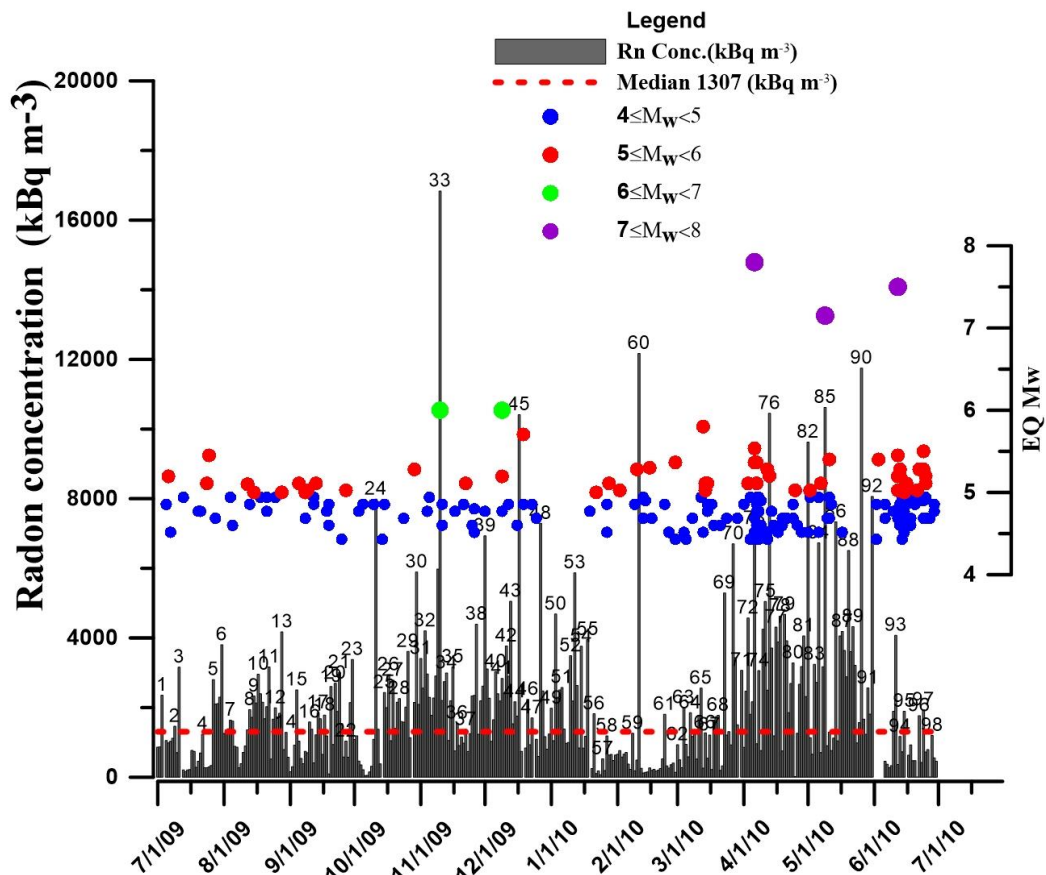
*Figure 4.*7   Radon concentration in soil gas (daily average) with the earthquake magnitude between July 1, 2009 to June 30, 2010 (seismic events databases from ANSS of Northern California Earthquake Data Center).

In addition, which a precursor time of 0-1 day with the earthquake $M_w \geq 4$. It is possible that radon can be seen as a precursor with 53 radon peak anomalies of total 98 peaks showed low signal 54.1 %, and behavior is not a precursor 45 of 98 peaks, 45.9 % or noise with no earthquakes $M_w \geq 4$ occurring after the radon spike-like anomaly (Table 4.3).

Upon observation, can be seen the seismic events have accurately followed measurements of radon peaks. In Figure 4.7, it can clearly be seen that these events are neither random nor outstanding. For example, peak 60 was measured on February 11, 2010 and had a radon concentration value of 12170 kBq m^{-3}, it can be observed as an earthquake precursor $M_w \geq 4$ after 5 events, $M_w \geq 5$ after one event and $4 \leq M_w < 5$ after 4 events. Peak 73 as well, with a radon concentration value of 7,143 kBq m^{-3} measured on April 6, 2010, can also be seen as an earthquake precursor $M_w \geq 4$ after 17 events, $M_w \geq 5$ after 5 events and $4 \leq M_w < 5$ after 12 events. And finally peak 85, with a radon concentration value of 10,622 kBq m^{-3} measured on May 9, 2010, will also be seen as an earthquake precursor $M_w \geq 4$ after 6 events, $M_w \geq 5$ after 2 events and $4 \leq M_w < 5$ after 4 events. Thus, it is highly possible that station ST-10 is able to detect changes in concentration of radon gas caused by the earthquake of $M_w > 4$, or may be able to detect changes in concentration of radon gas caused by the earthquake of $M_w < 4$.

During the period of observation, as seen in the alternate high and low measurements of radon concentration, few earthquakes occurred when higher radon concentrations were found. And in contrast, more earthquakes occurred when radon concentrations were at their lowest (Figure 4.7). This feature is called earthquake precursor or pre-earthquake phenomena, the high peak radon will behave as an earthquake warning in advance. The phenomenon can be explained by the interaction between the plates in this area.

Furthermore, Thailand, being situated in the Eurasian plate close to the subduction zone, is in a high risk area of collision with the Indian-Australian plate. The Indian-Australian plate situated in the south is moving and pushing the Eurasian plate in the Northeast (NE) direction (USGS, 2005). The collision of these two plates has caused the compression pressure in the subduction zone, creating an imbalance of the mechanism in this area, forcing the mass in Southeast Asia to move in a southeast direction, consistent with several major and minor faults and fault related structures (Duerrast et al., 2007). As a result, many earthquakes occurred in this area, associated with local earthquakes in trough fault of southern Thailand, especially, at the Ranong and Khlong Marui Fault

4.1.4   The result of cumulative radon concentration

Figure 4.8 shows radon concentrations in soil gas for daily in correlation to the cumulative radon concentrations, the earthquakes with $M_W \geq 4$ and the cumulative seismic moment in the same period time of data between July 1, 2009 to June 30, 2010. In an investigation of the cumulative radon concentrations, that are related to the daily radon concentration that occurred during the measurement. It can be observed that when the occurrence of radon peak or radon anomalies increased in over a period of time, as a result, the cumulative radon concentration in during that time has a high slope. While the cumulative radon concentration data values were analyzed, which by fitting trend lines through data to observe the linear equation that can be used to identify the four different slopes, show in Figure 4.8.

When considered in conjunction with the earthquakes $M_w \geq 4$ occurring at each of these intervals (shown in Figure 4.8) can be summarized as follows:

1. If the slope of the cumulative radon concentration is < 1500 kBq m^{-3} day^{-1}, the earthquake size $M_w < 6$ is likely to occur.

2. If the slope of the cumulative radon concentration is > 2500 kBq m^{-3} day^{-1}, the magnitude of the earthquake magnitude Mw > 6 is likely to occur.

3. If the slope of the cumulative radon concentration is > 3000 kBq m^{-3} day^{-1}, the magnitude of the earthquake magnitude Mw > 7 is likely to occur.

Table 4.3: A possibility of radon peak as an earthquake precursor $M_w \geq 4$ compared with $M_w \geq 5$.

Observation area	Earthquake Magnitude (Mw)	Number of Earthquake (events)	Number of radon peak (a)	Number of Rn peak correlated with EQ (b)	Number of Rn peak not correlated with EQ (c)	Signal (%) (b/a)	Noise (%) (c/a)	Confidence level (S/N)	Precursor Time (day)
	M ≥ 4	143		53	45	54.1	45.9	1.2	
	M ≥ 5	44	98	24	74	24.5	75.5	0.3	0-1
	4 ≤ M < 5	99		46	52	46.9	53.1	0.9	
	M ≥ 4	183		66	32	67.3	32.7	2.1	
	M ≥ 5	53	98	31	67	31.6	68.4	0.5	0-3
	4 ≤ M < 5	130		57	41	58.2	41.8	1.4	
135°	M ≥ 4	199		66	32	67.3	32.7	2.1	
	M ≥ 5	57	98	33	65	33.7	66.3	0.5	0-5
	4 ≤ M < 5	142		59	39	60.2	39.8	1.5	
	M ≥ 4	210		66	32	67.3	32.7	2.1	
	M ≥ 5	60	98	34	64	34.7	65.3	0.5	0-10
	4 ≤ M < 5	150		59	39	60.2	39.8	1.5	
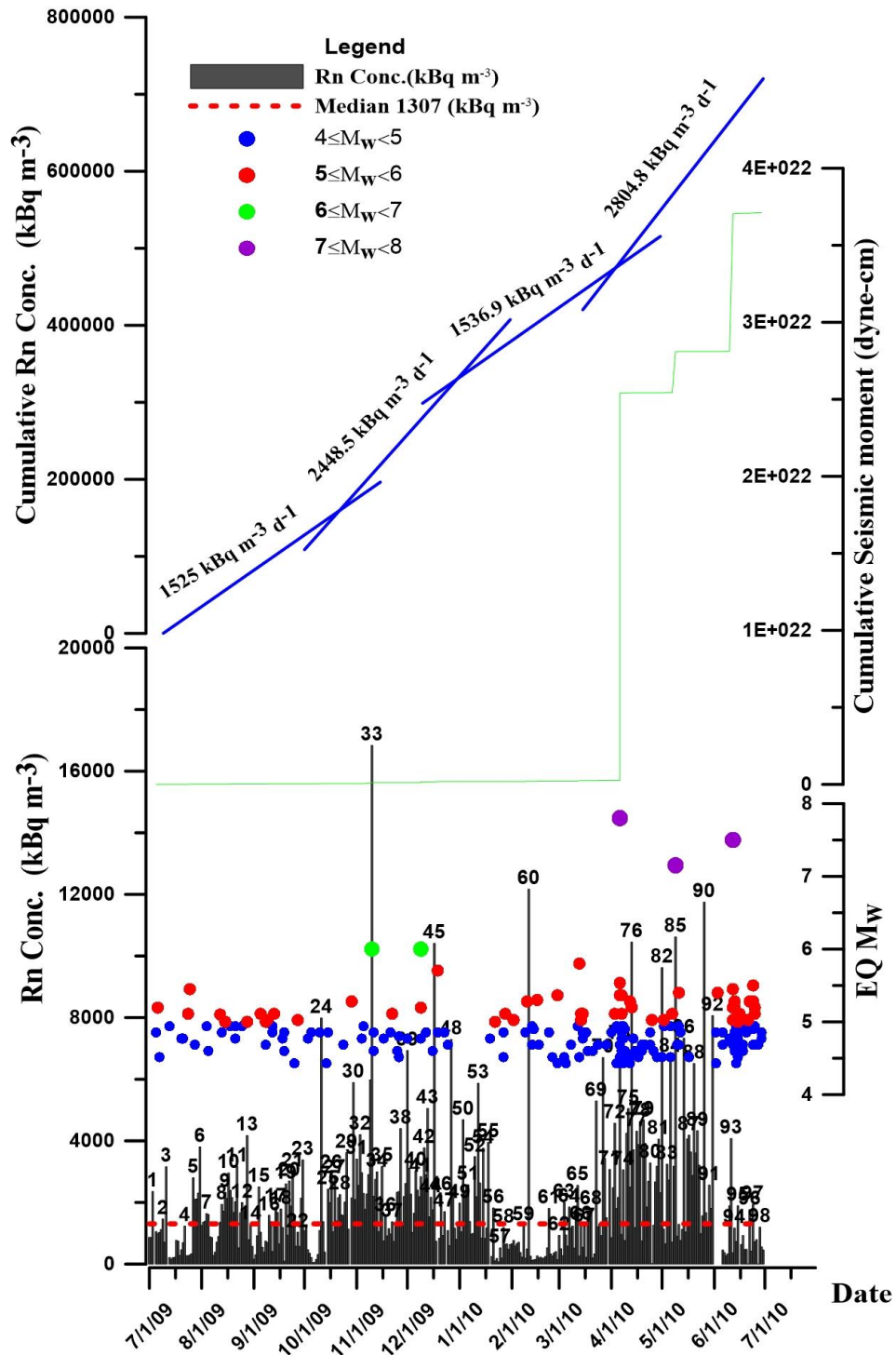
*Figure 4.*8   Graph shows the relative of radon concentration in soil gas (daily average), cumulative radon, the earthquake with $M_w \geq 4$ and cumulative seismic moment ,the data between July 1, 2009 to June 30, 2010.

4.2   Spatial variation of radon and application to radon exposure in Namom district

The study area, Namom district is located within the geologic units show in Figure 4.9 that is surrounded by mountains and hills. The rock structure of aquifers results from the erosion of bordering mountains and two main stream systems deliver water, sediments from the eastern and southern granitic highlands. As a result, this area has higher uranium concentration in the granite bedrock than other district in the vicinity (DMR, 1989). Corresponding to the general population in Namom district was carried out using case control of cancer risk from 1999-2004 (Hirunwatthanakul et al., 2006). Therefore, it is a reasonable to assume that high radon concentrations might be present in this area, as well as, greater health risks among inhabitants of Namom district. Thus, is important to assess the radiological hazards to population under investigations.

4.2.1   A possible correlation between soil radon concentration and radium content in soil samples and assess the potential radiological hazards

The main target of the present work is to study the possible correlation between soil radon concentration and radium content in soil samples and assess the potential radiological hazards associated with these materials by annual effective dose equivalent, radium equivalent activity, indices gamma radiation hazard index values and excess lifetime cancer risk associated with exposure to soil from Namom district, Songkhla province, Thailand.

Calculation radiological parameters

Radium equivalent activity (Ra_{eq})

The radium equivalent activity is a common index used to represent the specific activity of ^{226}Ra, ^{232}Th and ^{40}K. It is calculated on the assumption that 370

Bq kg^{-1} for ^{226}Ra or 259 Bq kg^{-1} for ^{232}Th or 4810 Bq kg^{-1} for ^{40}K produce the same gamma dose rate. Therefore, the Ra$_{eq}$ of the sample in (Bq kg^{-1}) can be expressed as:

$$Ra_{eq} = A_{Ra} + (A_{Th} \times 1.43) + (A_K \times 0.077), \qquad (4.1)$$

where A_{Ra}, A_{Th} and A_K are concentrations of the three radionuclides ^{226}Ra, ^{232}Th and ^{40}K respectively, which is expressed in Bq kg^{-1} (Najam et al., 2015).

Absorbed Gamma Dose Rate (*D*)

The external outdoor absorbed gamma dose rate due to terrestrial gamma rays from the nuclides ^{226}Ra, ^{232}Th and ^{40}K at 1m above the ground surface was calculated as follows:

$$D(nGy\ h^{-1}) = 0.462\ A_{Ra} + 0.604\ A_{Th} + 0.0417\ A_K. \qquad (4.2)$$

The annual effective dose equivalent E (μSv y^{-1}) was calculated from the relation (UNSCEAR, 1988):

$$E\ (\mu Sv\ y^{-1}) = D(nGy\ h^{-1}) \times 24h \times 365.25d \times 0.2 \times 0.7\ SvGy^{-1} \times 10^{-3}. \qquad (4.3)$$

External and Internal Hazard Indices (*H$_{ex}$* and *H$_{in}$*)

Radioactivity level can be calculated by the following expression of the external (H_{ex}) and internal (H_{in}) hazard index can be defined as follows:

$$H_{ex} = \frac{A_{Ra}}{370} + \frac{A_{Th}}{259} + \frac{A_K}{4810} \leq 1, \qquad (4.4)$$

$$H_{in} = \frac{A_{Ra}}{185} + \frac{A_{Th}}{259} + \frac{A_K}{4810} \leq 1. \qquad (4.5)$$

The limited average radioactivity level was found to be less than unity (Najam et al., 2015).

Gamma radiation hazard index ($I_{\gamma r}$)

The gamma radiation hazard index was suggested by a group of experts of the OECD (Organization of Economic Cooperation and Development) Nuclear Energy Agency for the external radiation due to different combinations of specific natural activities in a sample. Proceeding from these recommendations, another may be defined as:

$$I_{\gamma r} = \frac{A_{Ra}}{300} + \frac{A_{Th}}{200} + \frac{A_K}{3000} \qquad (4.6)$$

This index can be used to estimate the level of γ-radiation hazard associated with the natural radionuclides (European Commission, 1999).

Excess Lifetime Cancer Risk (*ELCR*)

The Excess Lifetime Cancer Risk (*ELCR*) was calculated using the following equation:

$$ELCR = E \times DL \times RF, \qquad (4.7)$$

where E is the annual effective dose equivalent, DL is the average duration of life (estimated to 70 years), and RF is the Risk Factor (Sv^{-1}), i.e. fatal cancer risk per Sievert. For stochastic effects, the ICRP (International Commission on Radiological Protection) uses RF as 0.05 for public (Taskin et al., 2009).

4.2.1.1 Correlation of radon and radium concentration in soil

The exposure due to radon inhalation and its daughters present in the environment is highest of natural radionuclides to which human being is exposed. Since radium is present at relatively low level in the natural environment, everyone has some level of exposure to its radiation. However, individuals may be exposed to higher level of radium and its associated external gamma radiation. If they live in an area where there is an elevated level of radium in soil. In addition, radium is

particularly hazardous because it continually produces radon, which can diffuse into nearby homes. So the radon measurement thus necessitates the need for radium estimation in parent source for public health risk evaluation.

In the present study, 20 sampling points were measured the radon concentration in soil along a line (L1, L2 and L3) with a difference geology, i.e., L1 in the Quaternary sediment (Qc) and Triassic Granite (Trgr), L2 in the Carboniferous shale, Quaternary sediment, and Triassic Granite. For the sampling site in L3 is a spot check of L1-7, based on the Quaternary sediment. Furthermore, 21 soil samples were collected for radium measurement at the same radon measuring point or relatively shorter distances less than 1 meters from radon sampling point, one sampling point in L3-3 is not to measure radon concentration (Figure 4.9 and Table 4.4).

The observation values of the radon concentration in soil gas are directly related to the radium content observed in the soil samples collected at the same location as shown in Table 4.4. It is evident from the Table 4.4 that the radon concentration in soil gas varies from 0 ± 0 kBq m^{-3} to 642 ± 6 kBq m^{-3} and radium content varies from 7 ± 3 Bq kg^{-1} to 279 ± 5 Bq kg^{-1}. The highest concentration of radon was found at sample code L1-7 with 642 ± 6 kBq m^{-3} corresponding to the highest radium content in soil (L1-7) at the same location with 279 ± 5 Bq kg^{-1} as well as the second highest of the radon concentration of 284 ± 3 kBq m^{-3} corresponds to the second highest of the radium content of 183 ± 9 Bq kg^{-1} found at L1-10 (also shown in Figure 4.10a). But, in the sample code of L1-3, L2-4, and especially on L2-6 the correlation of radon and radium concentration in soil is unclear, which show low radon soil gas concentration when compared to others with similar radium content. Such effect can be described by a target phenomena (e.g., Nazaroff and Nero, 1988; Markkanen and Arvela, 1992; Porstendörfer, 1993). In this case, if the soil is dry that radon atoms which are ejected from soil grains by the decay of radium on the mineral surfaces. Due to high ejected kinetic energy (86 keV) can pass through the pores, (if the pores are small enough) and stick to neighboring grains, and thus not any further available for exhalation as a result of radon concentration in soil gas should be low. Conversely, very significant outliers in the data shown in sample code L2-2, which has a very high radon concentration in soil gas compared with the lowest radium content in soil.

Figure 4.9   Sampling site locations in the simplified geologic map in Namom District, Songkhla province. Rock units include Trgr: Triassic Granite; Cy: Carboniferous shale; and Q: Quaternary sediment (Coordinates are in the UTM projection zone 47N).

Table 4.4: The observed values of radon concentration in soil gas and radium content in soil samples collected from Namom district, Songkhla province, Southern Thailand.

Sample code	Radon concentration $\pm$ SD* (kBq m^{-3})			Ra-226 content in soil $\pm$ SD* (Bq kg^{-1})		
L1-2	25	±	1	59	±	5
L1-3	1	±	0	84	±	6
L1-4	41	±	1	60	±	5
L1-5	24	±	1	53	±	8
L1-6	184	±	6	118	±	7
L1-7	642	±	6	279	±	5
L1-8	100	±	2	102	±	7
L1-9	91	±	2	70	±	5
L1-10	284	±	3	183	±	9
L1-11	202	±	2	130	±	8
L2-2	111	±	1	7	±	3
L2-4	2	±	0	54	±	2
L2-5	178	±	2	95	±	3
L2-6	0	±	0	94	±	3
L2-7	140	±	1	126	±	3
L2-8	233	±	5	141	±	8
L3-2	183	±	2	161	±	4
L3-5	90	±	2	108	±	3
L3-13	150	±	1	157	±	4
L3-14	99	±	2	142	±	4

* SD: standard deviation
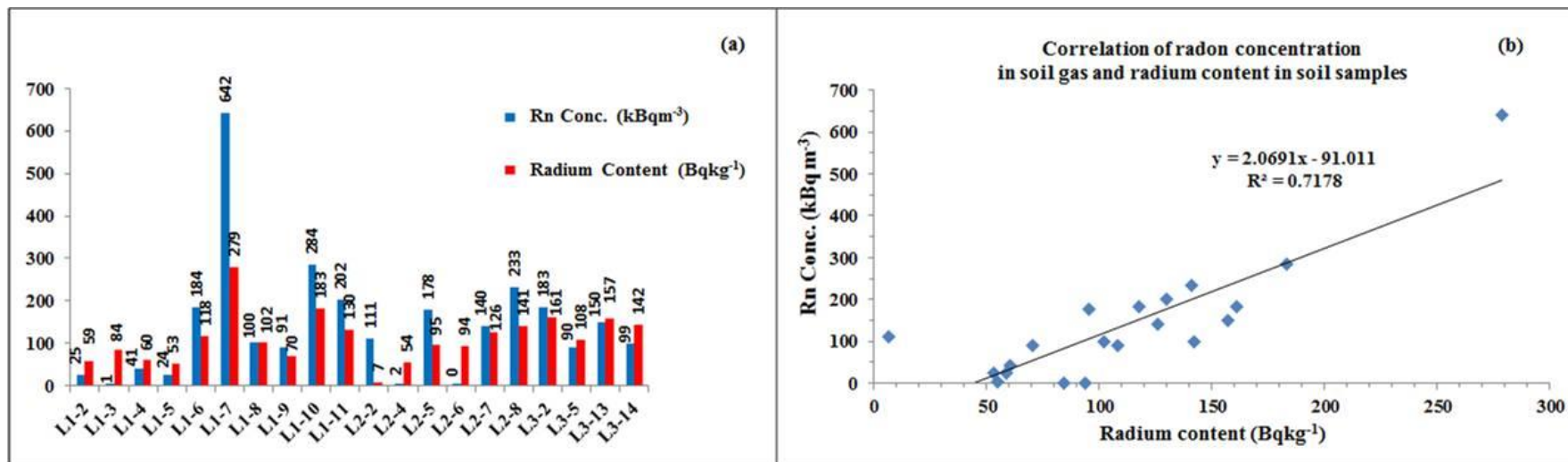
Figure 4.10 Correlation between radon and radium concentration in soil: (a) bar diagram showing radon in soil gas and radium content in different soil sample; (b) correlation graph between radon and radium concentration in soil.

Thus, it can be assumed that the high radon concentration may come from deep sources through a high permeability soil that might allow radon to move up more easily. Thus measured radon concentration in soil gas should be high.

Therefore, it is interesting to study correlation between radon concentration in soil gas and radium content in soil samples as shown in Figure 4.10b. The graph indicates a positive correlation coefficient, $R^2 = 0.72$ (the accuracy of the approximations). Similar results were reported by Sharma et al. (2003), Kakati et al. (2013).

However, the observed correlation depends on the geologic structure in the region when this region contains different rock formations such as granites, gneisses, schist and quartzite and is characterized by different mineral deposits (Pungrassami, 1984). As reported by Ishihara et al. (1980) and Sirijarukul (1994) that the Songkhla granite contained high uranium where decomposed granite has been exposed to ground or in the abandon tin mines (Pungrassami, 1984). The decomposed granite occurred under the influences of pneumatolytic and hydrothermal activities of coarse-grained biotite granite in the study area (Pungrassmi, 1984) is found also in the fault zones (Figure 4.9) and is probably a potential source of radium distributed in the area. Also signifies importance of high heat producing granites, which are known for high uranium, thorium and potassium contents in these rocks and soils (Atiphan ,2007; Kromkhun, 2010). However, the genesis has not been studied in detail. The question of why and how the granites contain unusually high uranium, thorium and potassium concentrations have not been satisfactorily answered (Kromkhun, 2010). Thus, it can be observed that wherever the radium content in the samples is more, the obvious offshoot radon concentration in soil gas has been also found to be high as well, as expected for a correlation between them (Singh et al., 2008).

4.2.1.2 Specific activity of radionuclides in soil samples

The specific activity of ^{226}Ra, ^{232}Th and ^{40}K in Bq kg^{-1} measured in soil samples are presented in Figure 4.11. It can be noticed that the specific activity concentrations of ^{226}Ra, ^{232}Th and ^{40}K were in the range of 7 to 279, 35 to 238 and 0.5 to 2306 (Bq kg^{-1}) with an average value of 108 $\pm$ 26 Bq kg^{-1}, 114 $\pm$ 22 Bq kg^{-1},

and 1081 ± 278 Bq kg^{-1}, respectively. The present results show that the values of the specific activity of natural isotopes in Namom district, Songkhla province are higher than the values of the specific activity of the latest global average limit which equal to 35 Bq kg^{-1} for ^{226}Ra, 45 Bq kg^{-1} for ^{232}Th and 412 Bq kg^{-1} for ^{40}K reported in United Nations Scientific Committee on the Effects of Atomic Radiation (UNSCEAR, 2008).
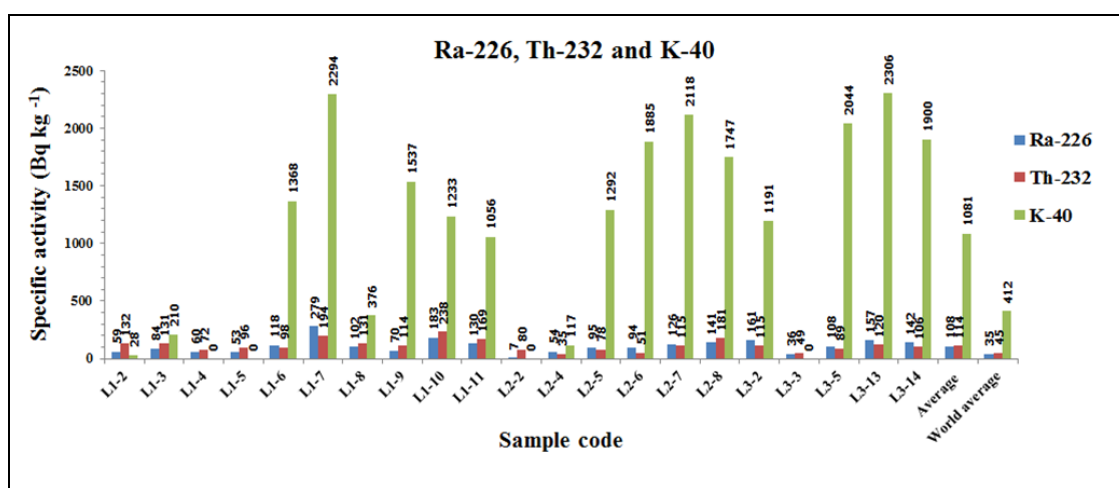
Figure 4.11   The specific activities of ^{226}Ra, ^{232}Th and ^{40}K in the soil samples collected from Namom district, Songkhla province, South of Thailand compared with the world-wide average specific activity (UNSCEAR 2008).

The variations of natural radioactivity levels at different sampling sites are due to the variation of concentrations of these elements in geological formations (being based on Figure 4.9). Concentrations of ^{226}Ra, ^{232}Th and ^{40}K is quite high in the southeast of the area, which contains a series of fault and fractures in granite bedrock. High ^{40}K activity while observing in all samples may be due to agricultural activities going on in the area. Considering the use of potassium fertilizers which may have been transported to the soil, given that ^{40}K should be high. Thus exposure to terrestrial radiation depends on radionuclide content in soil and in other environment but exposure also depends on human activities and practices (Wang, 2002).

4.2.1.3 Radiological Hazard Assessment

It is important to assess the health hazard of the radiation effects to human and environment, It has been defined in terms of "The radium equivalent activity" (Ra_{eq}), "Absorbed Dose Rate" (D), "Outdoor Annual Effective Dose" (E), "External and Internal hazard Index" (H_{ex} and H_{in}), "Gamma radiation hazard index" ($I_{\gamma r}$), and "Excess Lifetime Cancer Risk"(ELCR), respectively, the values are shown in Table 4.5, 4.6 and Figure. 4.12. The results shown in Table 4.5, 4.6 represent the values of radiological hazard assessment, with the average values and the uncertainty level of $\pm$ 2 SEM. The radium equivalent activity of all samples ranged from 107 to 733 Bq kg^{-1} with the average equivalent activity of 354 $\pm$ 72 Bq kg^{-1}. The highest of radium equivalent activity obtained in this study is higher than the world average limit of 370 Bq kg^{-1}.

The absorbed dose rates due to the terrestrial gamma rays at 1 m above ground surface are in the range of 47 to 342 nGy h^{-1} with an average of 164 $\pm$ 34 nGy h^{-1} for soil samples in the area under study. This value is higher than the world average value of 57 nGy h^{-1} (UNSCEAR, 2000). The ranges of annual effective dose estimated for all the samples are from 57 to 420 μSv y^{-1}, while the average value is 201 $\pm$ 42 μSv y^{-1}. This average value is comparable to the world average of 70 μSv y^{-1} as reported in UNSCEAR (2000).

On the other hand, the calculated values of the external and internal hazard index, gamma radiation hazard index and excess lifetime cancer risk for soil samples studied were above the safe limit as shown in Table 4.5, 4.6 and Figure 4.12. The results depict that the H_{in}, $I_{\gamma r}$ values for soil samples are higher than the limit of unity, which is above the permissible limit of 1 mSv y^{-1} recommended by the European Commission (European Commission, 1999).

Table 4.5:   Radiation hazard parameter values of each soil sample collected from different sites in Namom district of Songkhla province of Southern Thailand.

Sample code	Ra_{eq} (Bq kg^{-1})	D (nGy h^{-1})	E (µSv y^{-1})	H_{ex}	H_{in}	I_{gr}
L1-2	250	108	133	0.68	0.83	0.45
L1-3	287	127	155	0.78	1.00	0.52
L1-4	164	71	88	0.44	0.60	0.29
L1-5	190	82	101	0.51	0.66	0.34
L1-6	364	171	210	0.98	1.30	0.70
L1-7	733	342	420	1.98	2.73	1.41
L1-8	318	142	174	0.86	1.13	0.58
L1-9	351	165	203	0.95	1.14	0.68
L1-10	617	279	343	1.67	2.16	1.15
L1-11	453	206	253	1.22	1.57	0.85
L2-2	121	51	63	0.33	0.34	0.21
L2-4	114	51	63	0.31	0.45	0.21
L2-5	306	145	178	0.83	1.08	0.60
L2-6	312	153	188	0.84	1.10	0.63
L2-7	453	216	265	1.22	1.56	0.89
L2-8	534	247	303	1.44	1.82	1.02
L3-2	417	194	237	1.13	1.56	0.80
L3-3	107	47	57	0.29	0.39	0.19
L3-5	393	189	232	1.06	1.35	0.78
L3-13	506	241	296	1.37	1.79	0.99
L3-14	440	209	256	1.19	1.57	0.86
Average ± 2 SEM	354 ± 72	164 ± 34	201 ± 42	0.96 ± 0.20	1.25 ± 0.13	0.67 ± 0.14
World Average	370	57	70	1.00	1.00	1.00

* SEM: standard error of the mean; 2 SEM represent the 95% confidence limits

Table 4.6:   Radiation hazard parameter values of each soil sample collected from different sites in Namom district of Songkhla province of Southern Thailand.

Parameters	Average	±	2 SEM**	Max	±	SD*	Min	±	SD*	World recommended values
Ra_{eq} (Bq kg^{-1})	354	±	72	733	±	16	107	±	9	370
D (nGy h^{-1})	164	±	34	342	±	7	47	±	4	57
E (µSv y^{-1})	201	±	42	420	±	9	57	±	5	70
H_{ex}	0.96	±	0.2	1.98	±	0.04	0.29	±	0.03	1
H_{in}	1.25	±	0.13	2.73	±	0.06	0.34	±	0.03	1
I_{gr}	0.67	±	0.14	1.41	±	0.06	1.14	±	0.03	0.5

* SD: standard deviation;

** SEM: standard error of the mean ; 2 SEM represent the 95% confidence limits

External gamma dose estimation due to the terrestrial sources is essential not only because it contributes considerably (0.46 mSv y^{-1}) to the collective dose, but also because of the variations of the individual doses related to these sources. These doses vary depending upon the concentrations of the natural radionuclides, ^{238}U, ^{232}Th, their daughter products and ^{40}K, present in the soils and rocks, which in turn depend upon the local geology of each region in the world. To evaluate the terrestrial gamma dose rate, it is very important to estimate the natural radioactivity level in soils (Singh et al., 2005). The radium concentration in worldwide surface soil is relatively uniform, except in some well-defined areas that have a naturally higher concentration, such as some felsic volcanic soils and in some uranium mining regions (Rizzo et al., 2001). However, in buildings with high-radium levels, the radon exhalation from building materials may become of major importance. Higher indoor external dose rates may also arise from high concentrations of ^{226}Ra in soil. Elevated ^{222}Rn indoors may be explained by the fact that high radium soil concentrations remain embedded in the mineral grains. Radon can move through cracks in rocks and through pore spaces in soils to lead to higher inhalation doses. The computed Internal Hazard Index is given in the work.
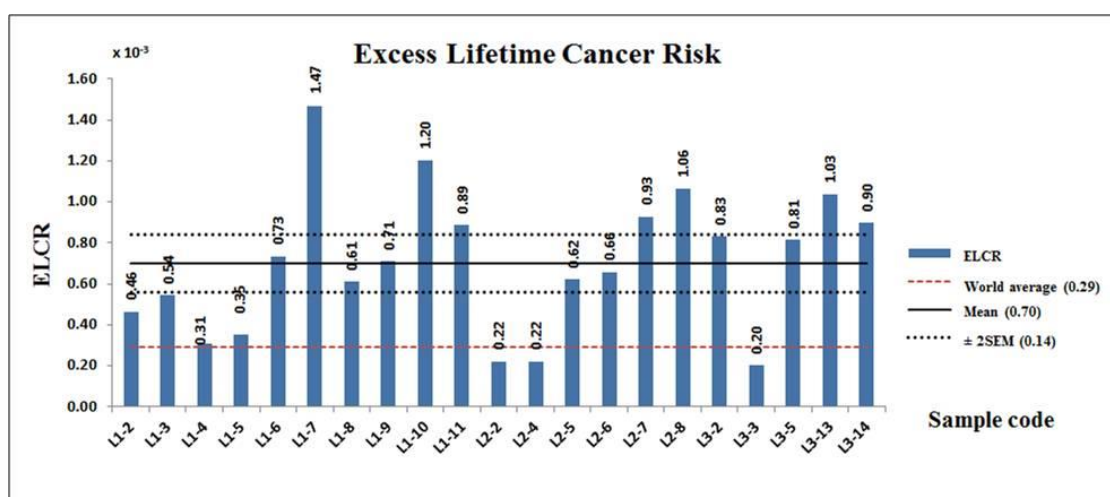
Figure 4.12   Excess lifetime cancer risk is compared with the mean and world average values.

.

Furthermore, the present values of the average excess lifetime cancer risk (ELCR) for all samples in Figure 4.12 are higher than the world average of 0.29×10^{-3} recommend by UNSCEAR (2000). This result indicated that the high radiation exposure is likely to increase risk of developing cancer in the general population where uranium and radium are significant components of the granite rock in this area (Wutthisasna et al., 2006). Corresponding to a population based case of incident cancers were observed in Namom district, identified by the cancer registry of Songkhla province, the Radiotherapy Unit, Prince of Songkla University, and Namom Hospital from 1999 to 2004. Thirty-two cases were identified and all had pathological diagnosis, while two men were living and 30 men were deceased. Also the information from the Songkhla Cancer Register found that oral and esophageal cancer in males, in Namom district is 5 times higher than the provincial level. These cancer cases were estimated to involve with exposure to radiation in the area, both ingestion and inhalation (Hirunwatthanakul et al., 2006).

4.2.2 Radon concentration in well water collected from Namom district: a factor influencing cancer risk?

This study aimed to investigate the radon levels in the water supplies to households, and to determine the health hazards due to radon gas that can accumulate and reach high concentration levels indoors, contributing significantly to human health risks as possible carcinogen.

Assessment of annual effective dose from drinking water

The annual effective dose E for general population caused by radon in drinking water and other domestic water use is the sum of effective doses from radon ingestion with water (E_{ing}) and from inhalation of water borne radon (E_{inh}). The ingestion dose for a particular radionuclide can be estimated as IAEA (1996):

$$E_{ing} = DCF \cdot A_{ing}, \tag{4.8}$$

where *DCF* (dose conversion factor) or dose coefficient is in Sv Bq^{-1}, and this is connected with the effective dose due to ingestion of unit activity of the particular radionuclide, while A_{ing} is the total activity ingested in Bq.

Regarding radon ingestion in drinking water Eq. (4.8), can be modified as follows Bem et al., 2014:

$$E_{ing} = DCF \cdot A_{Rn} \cdot V_A, \quad\quad\quad\quad (4.9)$$

where A_{Rn} is the average concentration of ^{222}Rn in drinking water in Bq l^{-1}, and V_A is the estimated annual volume of water consumed directly from tap in l.

The estimated dose coefficient due to ingestion of radon from water is 10^{-8} Sv Bq^{-1} for an adult (UNSCEAR, 2000). Since radon is readily lost from water by heating or boiling, the value of 60 l for the weighted direct annual consumption of tap water has been proposed in United Nations Scientific Committee on the Effects of Atomic Radiation (UNSCEAR) 2000 Report.

Exposure to radon is mainly affected by the inhalation of its decay products, which deposit homogeneously within the human respiratory tract and irradiate the bronchial epithelium (UNSCEAR, 2000). We assumed that the ratio of radon concentration in air to that in water is 10^{-4}, the equilibrium factor between radon and its progeny is 0.4, the average indoor occupation factor is 0.8 or 7000 h y^{-1}, and the dose conversion factor for radon exposure is 9 nSv Bq^{-1} m^3 h^{-1} (UNSCEAR, 2000). The annual effective dose due to inhalation corresponding to the concentration of 1 Bq l^{-1} in tap water is therefore 2.5 μSv y^{-1} (Binesh et al., 2012), and this scaling is applied here to estimate the inhalation doses.

The seasonal variations in rainfall impact on the radon concentration in well water were observed (e.g., Fuki, 1985; Hamada, 2000; Misha et al., 2013; Prasad et al., 2009; Zmazek et al., 2000). It was found that the overall average values of radon concentration reach maximum during rainy season and minimum during summer season (Misha et al., 2013; Zmazek et al., 2000). In the rainy season flow of water through rivers and canals come to the ground and increase the level of water. Because of this the radon kept low in the other season flow upwards with water level, thus the radon concentration in water slightly

increases (Misha et al., 2013). In addition, enrichment of radon in water after the rainfall is possible by increasing of more catchment area additional radon is supplied from the surrounding rock and soil (Prasad et al., 2009). Meanwhile flow of the radionuclides from hilly region reach into streams and the plane, which is one of the reason as an increase of radon in water (Misha et al., 2013).

The area under study (South of Thailand), really has only two seasons: the summer season (February- September) and the rainy season (October-January). Due to heavy rains, possibly 70 percent of the country is covered by forest. It is classified as monsoon forest, except in the South and South-East areas where tropical rain forest is more common (Jermsawatdi, 1979). Considering the radon concentration in water is strongly affected by the seasonal variation in rainfall. The sampling of this study was observed in the summer and assumed that sampling is representative of the annual average.

Well water sample collection

A total of 60 shallow well water samples were taken from different homes distributed within the study area. The well water sample collection was done in communities with comparatively high populations, as the villages and homes tend to be near the main water streams. Private wells have been dug to supply household water. In this case, well water samples were collected one sample per site from different homes along the village's main river (Figure 4.13). These water samples represent the residential well water of the study area. Most of these water samples were taken at depths less than 20 m in 250 ml plastic bottles (Durridge CO.) with water sampling equipment; a few samples were taken from sump pumps representing depths exceeding 20 m. Furthermore, when a well was equipped with a water pump, the water samples were collected immediately before being pumped into the storage tank. A precaution that needs to be exercised in the of any grab water is identical in that dissolved gases from water should not escape during transfer from water sample to the storage container. Aeration of water sample during collection could result in a loss of radon, and thus the sampling procedures need to be designed to minimize this effect.

The distribution of all well water samples in the district is as follows: 15 samples were taken from Pijit sub-district, north of Namom district; 6 samples from the Namom sub-district; 20 samples from Tungkamin sub-district (west of Namom district); and 19 samples from Klongrang sub-district to the east.
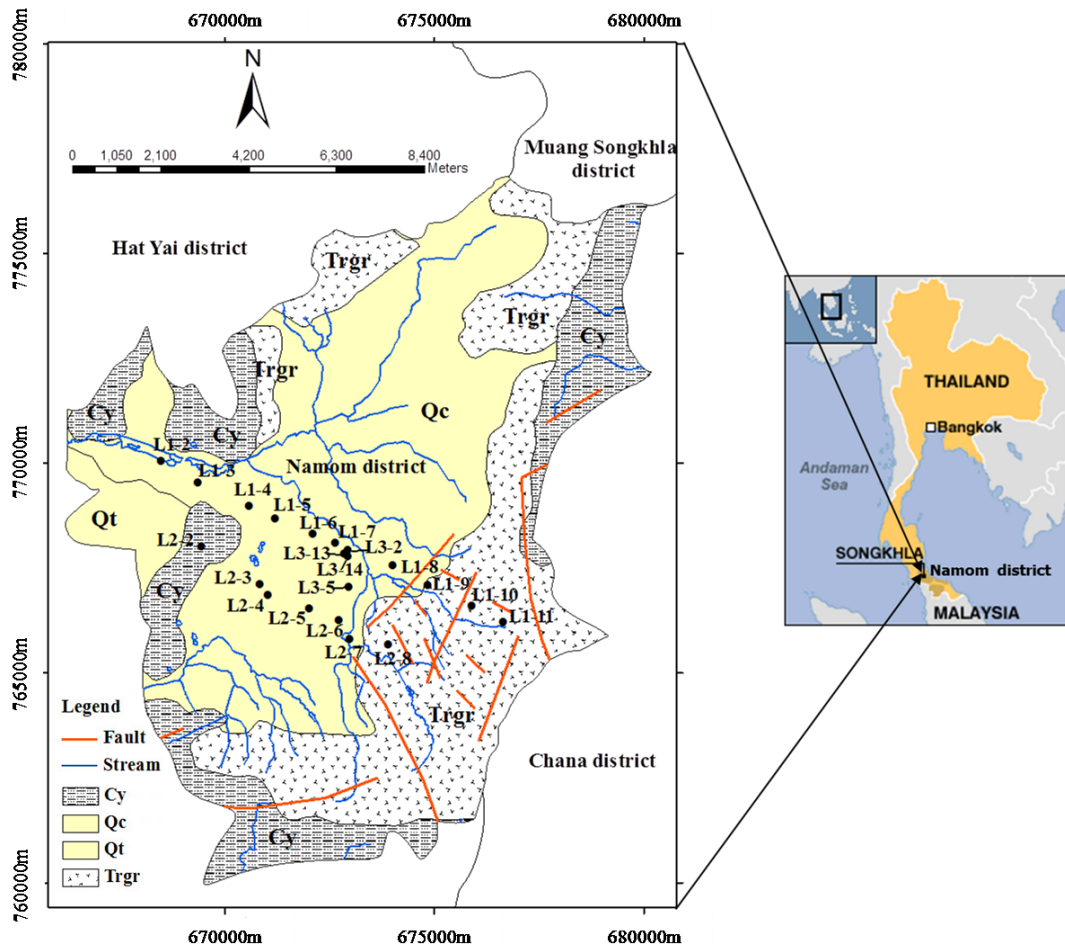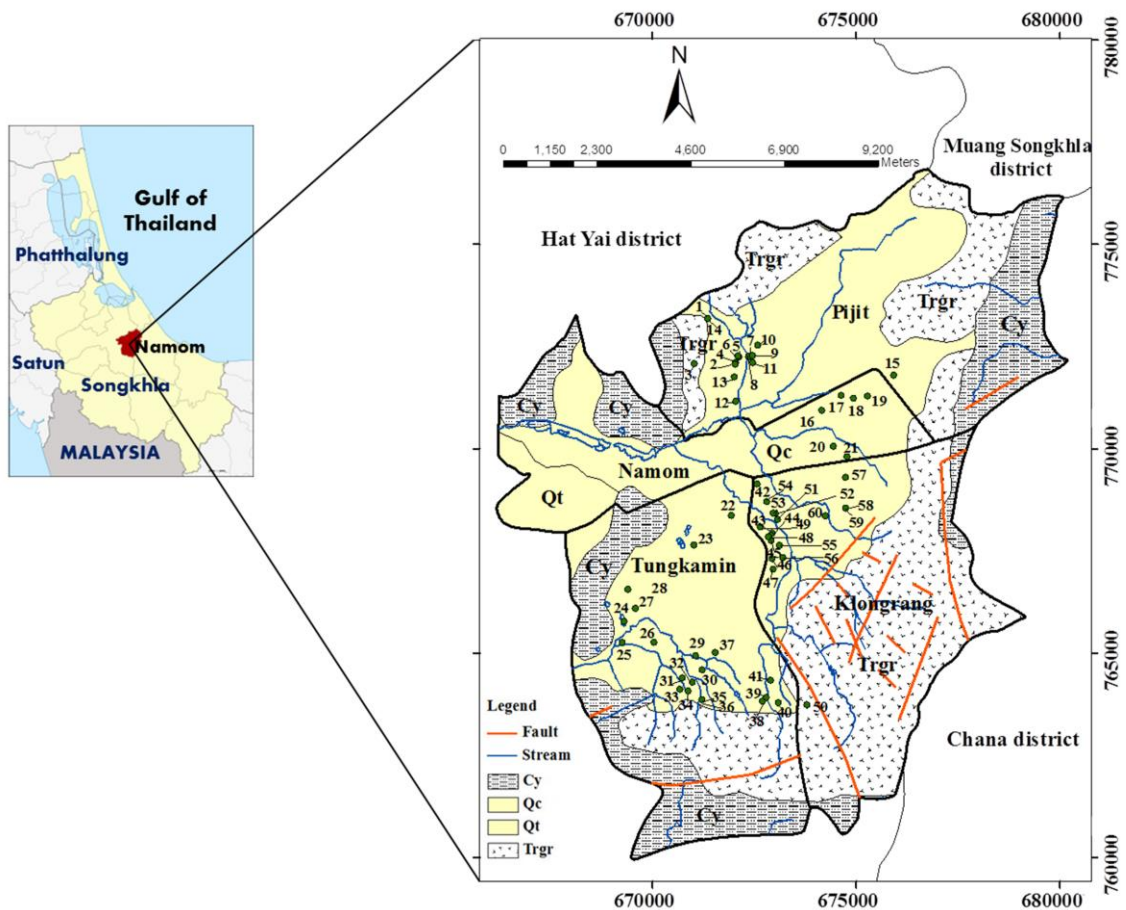

Figure 4.13   Sampling site locations on a simplified geologic map of Namom District, Songkhla province. Rock units include Trgr: Triassic Granite; Cy: Carboniferous shale; and Q: Quaternary sediment.

4.2.2.1 Radon concentration in well water samples

Totally 60 well water samples were collected from different sites in 4 sub-districts of Namom district, Songkhla province, Southern Thailand. Table 4.7 and Figures 4.13 show the radon concentrations varying across the 4 sub-districts.

A statistical summary of the radon concentrations in well water is given in Table 4.8. The mean ± SEM of radon concentration for each sub-district was 21.1 ± 10.7 Bq l^{-1} for Pijit, 13.9 ± 1.6 Bq l^{-1} for Namom, 16.9 ± 2.1 Bq l^{-1} for Tungkamin, and 62.1 ± 26.8 Bq l^{-1} for Klongrang; while the average across all measured samples was 32.0 ± 9.2 Bq l^{-1}. Fifteen out of the 20 well water samples (75%) from Tungkamin sub-district had radon concentrations exceeding the Maximum Contaminant Level for radon in drinking water (MCL = 11 Bq l^{-1}) reported by the US Environmental Protection Agency (USEPA,1999). Overall, approximately 63 % (38 samples) of the cases had radon concentrations above the MCL.

Table 4.7:   Concentration of ^{222}Rn in the 60 water samples collected from shallow wells in Namom district of Songkhla Province, Thailand.

Location Sub-district	Sample No.	Rn in water (Bq l^{-1})	SD (Bq l^{-1})	Location Sub-district	sample No.	Rn in water (Bq l^{-1})	SD (Bq l^{-1})
Pijit	1	20.49	1.29		31	15.75	2.21
(15 samples)	2	3.07	0.13		32	18.87	2.76
	3	2.63	0.22		33	14.70	1.00
	4	3.06	0.38		34	22.49	1.30
	5	8.30	0.70		35	19.45	0.32
	6	9.14	0.53		36	37.16	2.44
	7	26.24	1.33		37	24.06	2.06
	8	19.03	0.30		38	12.12	1.30
	9	11.30	0.64		39	33.72	3.56
	10	8.45	0.09		40	20.98	1.73
	11	4.17	0.09		41	19.58	1.91
	12	4.88	0.25	Klongrang	42	15.91	3.15
	13	7.76	2.34	(19 samples)	43	483.04	39.26
	14	169.00	3.50		44	64.80	0.80
	15	18.61	0.70		45	7.80	1.73
Namom	16	9.78	1.29		46	59.50	5.14
(6 samples)	17	13.94	1.33		47	4.55	0.64
	18	13.84	2.48		48	44.51	4.75
	19	9.63	1.38		49	40.53	11.39
	20	19.37	2.53		50	23.72	2.27
	21	16.57	1.33		51	67.11	14.60
Tungkamin	22	3.47	0.43		52	257.51	10.15
(20 samples)	23	11.09	1.80		53	1.53	0.64
	24	0.22	0.18		54	7.01	1.56
	25	9.39	0.70		55	37.60	4.59
	26	14.47	1.90		56	20.71	2.32
	27	15.96	2.70		57	17.90	1.30
	28	29.01	3.06		58	25.38	0.64
	29	9.89	0.58		59	0.05	0.09
	30	6.38	0.60		60	0.08	0.09

Table 4.8:   Statistical summary by sub-district of radon concentration in shallow well samples.

Location Sub-district	Number of samples	Average (SEM)* Bq l⁻¹	Min-Max Bq l⁻¹	E_{Inh} ** (μSv y⁻¹)	E_{ing}** (mSv y⁻¹)	% >11 Bq l⁻¹	% >32 Bq l⁻¹
Pijit	15	21.1 (10.7)	2.6-169.0	52.8	0.01	40.0	6.7
Namom	6	13.9 (1.6)	9.6-19.4	34.8	0.01	66.7	0.0
Tungkamin	20	16.9 (2.1)	0.2-37.2	42.3	0.01	75.0	10.0
Klongrang	19	62.1(26.8)	0.1-483.0	155.3	0.04	68.4	42.1
Namom district	60	32.0 (9.2)	0.1-483.0	80	0.02	63.3	18.3

*   SEM: The standard error of mean $= \frac{\sigma}{\sqrt{n}}$, σ : standard deviation, and n: number of samples

** E_{Inh} : Effective dose for inhalation; E_{ing} : Effective dose for ingestion
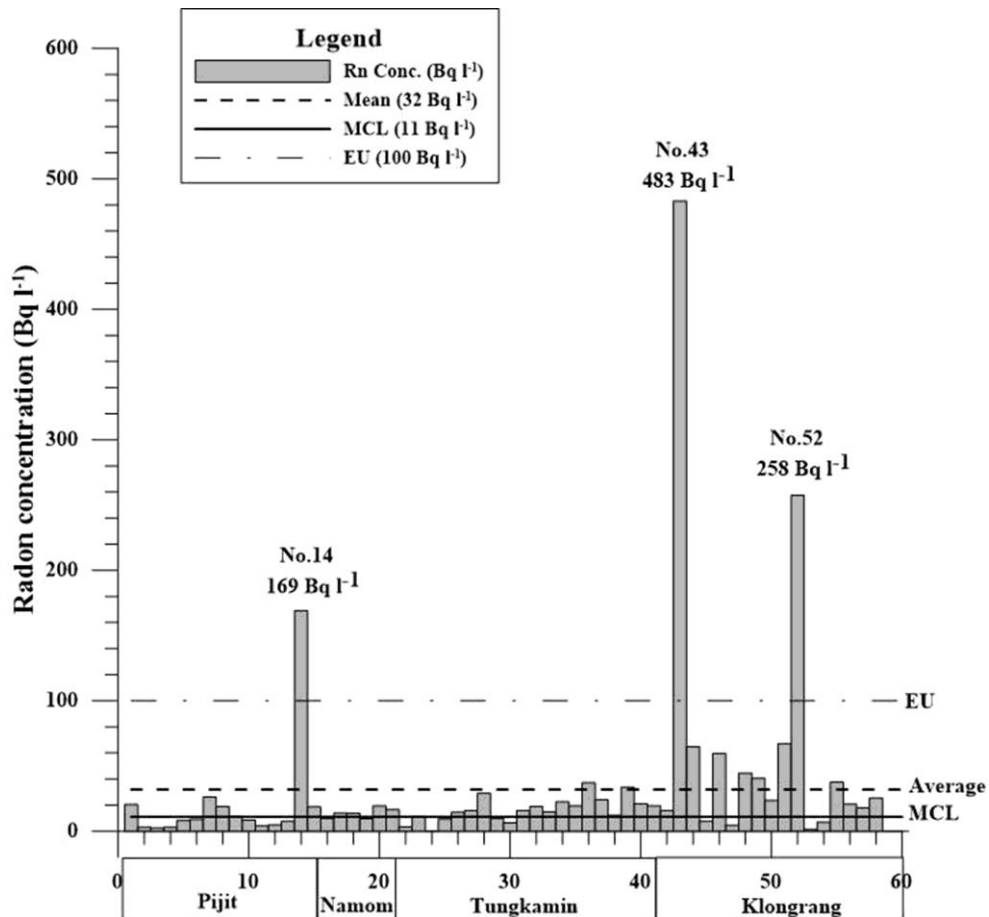
Figure 4.14   The distribution of radon concentrations in well water samples from Namom district, also showing the overall average and recommended limits with horizontal lines.

Further, in the results of Table 4.7 and Figure 4.14 it is of interest to note that the radon concentrations in well water samples No. 14 (169.0 ± 3.5 Bq l^{-1}), No. 43 (483.0 ± 39.3 Bq l^{-1}) and No. 52 (257.5 ± 10.2 Bq l^{-1}) were above the European Union Directive EC2013/51/EURATOM reference level of 100 Bq l^{-1}. Upon comparing the averages by the 4 sub-districts, the highest average was for Klongrang sub-district at 62.1 ± 26.8 Bq l^{-1}, with 42 % (8 of 19 well water samples) of cases having higher radon concentration than the average across all measured samples (32.0 ± 9.2 Bq l^{-1}), as shown in Table 4.8.

With respect to the annual effective dose received from drinking water consumption in Namom district, recalling the European Union Directive EC2013/51/EURATOM recommendations at 0.1 mSv y^{-1}, it can be seen from Table 4.8 that the annual effective dose from ingestion ranged from 0.01 mSv y^{-1} to 0.04 mSv y^{-1} with an average value of 0.02 mSv y^{-1}, and the annual effective dose from inhalation ranged from 0.03 mSv y^{-1} to 0.16 mSv y^{-1} with an average value of 0.08 mSv y^{-1}. Hence, in this study the total annual effective dose is estimated to equal 0.1 mSv y^{-1}. The dose due to inhalation of water-borne radon is higher than that from ingestion of drinking water, but does not exceed the recommended reference level of 0.1 mSv y^{-1} from drinking water consumption (EU Council Directive, 2013).

However, there are some controversies concerning human annual water intake in this study area. Because the Namom district area is in a tropical region and most of the population work in agriculture, 2 liters per day or 730 liters per year have been proposed as more realistic values by the International Commission on Radiological Protection (ICRP, 1996). When used with the average radon concentration of 32 Bq l^{-1} in the dose calculation according to Eq. (4.9), the effective dose from water ingestion becomes $E_{ing} = 10^{-8} \times 32 \times 730 = 0.0002$ Sv y^{-1} or 0.2 mSv y^{-1} that exceeds the recommended 0.1 mSv y^{-1} maximal dose. The total annual water intake is in general uncertain and should be adjusted for each individual study area.

In Table 4.9 the current results are compared to prior published similar studies, taking geological differences into consideration. On accounting for the geological differences there is reasonable concordance (Marques et al., 2006; Cosma et al., 2008; Tarim et al., 2012; Al-Zabadi et al., 2012). Because of a specific

geological characteristics of Namom district area is more complex of a series of faults and fractures in the granite bedrock, the migration of radon in ground water can occur through porous rocks or fractured rocks by advective transport (Ghasemizadeh et al., 2012). Therefore, the water originating from granitic basement tends to have high radon concentration along with other radionuclides in the uranium and thorium series (Tarim et al., 2012). The average radon concentration in well water of the current study area was also significantly higher than the MCL of 11 Bq l-1 set by USEPA (1999), as shown in Figure 4.14.

Table 4.9:   Literature curated radon concentrations in household water by country.

Region	Source	^{222}Rn Concentration (Bq l^{-1})	Reference
Italy	Well	12.7	(Kozłowska et al., 2009)
Brazil	Well	0.02-112.50(15.4)	(Bonotto, 2014)
Pakistan	Well	0.67-1.45(1.21)	(Nasir & Shah, 2012)
Malaysia (Sungai Petani)	Well	12.4-17 (14.7)	(Ahmad et al., 2015)
	Tap	2.7-7.0 (5.37)	
Romania	Well	5.6-35 (18.5)	(Nita et al., 2013)
	Tap	1.2-4.5 (2.5)	
	Spring waters	10.2-68.9 (22.7)	
China	Ground water	0.71-3735 (229.4)	(Zhuo et al., 2001)
	Tap	8-18(12)	(Xinwei, 2006)
Ghana	Well	8.1	(Darko et al., 2010)
India	Well	2.1	(Somashekar & Ravikumar, 2010)
	Tap	6.44-8.36 (7.35)	(Shivakumara et al., 2014)
Turkey	Well	1.42-53.64	(Tarim, 2012)
	Tap	0.91-12.58	
Jordan	Tap	2.5-4.7	(Al-Bataina et al., 1997)
Palestine	Well	2.9-23.4(9.5)	(Al-Zabadi et al., 2012)
	Spring waters	1.5-9.9 (4.6)	
Mexico	Well	1.78-39.75	(Villalba et al., 2005)
Thailand (Namom)	Well	0.05-483.04 (32)	(This study)

An important aspect of the high radon concentration is that it is hazardous to human health if the populace consumes the well water without any treatment. When household water is used for showering, laundry, washing, and cooking, radon and its progeny can be released, with contributions from spray water. This radioactive gas enters the human body through ingestion and inhalation of indoor air. Therefore, the radon in water is probably the major source of radiation doses to

stomach and lungs. So, the inhabitants of Namom district have comparatively high cancer risk due to consuming well water with high radon concentration. This agrees with the report by Hirunwatthanakul et al. (2006), who suggested, based on the uranium and radium being significant components in the granite rock, that people in the Namom area are exposed to radiation-contaminated drinking water, which is likely to increase the risk of developing cancer.

CHAPTER 5

CONCLUSION AND RECOMMENDATION

Based on the results and discussion presented in previous chapters, the conclusions can be drawn:

5.1 Conclusions regarding radon observations in soil gas as a possible earthquake precursor

During the period of this work, the objective was to conduct a daily study of a possible correlation between radon concentration in soil gas in ST-10, Muang district, Phang Nga Province, in relation to the 210 earthquakes of moment magnitude $M_w \geq 4$, reported by ANSS (Advanced National Seismic System) of NCEDC (Northern California Earthquake Data Center) on the website http://www.ncedc.org/anss/catalog-search.html. The earthquakes were selected only in the target area in the Andaman Sea and the Indian Ocean, where the maximum of epicentral distance from radon measuring stations was a distance of 855 km. Between July 1, 2009 and June 30, 2010, 210 earthquake events were recorded as follows.

- o $4 \leq M_w < 5$, 150 events

- o $5 \leq M_w < 6$, 55 events

- o $6 \leq M_w < 7$, 2 events

- o $7 \leq M_w < 8$, 3 events

In summary, the radon peak anomaly can be used as a possible earthquake precursor with the earthquake $M_W \geq 4$. It is a 67.3 % possibility that 1 peak of radon anomaly has at least 1 earthquake event that follows. In the remaining 30.7 %, not even one event of an earthquake of $M_w \geq 4$ occurred after the radon peak anomaly.

Additionally, each radon peak anomaly that is not an earthquake precursor can be caused by the following:

(1) a measurement of $M_w < 4$

(2) being a post seismic anomaly

(3) exclusion from the observation area

5.2   Conclusions regarding the health effect of radon exposure in Namom district

5.2.1   A possible correlation between soil radon concentration and radium content in soil samples and assess the potential radiological hazards

The results indicate that the study area under investigation has significantly high activity concentration of radon. It has been also found to have a high radium content. The correlation between soil gas radon concentration and soil sample radium content shows a positive correlation coefficient (R^2 = 0.72), whilst the present average values of the activity concentration of ^{226}Ra, ^{232}Th and ^{40}K obtained in the soil samples are higher than the world average for the region under consideration (UNSCEAR 2008).

In terms of evaluation, the natural radiation hazard indices confirm high levels of the natural radionuclides in this study area when compared with the various world averages and the recommended values. Significantly, this result indicated that the high radiation exposure is likely to cause additional radiological health risks to the population in the study area. Health effects of radiation released as a result of the investigation remain as a concern.

5.2.2   Radon concentration in well water collected from Namom district: a factor influencing cancer risk?

The present study found that household drinking water sampled from the Namom district of Songkhla province, Thailand, had ^{222}Rn concentrations exceeding the MCL recommended by the USEPA, and above 100 Bq l^{-1}, which is the safe limit in European Union Directive EC2013/51/EURATOM laying down requirements for protecting the public against exposure to radon in drinking water

supplies. Such hazardous levels were observed from well No. 14 (in Pijit sub-district), well No. 43 (in Klongrang sub-district) and well No. 52 (in Klongrang sub-district). Measures should be taken to reduce the radon concentration in consumed water. It is also important to periodically monitor the radon gas levels inside dwellings near the radon releasing rock complexes. The obtained data was used to estimate the total annual effective doses from radon in well water, clearly concluding with estimates greater than the permissible limit (0.1 mSv y^{-1}) recommended by the European Union Directive EC2013/51/EURATOM. The total annual water intake for this study area was estimated as 2 liters per day or 730 liters per year, which affects the exposure estimates.

For comprehensive health risk reduction, it is recommended to look at technical education on reduction techniques and ventilation methods. Regarding reduction of the ^{222}Rn concentrations in drinking water, granular activated carbon systems (GAC) have fine porous materials that trap and hold the radon, but these can easily be clogged by sediments or other contaminants in the water. Concerning the ventilation, spray aeration applies a nozzle spray in the storage tank. The high specific surface and short diffusion distance of the spray droplets allows radon gas to exit from the water, while air blowers vent out the released radon gas (Swistock, 2016).

In the future, it might be possible to continuous monitoring radon gas in the study area of Namom district, Songkhla province as a possible method for earthquake warning, which is comparable to the site selection in ST-10 in Phang Nga province.

REFERENCES

Ahmad, N., Jaafar, M.S., and Alsaffar, M.S. 2015. Study of radon concentration and toxic elements in drinking and irrigated water and its implications in Sungai Petani, Kedah, Malaysia. J Radiat Res Appl Sci. 8: 294-299.

Al-Bataina BA, Ismail AM, Kullab MK, Abumurad KM, Mustafa H (1997) Radon measurements in different types of natural waters in Jordan. Radiat Meas. 28: 591-594.

Alharbi, W.R., and Abbady, A.G.E. 2013. Measurement of radon concentration in soil and the extent of their impact on the environment from Al-Qassim, Saudi Arabia. Natural Science. 5(1): 93-98.

Al-Tamimi, M.H., and Abumurad, K.M. 2001. Radon anomalies along faults in North of Jordan. Radiation Measurements. 34: 397-400.

Alter, W.H., and Fleischer, R.L. 1981. Passive integrating radon monitor for environmental monitoring. Health Physics. 40: 693-697.

Al-Zabadi, H., Musmar, S., Issa, S., Dwaikat, N., and Saffarini, G. 2012. Exposure assessment of radon in the drinking water supplies: a descriptive study in Palestine. BMC Res Nots. 5(29): 1-8.

Atiphan, S. 2007. Boundary Delineation of high Background Radiation Area in Amphoe Namom Changwat Songkhla using Gamma-Ray Measurmaent. Master of Science Thesis in Geophysics, Prince of Songkla University, Hatyai, Thailand.

Baykara, O., and Doğru, M. 2006. Measurements of radon and uranium concentration in water and soil samples from East Anatolian Active Fault Systems (Turkey). Radiation. Measurement. 41, 362-367.

BEIR VI, 1999. Report of the Committee on the Biological Effects of Ionizing Radiation, Health effects of exposure to radon, National Research Council, The National Academies Press.

Bem, H., Plota, U., Staniszewska, M., Bem, E.M., and Mazurek, D. 2014. Radon (^{222}Rn) in underground drinking water supplies of the Southern Greater Poland Region. J Radioanal Nucl Chem. 299: 1307-1312.

Bhongsuwan, T., Chittrakarn, T., Chongkum, S., Polapongs, P., Sirijarukal, S, Thitipornpan, A., Wattanavatee, K., and Wutthisasna, J. 2001. Radon risk assessment, indoor/outdoor to public communities in Songkhla Lake Basin. In: Proceedings of the 8th Nuclear Science and Technology Conference., Bangkok, Thailand, June 20-21, 2001: 757-768.

Bilham, R. 2005. A Flying Start, Then a Slow Slip. Science. 308: 1126-1127.

Bodansky, D., Robkin, M.A., and Stadler D.R. 1987. Indoor Radon and Its Hazards. University of Washington Press: USA.

Bonotto, D.M. 2014. ^{222} Rn, ^{220} Rn and other dissolved gases in mineral waters of southeast Brazil. J Environ Radioact. 132: 21-30.

Brill, A.B.1994. Radon Update. The Journal of Nuclide Medicine. 35, 2.

Garson, M.S., Young, B., Mitchell, A.H.G. and Tait, B.A.R. 1975. Geological map of Phuket/Phannga/Krabi, 1:125,000. In: Garson, M.S., Young, B., Mitchell, A.H.G. and Tait, B.A.R., the geology of the tin belt in Peninsular Thailand around Phuket, Phangnga, and Takua Pa. In: Overseas Memoir of the Institute of Geological Sciences. 1:112.

CGS, 2008. California Geological Survey [online]. Available from: http://206.170.189.143/CGS/minerals/hazardous_minerals/radon/index.htm [3 June 2008].

Chyi, L.L., Chou, C.Y., Yang, F.T., and Chen, C.H. 2001. Continuous radon measurements in faults and earthquake precursor pattern recognition. Western Pacific Earth Science. 2: 227-246.

Cosma, C., Moldovan, M., Dicu, T., and Kovacs, T. 2008. Radon in water from Transylvania (Romania). Radiat Meas. 43: 1423 – 1428.

Cothern, C.R., James, E., and Smith, Jr. 1987. Environmental Radon. Plenum Press: New York.

Cummins, P., and Leonard, M. 2004. Small Threat but Warning Sounded for Tsunami Research. AUSGEO News, 75: (September).

Dangmuan, S. 2008. Seismic study of Southern Thailand after the 26 December 2007 Sumastra Andaman Earthquake. Master of Science Thesis in Geophysics, Prince of Songkla University, Hatyai, Thailand.

Darko, E.O., Adukpo, O.K., Fletcher, J.J., Awudu, A.R., and Otoo, F. 2010. Preliminary studies on Rn-222 concentration in ground water from selected areas of the Accra metropolis in Ghana. J Radioanal Nucl Chem. 283: 507-512.

David Suzuki Foundation. 2015. Revisiting Canada's Radon Guideline. [online]. Available from: http://www.davidsuzuki.org/publications/downloads/2015/revisiting_canadas_radon_guideline.pdf.

DMR, 1989. Thailand nationwide airborne geophysical survey: Bangkok, Department of Mineral Resources.

DMR, 2005. Geological map of Thailand, scale 1:2,500,000.

Duerrast, H, Dangmuan, S. and Lohawijarn, W. 2007. Khlong Marui and Ranong Fault Zones in Southern Thailand Re-Activated The 26 December 2004 M_w 9.3 Sumatra- Andaman Earthquake. GEOTHAI'07 International Conference on Geology of Thailand: Towards Sustainable Development and Sufficiency Economy. pp.141-144.

Duggal, V., Mehra, R., and Rani, A. 2013. Determination of ^{222}Rn level in groundwater using a Rad7 detector in the Bathinda district of Punjab. Radiat Prot Dosim. 156(2):239-245.

Durrani, S.A., and Ilíc, R., 1997. Radon Measurements by Etched Track Detectors. World Scientific Publishing Co. Pte. Ltd, Singapore.

Durridge Company, Inc. 2012. RAD7-RAD H_2O. Radon in Water Accessory, Owner's Manual.

Einarssón, P., Theodórsson, P., Hjartardóttir, A.R., and Guðjónsson, I.G. 2008. Radon Changes Associated with the Earthquake Sequence in June 2000 in the South Iceland Seismic Zone. Pure and Applied Geophysics. 165: 63-74.

Etiope, G., and Martinelli, G. 2002. Migration of carrier and trace gases in the geosphere: an overview. Physics of the Earth and Planetary Interiors. 129: 185-204.

EU (European Union), 2013. Council Directive 2013/51/EURATOM of 22 October 2013. Laying down requirements for the protection of the health of the general public with regard to radioactive substances in water intended for human consumption. Off J Eur Commun 2013:L296:12-21.

European Commission. 1999. Radiation protection 112, radiological protection principles concerning the natural radioactivity of building materials. Directorate-General Environment, Nuclear Safety and Civil Protection.

Friedmann, H., 1991: Continuous spring water radon measurement in Austria and possible relations to earthquakes. Inter. Conf. on Earthquake Prediction, Strasbrourg, France.

Ghasemizadeh, R., Hellweger, F., Butscher, C., Padilla, I., Vesper, D., Field, M., and Alshawabkeh, A. 2012. Review: Groundwater flow and transport modeling of karst aquifers, with particular reference to the North Coast Limestone aquifer system of Puerto Rico. Hydrogeol J. 20(8): 1441-1461.

Ghosh, D., Deba, A., Sengupta, R., Patraa,K.K., and Bera, S., 2007. Pronounced soil-radon anomaly-Precursor of recent earthquakes in India. Radiation Measurements, 42, pp, 466- 471.

Hanks, T., and Kanamori, H. 1979. A moment magnitude scale, J. Geophys. Res. 84, 2348–2350.

Harris, R.C., and Pearthree, P.A. 2002. A home buyer's guide to geologic hazards in Arizona. Ariz. Geol. Surv. Down-To-Earth 13, 1-36 [online] Available from : http://www.azgs.az.gov/HomeOwners-OCR/home_buyers_guide_2002_full. pdf.

Hauksson, E., and J. G. Goddard, 1981: Radon earthquake precursor studies in Iceland. J. Geophys. Res., 86, pp7037-7054, doi: 10.1029/JB086iB08p07037.

Hinkle, M. 1994. Environmental conditions affecting concentrations of He, CO2, O2 and N2 in soil gases, Appl Geochem 9:53-63.

Hirunwatthanakul, P., Sriplung, H., Geater, A. 2006. Radium-Contaminated Water: a Risk Factor for Cancer of the Upper Digestive Tract. Asian Pacific J Can. Prevent. 7:295-298.

HPS: Health Physics Society. Specialists in radiation safety. Founded 1956 update 2008 http://hps.org.

IAEA, 1996. Basic safety standards for protection against ionizing radiation and for safety of radiation sources. Safety series No 115. IAEA, Vienna.

ICRP, 1996. Age-dependent doses to members of the public from intake of radionuclides: Part 5. Compilation of ingestion and inhalation dose coefficients (ICRP Publication 72), Pergamon Press, Oxford.

Inceoz, M., Baykara, O., Aksoy, E., and Dogru, M., 2006. Measurements of soil gas radon in active fault systems: A case study along the North and East anatolian fault systems in Turkey. Radiation Measurements, 41, pp. 349–353.

Ishihara, S., Sawata, H, Shibata, K., Terashima, S., Arrykul, S., Sato, K. 1980. Granites and Sn-W deposits of peninsular Thailand. In: Mining Geol. Spec. Issue, 8, Japan.

Jónsson, S., and Einasson, P. 1996. Radon anomalies and earthquakes in the South Iceland Seismic Zone 1977–1993. In Seismology in Europe (ed. Thorkelsson, B. et al.), European Seismology. Commission, Reykjavıˊk, pp. 247–252.

Kakati, R.K., Kakati, L., and Ramachandran, T.V. 2013. Measurement of uranium, radium and radon exhalation rate of soil samples from Karbi Anglong district of Assam, India using EDXRF and Can technique method. APCBEE Procedia. 5: 186-191.

Khan, M.S., Srivastava, D.S, Azam, A. 2012. Study of radium content and radon exhalation rates in soil samples of northern India. Environ Earth Sci doi:10.1007/s12665-012-1581-7.

Kozłowska, B., Morelli, D., Walencik, A., Dorda, J., Altamore, I., Chieffalo, V., Giammanco, S., Immè, G., and Zipper, W. 2009. Radioactivity in waters of Mt. Etna (Italy). Radiat Meas. 44: 384-389.

Kromkhun, K. 2010. Petrogennesis of High Heat Producing Granite: Implication for Mt Painter Province, South of Australia. Ph.D. thesis in Geology and Geophysics, Faculty of Science, University of Adelaide.

Lay, T., Kanamori, H., Ammon, C.J., Nettles, M., Ward, S.N., Aster, R.C., Beck, S.L., Bilek, S.L., Brudzinski, M.R., Butler, R., DeShon, H.R., Ekström, G., Satake, K., and Sipkin, S. 2005. The Great Sumatra-Andaman Earthquake of 26 December 2004. Science 308: 1127-1133.

Mahur, A.K., Kumar, R., Sonkawade, R.G., Sengupta, D., and Prasad, R. 2008. Measurement of natural radioactivity and radon exhalation rate from rock

samples of Jaduguda uranium mines and its radiological implications. Nucl Instrum Methods Phys Res B 266:1591-1597.

Markkanen, M., and Arvela, H. 1992. Radon emanation from soil. Radiat Protect Dosim. 45: 269-272.

Marques, A.L., Geraldo, L.P., Santos, and W. 2006. Levels of natural radon-radioactivity in the São Vicente, SP, rock massif. Radiol Bras. 39(3): 1-8.

Mose, D.G., Mushrush, G.W., and Chrosinak, C. 1990, Radioactive hazard of potable water in Virginia and Maryland: Bulletin of Environmental Contamination andToxicology.44(4): 508-513.

Mullinger, N.J., Binley, A.M., Pates, J.M., and Crook, N.P. 2007. Radon in Chalk streams: Spatial and temporal variation of groundwater sources in the Pang and Lambourn catchments, UK. Journal of Hydrology. 339:172– 182.

Najam, A.L, Younis, A.S., and Kithah, H.F. 2015. Natural radioactivity in soil samples in Nineveh Province and the associated radiation hazards. Int J Phy. 3(3): 126-132.

Nasir, T., and Shah, M. 2012. Measurement of annual effective doses of radon from drinking water and dwellings by CR-39 track detectors in Kulachi city of Pakistan. J Basic Appl Sci. 8: 528-536.

Nazaroff, W.W., and Nero, A.V. 1988. Radon and Decay Products in Indoor Air. Wiley, New York.

NCEDC, (Northern California Earthquake Data Center) on the website http://www.ncedc.org/anss/catalog-search.html.

NCRP, 1987. Report No. 93. Ionizing radiation exposure of the population of the United States

Nevada radon education program, University of Nevada Cooperative Extension. How radon gets into home. [online]. Available from: https://www.unce.unr.edu/pro grams/sites/radon/homes/.

Ni, S., Kanamori, H., and Helmberger, D. 2005. Energy radiation from the Sumatra earthquake. Nature 434: 582.

Nita, D.C., Moldovan, M., Sferle, T., Ona, V.D., and Burghele, B.D. 2013. Radon concentrations in water and indoor air in north‐west regions of Romania. Rom Journ Phys. 58: S196–S201.

Nutalaya, P., Sodsri, S., and Arnold, E.P. 1985. Seismicity Data of Thailand and Adjacent Areas. (Part B) in Arnold, E.P. (ed.) Thailand, Series on Seismology Volume II, Southeast Asia Association of Seismology and Earthquake Engineering, 403 pp, ISBN 974-8202-13-5.

Nutlaya, P., and S. Sodsri 1984. Earthquake Data of Thailand and Adjacent Areas Supplementary data, The Asian Institute of Technology, Bangkok, Thailand.

Ortiz, M., and Bilham, R. 2003. Source area and rupture parameters of the 31 December 1881 Mw = 7.9 Car Nicobar earthquake estimated from tsunamis recorded in the Bay of Bengal. Journal of Geophysical Research 108 (B4) 2215http://cires.colorado.edu/~bilham/Andaman.pdf.

Papp, B., Deak, F., Horvath, A., Kiss, A., Rajnai, G., Szabo, Cs. 2008. A new method for the determination of geophysical parameters by radon concentration measurements in borehole. Journal of Environmental Radioactivity, 99(11): 1731-1735.

Petersen, M.D., Dewey, J., Hartzell, S., Mueller, C., Harmsen, S., Frankel, A.D., and Rukstales, K. 2004. Probabilistic seismic hazard analysis for Sumatra, Indonesia and the Southern Malaysian Peninsula. Tectonophysics, 390, pp 141-158.

Pisapak, P. 2009. Preliminary Monitoring of the Change of Soil Gas Radon for Earthquake Pre- warning in the Khlong Marui Fault Zone. Master of Science Thesis in Geophysics, Prince of Songkla University, Hatyai, Thailand.

Planiníc, J., Radolíc, V., and Lazanin, Ž. 2001. Temporal variations of radon in soil related to earthquakes. Applied Radiation and Isotopes. 55: 267–272.

Planinic, J., Radolic, V., and Vukoric, V., 2004. Radon as an earthquake precursor. Nuclear Instruments and Methods in Physics Research A 530, pp. 568–574 .

Poobrasert, S. 1987. Country Report on Earthquake Preparedness in Thailand, Report on Geodetic and geophysical Activities of the Thai National Committee on Geodesy and Geophysics period 1983-1986, Paper Subrnitted by the Royal Thai Survey Department, Thailand.

Porstendörfer, J. 1993. Properties and behaviour of radon and thoron and their decay products in the air. Proceedings of the Fifth International Symposium on the

Natural Radiation Environment, Tutorial Session. Luxembourg, Belgium pp 73-139.

Pungrassami, T. 1984. Tin mineralization of the Thung Pho-Thung Khamin District Changwat Songkhla, Prince of Songkla University, Thailand.

Ristoiu, D., Cosma, C., Ristoiu, T., and Miles, J. 1996. Radon mitigation in soils. Symposium on Radiation Protection in Neighbouring Countries in Central Europe-1995, Proceedings, Portorož, Slovenia, September 4-8,1995, Ed. By Denis Glavič-Cindro, p.119-122.

Rizzo, S., Brai, M., Basile, S., Bellia, S., and Hauser, S. 2001. Gamma activity and geochemical features of building materials: estimation of gamma dose rate and indoor radon levels in Sicily. Appl Radiat Isot. 55: 259-265.

SARAD GmbH, 2007. User Manual RTM 1688-2 Version 12/2007, Germany.

Sciarra, A., Cantucci, B., Buttinelli, M., Galli, G., Nazzari, M., Pizzino, L., and Quattrocchi, F. 2012. Soil-gas survey of liquefaction and collapsed caves during the Emilia seismic sequence. Ann Geophys 55(4): 803-809.

Scordilis, E.M., 2006. Empirical global relations converting M_S and m_b to moment magnitude. J. Seismol. 10: 225-236. DOI: 10.1007/s10950-006-9012-4.

Sharma, D.K,, Kumar, A., Kumar, M., and Singh, S. 2003. Study of uranium, radium and radon exhalation rate in soil samples from some areas of Kangra district, Himachal Pradesh, India using solid-state nuclear track detectors. Radiat Meas 36:363-366.

Shivakumara, B.C., Chandrashekara, M.S., Kavitha, E., and Paramesh, L. 2014. Studies on [226]Ra and 222Rn concentration in drinking water of Mandya region, Karnataka State. India. J Radiat Res Appl Sci. 7: 491- 498.

Singh, H., Singh, J., Singh, S., and Bajwa, B.S. 2008. Radon exhalation rate and uranium estimation study of some soil and rock samples from Tusham ring complex, India using SSNTD technique. Radiat Meas. 43: 459-462.

Singh, S., Rani, A., and Mahajan, R.K. 2005. [226]Ra, [232]Th and [40]K analysis in soil samples from some areas of Punjab and Himachal Pradesh, India using gamma ray spectrometry. Radiat Meas. 39: 431-439.

Sirijarukul, S. 1994. A measurement of U-238 in rocks in Songkhla, Phatthalung and Pattani province. Physics project, Faculty of Science, Prince of Songkla University, Hat Yai.

Somashekar, R.K., and Ravikumar, P. 2010. Radon concentration in groundwater of Varahi and Markandeya river basins, Karnataka State, India. J Rad Nucl Chem. 285: 343-351

Stein, S., and Okal, E.A. 2005. Size and speed of the Sumatra earthquake. Nature, 434, 581–582.

Sumesh, C.G., Vinod, K.A., Tripathi, R.M., and Puranik, V.D. 2011. Thoron interference test of different continuous passive radon monitors. Radiat Protect Environ 34(4): 257-261.

Swistock, B. 2016. Reducing Reducing Radon in Drinking Water, The Pennsylvania State University:Penn State Cooperative Extension. Available at: http://extension.psu.edu/natural-resources/water/drinking-water/water-testing/pollutants/reducing-radon-in-drinking-water

Tapponnier, P., Peltzer, G., Armijo, R. 1986. On the mechanics of the collision between India and Asia. In: Coward, M.P., Ries, A.C. (Eds.), Collision Tectonics. Geological Society Special Publication. 19: pp 115–157.

Tarim, U.A, Gurler, O., Akkaya, G., Kilic, N., Yalcin, S., Kaynak, G., and Gundogdu, O. 2012. Evaluation of radon concentration in well and tap waters in Bursa, Turkey, Radiat. Prot Dosim. 150(2): 207-212.

Taskin, H., Karavus, M., Ay, P., Topuzoglu, A., Hidiroglu, S., and Karahan, G. 2009. Radionuclide concentration in soil and lifetime cancer risk due to the gamma radioactivity in Kirklareli, Turkey. J Environ Radioact. 100:49-53.

Toscani, L., Martinelli, G., Dalledonne, C., Gadidolfi, L., Ortalli, I., Sogni, R., Vaccari, S., and Venturelli, G. 2001. Radon in underground waters of Northern Apennines as determined by four different analytical methods. Proceedings 5th International Conference on Rare Gas Geochemistry (Eds. I Hunyadi, I ceige and J Hakl) Hungary, 321-328.

Ulamov, V.I. and Mavashev, B.Z. 1967. On fore – runners of a strong tectonic earthquakes. Dokl. USSR Academy of Science. 176: 319-322

UNSCEAR, 1988. United Nations Scientific Committee on the Effects of Atomic Radiation. Report of the General Assembly, New York, United Nations.

UNSCEAR, 2000. United Nation Scientific Committee on the Effect of Atomic Radiation. Sources and Effects of Ionizing Radiation. Report to General Assembly, with Scientific Annexes, New York, United Nation.

UNSCEAR, 2008. United Nation Scientific Committee on the Effect of Atomic Radiation. Sources and Effects of Ionizing Radiation. Report to General Assembly, with Scientific Annexes, New York, United Nation

USEPA, 1999. United States Environmental Protection Agency. National primary drinking water regulations for radon-222. EPA 815-F-99-009. U.S. Government Printing Office, Washington, DC.

USEPA, 2001. Radon in Drinking Water: Question and Answers, US Environmental Protection Agency. Washington, D.C.

USGS, 2005. Summary of Magnitude 9.0 Sumatra-Andaman Islands Earthquake & Tsunami Sunday, December 26, 2004 at 00:58:53 UTC [online]. Available from:http://neic.usgs.gov/neis/bulletin/neic_slav_ts.html.

Vigny, C., Simons, W.J.F., Abu, S., Bamphenyu, R., Satirapod, C., Choosakul, N., Subarya, C., Socquet, A., Omar, K., Abidin, H.Z., and Ambrosius, B.A.C. 2005. Insight into the 2004 Sumatra−Andaman earthquake from GPS measurements in southeast Asia. Nature 436: 201-206 [online]. Available from:http://www.nature.com/nature/journal/v436/n7048/full/nature03937.html

Villalba, L., Colmenero Sujo, L., Montero Cabrera , M.E., Cano Jiménez, A., Rentería Villalobos, M., Delgado Mendoza, C.J., Jurado Tenorio, L.A., Dávila Rangel, I., and Herrera Peraza, E.F. 2005. Radon Concentrations in Ground and Drinking Water in the State of Chihuahua, Mexico. J Environ Radioact. 80: 139-151.

Wang, Z. 2002. Natural radiation environment in China. Int Congr Ser. 1225: 39-46.

Watkinson, I., Chris, E., and Hall, R. 2008. The kinematic history of the Khlong Marui and Ranong Faults, southern Thailand. Structural Geology. [Online]. Available from:http://doi:10.1016/j.jsg.2008.09.001.

Wattananikorn, K., Kanaree, M. and Wiboolsake, S. 1998. Soil gas radon as an earthquake precursor: some considerations on data improvement. Radiation Measurements. 29: 593-598.

Wutthisasna, J., Chittrakarn. T., Bhongsuwan, D., Bhongsuwan, T. 2006. Concentration of Ra-226 in shallow well water and its relation with the evidence of oral and esophagus cancers in Namom District. Songkhla Province. Songklanakarin J Sci Technol. 28:201-215.

Xinwei, L. 2006. Analysis of radon concentration in drinking water in Baoji (China) and the associated health effects. Radiat Prot Dosim. 121(4): 452-455

Zhuo, W., Iida, T., and Yang, X. 2001. Occurrence of ^{222}Rn, ^{226}Ra, ^{228}Ra and U in groundwater in Fujian Province, China. J Environ Radioact. 53: 111-120.

APPENDICES

APPENDIX A
RADON DATA

APPENDIX A1

THE NUCLEAR TRACK-ETCHED
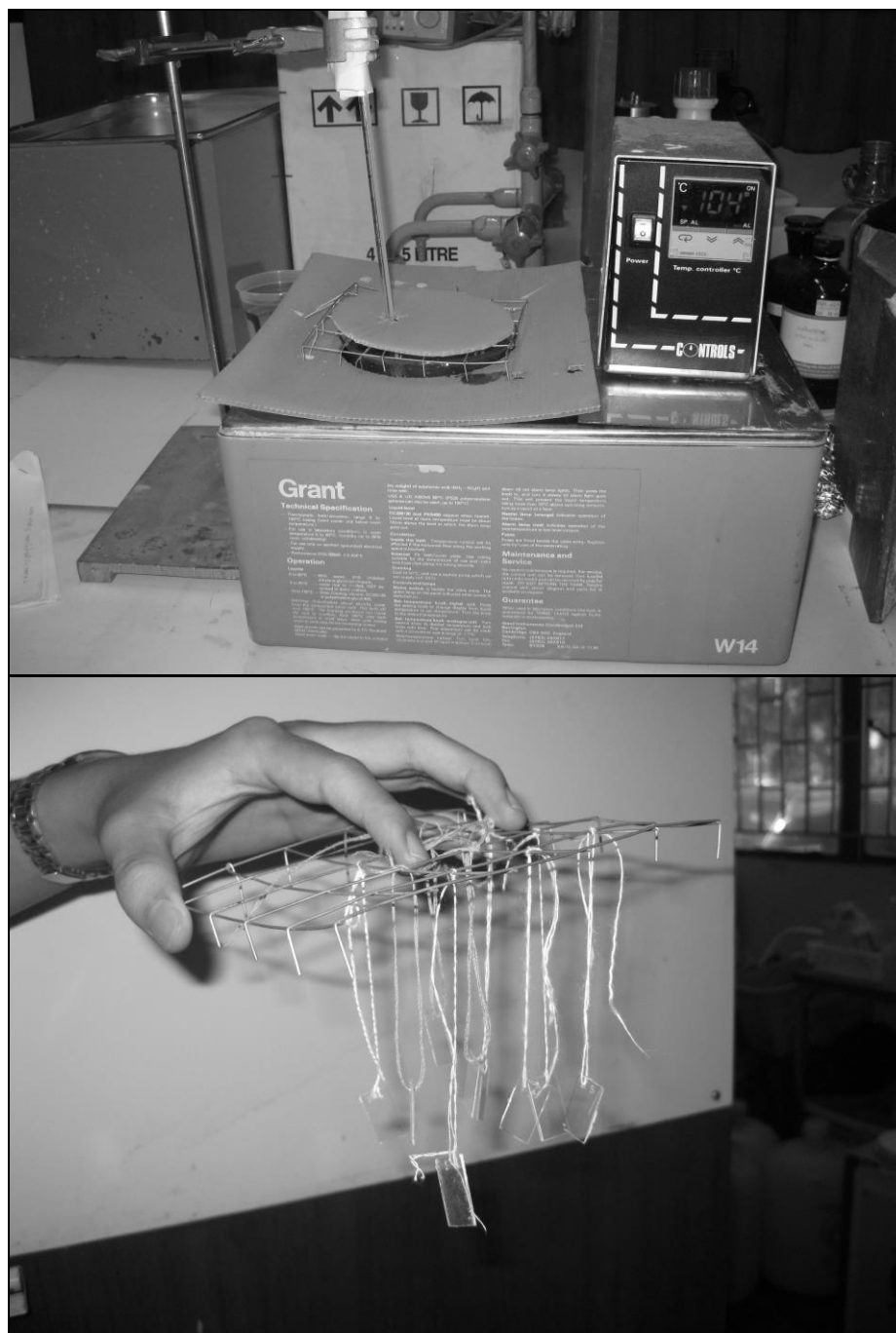
Figure A1.1   Water bath (Grant- W14) setup of the nuclear track-etched detector.
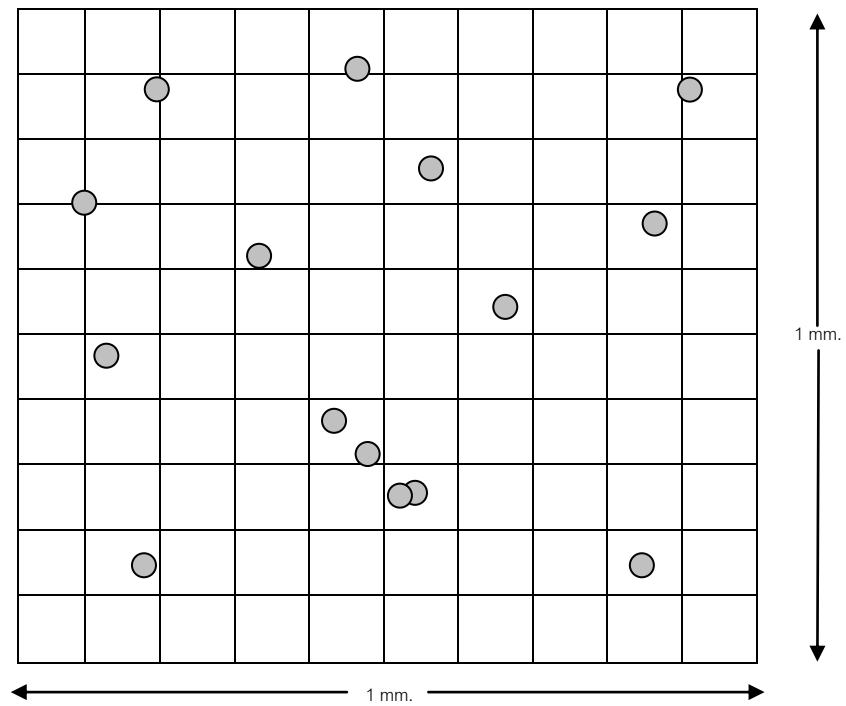
Figure A1.2   Schematic sketch of a frame of 1 mm ^{2} with a 10x10 raster for counting apparent density of the tracks using an optical microscope.

Figure A1.3   Counting tracks by using an optical microscope (OLYMPUS-BHC) at magnifications 10x10 (x100).

APPENDIX A2

DATA OF ALPHA TRACK RADON CONCENTRATION IN SOIL GAS

Table A2.1: The daily data of alpha track radon concentrations (kBq m^{-3}) at station ST-10 was observed in Phang Nga Province over a three months from July 1 to September 30, 2009.

Date	July 09		August 09		September 09	
	Rn_Conc.	SD.Er.	Rn_Conc.	SD.Er.	Rn_Conc.	SD.Er.
1	866.12	7.23	1257.07	5.33	156.67	1.12
2	868.25	3.38	1358.26	6.94	303.68	1.20
3	2356.39	6.95	1389.16	4.52	922.58	2.72
4	-	-	1639.49	7.46	2508.72	7.31
5	1053.61	3.33	1609.66	5.32	1034.43	3.36
6	987.56	3.03	886.36	3.93	542.29	2.24
7	1029.11	2.79	862.93	3.47	387.83	1.54
8	1120.72	4.95	275.98	2.01	744.69	3.11
9	1462.66	4.96	389.96	2.70	702.08	3.58
10	709.53	3.63	712.73	3.99	1585.16	2.31
11	3160.65	6.84	897.02	3.57	1377.44	3.93
12	-	-	1359.33	3.10	411.27	2.07
13	212.07	1.59	1938.82	7.40	1215.52	3.21
14	155.61	1.15	1718.32	10.59	1852.54	2.61
15	207.81	1.19	2331.89	7.63	1679.97	3.06
16	218.46	1.54	2129.50	5.72	653.08	2.04
17	770.25	2.69	2958.26	7.71	1786.49	3.23
18	744.69	2.73	2395.81	4.49	1186.76	4.61
19	286.63	1.65	2156.13	8.81	93.82	1.22
20	461.33	1.55	1676.77	7.07	2606.73	7.42
21	696.75	1.87	2025.10	6.83	936.43	3.54
22	1235.76	5.00	3169.17	8.92	2699.40	7.34
23	274.92	1.46	524.18	2.44	1887.69	3.83
24	273.85	9.31	1669.31	3.64	3008.32	4.23
25	295.16	2.56	1994.21	6.38	1538.29	5.29
26	337.76	2.39	1731.10	5.01	580.64	2.83
27	2802.73	8.24	1834.43	5.85	1037.63	4.39
28	2102.87	7.80	4174.76	9.96	575.31	2.60
29	2111.39	3.64	792.62	2.63	2141.22	4.07
30	2301.00	6.89	1287.96	3.30	3381.16	8.80
31	3804.06	6.45	574.25	1.91	-	-
Mean	1134.75	4.03	1603.89	5.44	1317.93	3.63
S.D.	985.89	2.44	856.98	2.39	885.94	1.94
Min	155.61	1.15	275.98	1.91	93.82	1.12
Max	3804.06	9.31	4174.76	10.59	3381.16	8.80
SD. ER	183.08	0.45	153.92	0.44	161.75	0.36

Table A2.2:   The daily data of alpha track radon concentrations (kBq m^{-3}) at station
ST-10 was observed in Phang Nga Province over a three months from
October 1 to December 31, 2009.

Date	October 09		November 09		December 09	
	Rn_Conc.	SD.Er.	Rn_Conc.	SD.Er.	Rn_Conc.	SD.Er.
1	1081.30	2.54	3408.85	6.36	6931.60	25.86
2	1187.83	3.49	2557.72	5.92	3108.45	6.22
3	465.59	1.94	4204.59	12.21	2271.18	4.27
4	351.61	2.53	2963.58	4.63	1031.24	2.80
5	215.26	1.46	2294.61	4.51	1649.08	4.08
6	48.02	1.17	1777.97	6.92	3029.63	5.38
7	55.48	0.80	2273.31	4.23	2400.07	4.40
8	149.22	1.29	2908.19	6.82	2190.22	7.00
9	315.39	2.63	5980.34	14.08	2836.82	6.46
10	1087.69	4.60	16837.27	52.92	2416.05	10.14
11	7987.25	14.87	2201.93	6.64	3771.03	12.83
12	1377.44	6.17	2747.34	6.91	2898.60	12.61
13	385.70	1.51	2994.47	9.13	5052.52	10.74
14	-	-	1055.74	3.04	1535.09	4.51
15	2433.09	5.85	2196.61	5.61	2167.85	2.31
16	1995.28	5.62	3171.30	5.23	1757.73	4.92
17	2940.15	9.21	752.14	2.75	10411.74	18.12
18	1048.28	3.13	1554.27	6.58	741.49	1.85
19	2786.75	7.74	911.93	2.95	-	-
20	1403.00	4.57	1151.61	4.00	840.56	1.84
21	2154.00	7.84	976.91	2.48	2236.02	5.43
22	2257.33	5.46	1371.05	4.11	933.23	3.23
23	1596.88	4.81	734.03	3.66	1703.40	5.65
24	1578.77	3.31	1253.87	3.52	-	-
25	2013.39	4.62	2334.02	6.65	1089.82	3.39
26	3614.44	7.28	2353.20	5.98	596.62	2.96
27	1134.56	3.27	4396.33	11.78	7291.65	9.94
28	-	-	1236.83	2.80	2475.70	8.27
29	2148.67	5.47	2193.41	6.84	1166.52	3.31
30	5894.06	7.33	2615.25	7.70	807.54	2.48
31	2093.28	4.12	-	-	1238.96	4.26
Mean	1786.20	4.64	2780.29	7.56	2640.70	6.73
S.D.	1730.97	3.00	2906.42	9.02	2229.38	5.33
Min	48.02	0.80	734.03	2.48	596.62	1.84
Max	7987.25	14.87	16837.27	52.92	10411.74	25.86
SD. ER	321.43	0.56	530.64	1.68	413.98	0.99

Table A2.3: The daily data of alpha track radon concentrations (kBq m^{-3}) at station ST-10 was observed in Phang Nga Province over a three months from January 1 to March 31, 2010.

Date	January 10		February 10		March 10	
	Rn_Conc.	SD.Er.	Rn_Conc.	SD.Er.	Rn_Conc.	SD.Er.
1	1981.43	3.51	659.47	3.13	934.30	3.09
2	1049.35	3.45	768.12	3.72	500.75	2.47
3	4687.14	12.77	579.57	2.72	270.65	1.33
4	2291.41	7.71	663.73	2.77	1998.47	4.75
5	2507.66	4.38	710.60	3.24	943.89	2.54
6	2575.83	8.39	376.11	1.80	583.84	1.85
7	1381.70	4.61	224.85	1.02	1850.41	4.02
8	972.65	3.34	1260.26	3.53	1172.91	3.59
9	996.08	3.59	188.63	1.26	1235.76	4.41
10	3488.74	7.65	491.16	1.86	519.92	2.02
11	2189.15	7.49	12170.45	16.19	1775.84	3.82
12	5870.62	16.81	257.87	1.51	2557.72	7.57
13	2635.49	4.87	122.59	1.16	263.20	0.82
14	842.69	4.06	138.56	0.94	1275.18	3.60
15	3760.38	11.12	153.48	0.94	543.36	1.73
16	832.04	2.70	268.52	1.05	1212.33	2.74
17	1173.98	4.18	199.28	0.81	218.46	1.08
18	3954.25	10.68	226.98	1.70	1638.42	4.07
19	-	-	176.91	1.13	1735.36	3.21
20	248.28	1.10	201.41	1.31	1777.97	2.25
21	1821.64	4.38	250.42	1.61	200.35	0.75
22	106.61	1.32	526.31	2.29	328.18	0.47
23	181.17	1.16	1805.67	5.44	5293.26	7.57
24	68.26	0.99	328.18	1.70	1210.20	2.83
25	528.44	1.73	262.13	0.78	1307.13	2.59
26	195.02	1.19	360.13	1.58	924.71	2.74
27	1185.70	5.75	408.07	1.19	6703.64	8.32
28	640.29	2.39	140.70	0.74	3432.29	4.06
29	654.14	2.71	-	-	1507.40	3.97
30	480.51	2.38	-	-	-	-
31	639.23	2.45	-	-	3071.17	5.70
Mean	1664.66	4.96	854.29	2.40	1566.23	3.33
S.D.	1479.11	3.85	2248.46	2.92	1463.42	1.97
Min	68.26	0.99	122.59	0.74	200.35	0.47
Max	5870.62	16.81	12170.45	16.19	6703.64	8.32
SD. ER	265.66	0.71	424.92	0.54	267.18	0.37

Table A2.4:   The daily data of alpha track radon concentrations (kBq m^{-3}) at station
ST-10 was observed in Phang Nga Province over a three months from
April 1 to June 30, 2010.

Date	April 10		May 10		June 10	
	Rn_Conc.	SD.Er.	Rn_Conc.	SD.Er.	Rn_Conc.	SD.Er.
1	857.60	2.81	9625.59	24.06	-	-
2	2,474.64	6.43	1136.69	5.55	-	-
3	4,574.22	8.04	661.60	2.49	-	-
4	1,805.67	3.04	3241.61	11.47	-	-
5	2,163.59	7.59	2723.90	6.14	-	-
6	7,142.52	7.65	6729.20	7.77	458.14	2.21
7	959.86	2.20	709.53	3.78	371.85	1.14
8	3,060.52	4.79	3175.56	12.78	270.65	1.11
9	765.99	2.31	10621.59	30.24	329.24	1.75
10	4,249.33	14.38	906.60	2.21	1891.95	2.88
11	5,046.1	12.7	1291.15	3.45	4074.63	2.68
12	2,500.2	8.8	767.06	2.08	366.53	0.92
13	10,451.2	15.5	1126.04	4.29	1170.78	2.72
14	3,710.3	7.6	7335.33	24.38	732.97	2.45
15	1,188.89	4.42	1044.02	3.30	1893.02	4.15
16	4,311.11	10.07	4060.78	10.33	-	-
17	3,885.01	8.92	4186.48	11.61	634.97	4.18
18	4,626.42	15.60	3640.01	14.92	928.97	3.22
19	754.27	4.03	2881.56	9.53	474.12	3.18
20	4,679.68	17.74	6509.77	23.49	478.38	2.87
21	3,916.97	7.58	3604.86	11.84	6.48	0.50
22	1,852.54	4.14	4327.09	11.95	1767.32	2.47
23	2,691.95	7.19	3211.78	9.82	424.05	2.89
24	3,284.22	8.39	987.56	3.46	1935.62	5.71
25	19.26	1.11	1571.31	6.12	722.32	4.31
26	1,262.39	3.04	11750.75	24.99	791.56	1.68
27	2,670.64	8.01	1669.31	8.03	6.48	0.50
28	3,179.83	10.09	1234.70	4.73	1199.54	2.32
29	4,057.58	12.37	2563.05	7.62	555.07	2.80
30	2,314.85	8.83	1809.93	8.00	457.07	2.25
31	-	-	8065.02	19.91	-	-
Mean	3,148.58	7.84	3650.63	10.66	914.24	2.54
S.D.	2,112.40	4.35	3097.34	7.81	888.37	1.26
Min	19.26	1.11	661.60	2.08	6.48	0.50
Max	10,451.15	17.74	11750.75	30.24	4074.63	5.71
SD. ER	385.67	0.81	556.30	1.45	181.34	0.23

APPENDIX B
EARTHQUAKE DATA

APPENDIX B1

ORDER OF EARTHQUAKE EVENTS

Table B1: The earthquake magnitude (M_W (4) was selected from ANSS of Northern California Earthquake Data Center, 210 seismic events occurred between July 1, 2009 to June 30, 2010.

Order	dd/mm/yyyy	Time	Lat	Long	Depth (km)	Mag	Magt	Mw	Epic. Dis. (km)	Mo (dyne-cm)
1	5/7/2009	25:37.0	1.306	99.704	181.9	4.5	Mb	4.9	797	9.61E+17
2	6/7/2009	00:39.3	3.06	93.318	33.4	4.9	Mb	5.2	826	3.11E+18
3	7/7/2009	44:00.6	1.294	97.101	35	4.1	Mb	4.5	805	2.97E+17
4	13/7/2009	52:38.8	2.041	97.994	71.7	4.6	Mb	4.9	709	1.29E+18
5	20/7/2009	49:27.9	3.504	92.68	35.9	4.4	Mb	4.8	844	7.16E+17
6	21/7/2009	51:55.5	4.446	96.658	46.2	4.4	Mb	4.8	488	7.16E+17
7	24/7/2009	45:33.5	5.223	94.719	35	4.8	Mb	5.1	551	2.32E+18
8	25/7/2009	41:58.0	1.869	97.02	39.2	5.2	Mb	5.5	745	7.50E+18
9	28/7/2009	18:09.9	2.293	97.077	35	4.3	Mb	4.7	698	5.34E+17
10	4/8/2009	32:49.4	2.43	96.312	49.1	4.6	Mb	4.9	708	1.29E+18
11	5/8/2009	08:13.3	2.091	96.108	35	4.2	Mb	4.6	751	3.98E+17
12	12/8/2009	33:25.7	9.018	93.723	50.7	5.1	Mw	5.1	531	2.24E+18
13	13/8/2009	37:31.5	5.208	94.744	61.2	4.5	Mb	4.9	550	9.61E+17
14	15/8/2009	04:32.2	4.603	96.625	54.3	5	Mw	5.0	475	1.58E+18
15	18/8/2009	28:08.2	2.283	96.404	54.5	4.6	Mb	4.9	720	1.29E+18
16	21/8/2009	27:29.6	0.844	97.409	35	4.4	Mb	4.8	847	7.16E+17
17	21/8/2009	09:16.0	0.963	97.432	30	4.6	Mb	4.9	834	1.29E+18
18	25/8/2009	26:51.9	5.361	94.693	80.5	4.6	Mb	4.9	544	1.29E+18
19	28/8/2009	45:18.3	5.475	94.659	55.3	5	Mw	5.0	539	1.58E+18
20	5/9/2009	19:36.1	1.129	97.191	35	4.8	Mb	5.1	820	2.32E+18
21	8/9/2009	39:52.6	5.26	94.315	57.5	5	Mw	5.0	583	1.58E+18
22	8/9/2009	33:48.1	2.508	96.13	62.1	4.3	Mb	4.7	707	5.34E+17
23	9/9/2009	07:16.7	10.261	93.82	169.9	4.7	Mb	5.0	552	1.73E+18
24	12/9/2009	43:29.5	8.572	93.901	28.7	4.6	Mb	4.9	508	1.29E+18
25	12/9/2009	48:42.6	5.177	94.619	35	4.5	Mb	4.9	563	9.61E+17
26	13/9/2009	11:23.3	4.654	95.011	10	4.8	Mb	5.1	571	2.32E+18
27	18/9/2009	52:22.8	0.876	97.493	35	4.4	Mb	4.8	843	7.16E+17
28	19/9/2009	28:16.0	1.424	97.005	36.5	4.2	Mb	4.6	793	3.98E+17
29	19/9/2009	35:29.2	0.732	99.386	116.4	4.5	Mb	4.9	855	9.61E+17
30	25/9/2009	06:12.1	2.404	96.159	35	4	Mb	4.4	717	2.21E+17
31	27/9/2009	26:03.6	1.967	97.075	43	4.7	Mb	5.0	733	1.73E+18
32	3/10/2009	52:32.7	4.807	96.066	35	4.4	Mb	4.8	486	7.16E+17
33	5/10/2009	46:59.4	10.696	91.566	10	4.5	Mb	4.9	798	9.61E+17
34	10/10/2009	33:31.0	3.308	96.176	35	4.5	Mb	4.9	624	9.61E+17
35	14/10/2009	04:54.9	10.885	92.139	21.2	4	Mb	4.4	747	2.21E+17
36	15/10/2009	17:34.2	10.7	91.73	10	4.5	Mb	4.9	782	9.61E+17
37	24/10/2009	27:31.3	1.019	97.244	35	4.3	Mb	4.7	831	5.34E+17
38	29/10/2009	05:20.0	8.151	91.759	29.6	5	Mb	5.3	742	4.17E+18
39	4/11/2009	42:30.3	3.726	95.465	63.7	4.4	Mb	4.8	622	7.16E+17
40	5/11/2009	21:30.9	2.876	98.919	161	4.6	Mb	4.9	615	1.29E+18
41	10/11/2009	48:46.8	8.082	91.899	23	6	Mw	6.0	727	5.01E+19
42	11/11/2009	09:59.7	10.282	93.803	35	4.5	Mb	4.9	555	9.61E+17
43	11/11/2009	34:15.0	5.523	94.701	95.5	4.2	Mb	4.6	532	3.98E+17
44	17/11/2009	40:16.2	1.261	97.067	35	4.4	Mb	4.8	809	7.16E+17
45	21/11/2009	10:18.2	7.877	93.838	39.9	4.5	Mb	4.9	519	9.61E+17
46	22/11/2009	45:53.8	2.71	95.533	35	4.8	Mb	5.1	714	2.32E+18
47	25/11/2009	50:42.7	0.967	98.669	70.9	4.2	Mb	4.6	824	3.98E+17
48	26/11/2009	27:41.8	4.694	96.202	33.1	4.8	Mw	4.8	488	7.94E+17
49	26/11/2009	00:37.8	1.327	99.286	8.6	4.1	Mb	4.5	789	2.97E+17
50	1/12/2009	16:57.3	7.628	94.566	56.2	4.4	Mb	4.8	446	7.16E+17

Table B1：   (continued)

Order	dd/mm/yyyy	Time	Lat	Long	Depth (km)	Mag	Magt	Mw	Epic. Dis. (km)	Mo (dyne-cm)
51	9/12/2009	37:19.8	1.339	99.975	206.8	4.9	Mb	5.2	798	3.11E+18
52	9/12/2009	17:00.9	2.419	99.212	166.2	4.4	Mb	4.8	668	7.16E+17
53	9/12/2009	29:02.9	2.759	95.91	21	6	Mw	6.0	691	5.01E+19
54	12/12/2009	18:14.9	2.576	95.9	35	4.5	Mb	4.9	710	9.61E+17
55	12/12/2009	34:02.6	1.955	99.371	163.3	4.5	Mb	4.9	721	9.61E+17
56	16/12/2009	49:22.2	0.93	97.403	35	4.2	Mb	4.6	838	3.98E+17
57	19/12/2009	43:57.3	2.675	96.062	43.9	5.5	Mb	5.7	693	1.81E+19
58	19/12/2009	30:04.1	2.618	96.204	68.1	4.5	Mb	4.9	693	9.61E+17
59	23/12/2009	23:06.4	7.3	92.502	73.2	4.5	Mb	4.9	673	9.61E+17
60	25/12/2009	28:41.5	2.103	96.744	35	4.3	Mb	4.7	727	5.34E+17
61	19/1/2010	23:59.0	1.019	97.298	35	4.4	Mb	4.8	830	7.16E+17
62	22/1/2010	46:17.3	3.025	93.789	36.9	5	Mw	5.0	794	1.58E+18
63	27/1/2010	58:26.7	1.698	97.719	50.3	4.5	Mb	4.9	750	9.61E+17
64	27/1/2010	46:40.8	7.754	94.686	58.4	4.1	Mb	4.5	430	2.97E+17
65	28/1/2010	12:51.7	4.64	96.832	8.4	4.8	Mb	5.1	461	2.32E+18
66	2/2/2010	54:56.3	10.768	92.07	38.3	4.7	Mb	5.0	749	1.73E+18
67	9/2/2010	58:29.2	1.199	96.932	12.7	4.5	Mb	4.9	819	9.61E+17
68	10/2/2010	48:44.5	1.522	97.063	30.9	5	Mb	5.3	781	4.17E+18
69	13/2/2010	31:28.5	8.588	92.07	27	4.6	Mb	4.9	707	1.29E+18
70	13/2/2010	19:03.0	3.338	96.543	92.5	4.3	Mb	4.7	605	5.34E+17
71	14/2/2010	09:13.2	2.766	94.285	44.3	4.9	Mw	4.9	782	1.12E+18
72	16/2/2010	08:24.1	4.624	93.136	34.1	5.3	Mw	5.3	728	4.47E+18
73	17/2/2010	32:15.6	1.329	98.341	61.5	4.3	Mb	4.7	785	5.34E+17
74	23/2/2010	24:13.0	2.338	96.312	49.6	4.5	Mb	4.9	717	9.61E+17
75	25/2/2010	57:48.8	2.637	93.422	46.5	4.1	Mb	4.5	853	2.97E+17
76	28/2/2010	13:27.9	2.112	99.015	58.1	5.1	Mb	5.4	700	5.59E+18
77	28/2/2010	55:31.4	2.067	98.872	25.6	4	Mb	4.4	704	2.21E+17
78	28/2/2010	39:30.6	1.975	98.998	10	4	Mb	4.4	715	2.21E+17
79	4/3/2010	24:11.7	7.186	92.585	35	4.1	Mb	4.5	667	2.97E+17
80	5/3/2010	53:16.1	3.192	97.035	73.3	4	Mb	4.4	603	2.21E+17
81	8/3/2010	35:59.8	4.575	95.695	97.2	4.3	Mb	4.7	530	5.34E+17
82	12/3/2010	58:34.0	1.356	97.085	35	4.6	Mb	4.9	798	1.29E+18
83	13/3/2010	59:01.0	1.323	97.171	19	5.8	Mw	5.8	800	2.51E+19
84	13/3/2010	17:18.6	1.244	97.094	37	4.1	Mb	4.5	810	2.97E+17
85	14/3/2010	43:26.4	8.756	92.296	37.7	4.7	Mb	5.0	683	1.73E+18
86	14/3/2010	21:50.7	0.929	99.467	26.4	4.8	Mb	5.1	834	2.32E+18
87	15/3/2010	43:55.1	5.01	94.736	45.6	4.4	Mb	4.8	565	7.16E+17
88	15/3/2010	21:18.4	4.444	96.556	38.4	4.5	Mb	4.9	494	9.61E+17
89	15/3/2010	54:23.3	1.187	97.135	36.7	4.8	Mb	5.1	815	2.32E+18
90	17/3/2010	44:55.9	4.505	95.62	84.4	4.5	Mb	4.9	541	9.61E+17
91	18/3/2010	04:43.3	2.212	96.353	50.7	4.2	Mb	4.6	729	3.98E+17
92	21/3/2010	23:05.1	2.108	98.93	35	4.2	Mb	4.6	700	3.98E+17
93	24/3/2010	13:51.5	7.649	92.127	35	4.3	Mb	4.7	707	5.34E+17
94	29/3/2010	00:57.6	0.802	97.417	21.2	4.3	Mb	4.7	852	5.34E+17
95	1/4/2010	51:15.7	4.944	93.997	35	4.5	Mb	4.9	632	9.61E+17
96	3/4/2010	50:01.3	1.767	99.011	121.4	4.8	Mb	5.1	738	2.32E+18
97	4/4/2010	40:58.6	10.855	92.134	34.8	4	Mb	4.4	746	2.21E+17
98	4/4/2010	43:15.6	2.536	95.867	35	4.6	Mb	4.9	716	1.29E+18
99	6/4/2010	36:14.3	5.515	93.201	30	4.3	Mb	4.7	670	5.34E+17
100	6/4/2010	15:01.6	2.383	97.048	31	7.8	Mw	7.8	689	2.51E+22

Table B1:   (continued)

Order	dd/mm/yyyy	Time	Lat	Long	Depth (km)	Mag	Magt	Mw	Epic. Dis. (km)	Mo (dyne-cm)
101	6/4/2010	26:09.6	2.4	97.069	35	4.1	Mb	4.5	687	2.97E+17
102	6/4/2010	34:29.3	1.501	97.124	35	4	Mb	4.4	782	2.21E+17
103	6/4/2010	54:06.0	2.346	97.17	35	5.3	Mb	5.5	690	1.01E+19
104	6/4/2010	35:38.2	1.911	96.721	28.1	5.1	Mb	5.4	748	5.59E+18
105	7/4/2010	32:42.1	2.319	96.98	35	4.4	Mb	4.8	698	7.16E+17
106	7/4/2010	03:48.7	1.839	96.597	35	4	Mb	4.4	760	2.21E+17
107	7/4/2010	22:15.9	2.63	96.928	35	5.1	Mb	5.4	666	5.59E+18
108	7/4/2010	05:12.3	2.076	96.7	35	4	Mb	4.4	731	2.21E+17
109	7/4/2010	34:41.5	2.032	96.66	40.6	4	Mb	4.4	737	2.21E+17
110	7/4/2010	54:23.7	2.282	96.505	35	4.6	Mb	4.9	716	1.29E+18
111	7/4/2010	17:01.8	2.251	96.493	35	4.8	Mb	5.1	720	2.32E+18
112	7/4/2010	41:24.2	2.341	96.998	54	4.5	Mb	4.9	695	9.61E+17
113	7/4/2010	41:07.3	0.984	96.863	35	4.4	Mb	4.8	843	7.16E+17
114	7/4/2010	45:06.1	0.948	96.881	35	4.2	Mb	4.6	847	3.98E+17
115	7/4/2010	21:11.5	2.106	96.892	46.3	4	Mb	4.4	723	2.21E+17
116	8/4/2010	59:55.6	2.279	97.047	35	4.1	Mb	4.5	700	2.97E+17
117	8/4/2010	49:24.1	2.427	97.045	35	4.4	Mb	4.8	684	7.16E+17
118	8/4/2010	44:16.2	2.122	96.662	35	4	Mb	4.4	728	2.21E+17
119	8/4/2010	47:57.3	1.655	97.077	31.4	4.6	Mb	4.9	766	1.29E+18
120	8/4/2010	28:12.6	1.655	96.946	35	4.2	Mb	4.6	769	3.98E+17
121	9/4/2010	29:37.7	1.855	99.174	34.6	4.9	Mw	4.9	730	1.12E+18
122	9/4/2010	07:39.5	1.655	99.174	35	4.2	Mb	4.6	751	3.98E+17
123	12/4/2010	58:04.7	2.02	96.732	42.8	4	Mb	4.4	736	2.21E+17
124	12/4/2010	01:47.2	1.985	96.804	46.4	4.1	Mb	4.5	738	2.97E+17
125	12/4/2010	33:29.6	2.383	97.205	57	5	Mb	5.3	685	4.17E+18
126	13/4/2010	14:56.8	7.805	91.843	21.1	5.2	Mw	5.2	736	3.16E+18
127	14/4/2010	58:33.4	1.98	97.072	41.3	4.4	Mb	4.8	731	7.16E+17
128	15/4/2010	37:09.3	2.044	96.682	26.9	4.2	Mb	4.6	735	3.98E+17
129	17/4/2010	50:56.0	1.786	96.919	35	4.1	Mb	4.5	756	2.97E+17
130	19/4/2010	42:31.2	2.113	96.782	45	4.2	Mb	4.6	725	3.98E+17
131	19/4/2010	47:14.5	2.09	96.706	36.6	4.3	Mb	4.7	730	5.34E+17
132	21/4/2010	39:46.6	2.089	96.656	35	4.3	Mb	4.7	731	5.34E+17
133	24/4/2010	08:30.1	2.617	96.989	35	4.3	Mb	4.7	666	5.34E+17
134	24/4/2010	45:42.3	6.161	93.067	18.3	4.5	Mb	4.9	651	9.61E+17
135	25/4/2010	59:46.7	5.272	94.415	55.1	4.7	Mb	5.0	573	1.73E+18
136	26/4/2010	02:35.5	2.47	95.819	35	4.2	Mb	4.6	724	3.98E+17
137	28/4/2010	49:12.9	1.946	96.556	12.1	4.1	Mb	4.5	750	2.97E+17
138	1/5/2010	02:26.8	7.877	93.527	81.5	4.1	Mb	4.5	553	2.97E+17
139	2/5/2010	44:46.4	6.567	92.804	22.1	4.7	Mb	5.0	662	1.73E+18
140	2/5/2010	23:25.9	7.22	92.332	36.6	4.6	Mb	4.9	693	1.29E+18
141	6/5/2010	40:32.0	2.072	96.715	10	4.6	Mb	4.9	731	1.29E+18
142	6/5/2010	49:39.2	2.08	96.694	40.1	4.1	Mb	4.5	731	2.97E+17
143	7/5/2010	58:36.8	9.396	93.073	70.2	4.8	Mb	5.1	606	2.32E+18
144	9/5/2010	59:41.6	3.748	96.018	38	7.2	Mw	7.2	589	2.66E+21
145	10/5/2010	36:57.4	3.213	95.983	55.2	4.3	Mb	4.7	643	5.34E+17
146	11/5/2010	01:33.9	2.029	96.708	39.4	4.3	Mb	4.7	736	5.34E+17
147	11/5/2010	17:47.1	3.498	95.845	40.5	5.4	Mw	5.4	622	6.31E+18
148	11/5/2010	28:32.5	4.606	95.037	55	4.6	Mb	4.9	573	1.29E+18
149	12/5/2010	37:58.6	1.974	96.732	38.8	4.5	Mb	4.9	741	9.61E+17
150	17/5/2010	59:09.0	1.857	96.972	34	4.1	Mb	4.5	747	2.97E+17

Table B1:　　(continued)

Order	dd/mm/yyyy	Time	Lat	Long	Depth (km)	Mag	Magt	Mw	Epic. Dis. (km)	Mo (dyne-cm)
101	6/4/2010	26:09.6	2.4	97.069	35	4.1	Mb	4.5	687	2.97E+17
102	6/4/2010	34:29.3	1.501	97.124	35	4	Mb	4.4	782	2.21E+17
103	6/4/2010	54:06.0	2.346	97.17	35	5.3	Mb	5.5	690	1.01E+19
104	6/4/2010	35:38.2	1.911	96.721	28.1	5.1	Mb	5.4	748	5.59E+18
105	7/4/2010	32:42.1	2.319	96.98	35	4.4	Mb	4.8	698	7.16E+17
106	7/4/2010	03:48.7	1.839	96.597	35	4	Mb	4.4	760	2.21E+17
107	7/4/2010	22:15.9	2.63	96.928	35	5.1	Mb	5.4	666	5.59E+18
108	7/4/2010	05:12.3	2.076	96.7	35	4	Mb	4.4	731	2.21E+17
109	7/4/2010	34:41.5	2.032	96.66	40.6	4	Mb	4.4	737	2.21E+17
110	7/4/2010	54:23.7	2.282	96.505	35	4.6	Mb	4.9	716	1.29E+18
111	7/4/2010	17:01.8	2.251	96.493	35	4.8	Mb	5.1	720	2.32E+18
112	7/4/2010	41:24.2	2.341	96.998	54	4.5	Mb	4.9	695	9.61E+17
113	7/4/2010	41:07.3	0.984	96.863	35	4.4	Mb	4.8	843	7.16E+17
114	7/4/2010	45:06.1	0.948	96.881	35	4.2	Mb	4.6	847	3.98E+17
115	7/4/2010	21:11.5	2.106	96.892	46.3	4	Mb	4.4	723	2.21E+17
116	8/4/2010	59:55.6	2.279	97.047	35	4.1	Mb	4.5	700	2.97E+17
117	8/4/2010	49:24.1	2.427	97.045	35	4.4	Mb	4.8	684	7.16E+17
118	8/4/2010	44:16.2	2.122	96.662	35	4	Mb	4.4	728	2.21E+17
119	8/4/2010	47:57.3	1.655	97.077	31.4	4.6	Mb	4.9	766	1.29E+18
120	8/4/2010	28:12.6	1.655	96.946	35	4.2	Mb	4.6	769	3.98E+17
121	9/4/2010	29:37.7	1.855	99.174	34.6	4.9	Mw	4.9	730	1.12E+18
122	9/4/2010	07:39.5	1.655	99.174	35	4.2	Mb	4.6	751	3.98E+17
123	12/4/2010	58:04.7	2.02	96.732	42.8	4	Mb	4.4	736	2.21E+17
124	12/4/2010	01:47.2	1.985	96.804	46.4	4.1	Mb	4.5	738	2.97E+17
125	12/4/2010	33:29.6	2.383	97.205	57	5	Mb	5.3	685	4.17E+18
126	13/4/2010	14:56.8	7.805	91.843	21.1	5.2	Mw	5.2	736	3.16E+18
127	14/4/2010	58:33.4	1.98	97.072	41.3	4.4	Mb	4.8	731	7.16E+17
128	15/4/2010	37:09.3	2.044	96.682	26.9	4.2	Mb	4.6	735	3.98E+17
129	17/4/2010	50:56.0	1.786	96.919	35	4.1	Mb	4.5	756	2.97E+17
130	19/4/2010	42:31.2	2.113	96.782	45	4.2	Mb	4.6	725	3.98E+17
131	19/4/2010	47:14.5	2.09	96.706	36.6	4.3	Mb	4.7	730	5.34E+17
132	21/4/2010	39:46.6	2.089	96.656	35	4.3	Mb	4.7	731	5.34E+17
133	24/4/2010	08:30.1	2.617	96.989	35	4.3	Mb	4.7	666	5.34E+17
134	24/4/2010	45:42.3	6.161	93.067	18.3	4.5	Mb	4.9	651	9.61E+17
135	25/4/2010	59:46.7	5.272	94.415	55.1	4.7	Mb	5.0	573	1.73E+18
136	26/4/2010	02:35.5	2.47	95.819	35	4.2	Mb	4.6	724	3.98E+17
137	28/4/2010	49:12.9	1.946	96.556	12.1	4.1	Mb	4.5	750	2.97E+17
138	1/5/2010	02:26.8	7.877	93.527	81.5	4.1	Mb	4.5	553	2.97E+17
139	2/5/2010	44:46.4	6.567	92.804	22.1	4.7	Mb	5.0	662	1.73E+18
140	2/5/2010	23:25.9	7.22	92.332	36.6	4.6	Mb	4.9	693	1.29E+18
141	6/5/2010	40:32.0	2.072	96.715	10	4.6	Mb	4.9	731	1.29E+18
142	6/5/2010	49:39.2	2.08	96.694	40.1	4.1	Mb	4.5	731	2.97E+17
143	7/5/2010	58:36.8	9.396	93.073	70.2	4.8	Mb	5.1	606	2.32E+18
144	9/5/2010	59:41.6	3.748	96.018	38	7.2	Mw	7.2	589	2.66E+21
145	10/5/2010	36:57.4	3.213	95.983	55.2	4.3	Mb	4.7	643	5.34E+17
146	11/5/2010	01:33.9	2.029	96.708	39.4	4.3	Mb	4.7	736	5.34E+17
147	11/5/2010	17:47.1	3.498	95.845	40.5	5.4	Mw	5.4	622	6.31E+18
148	11/5/2010	28:32.5	4.606	95.037	55	4.6	Mb	4.9	573	1.29E+18
149	12/5/2010	37:58.6	1.974	96.732	38.8	4.5	Mb	4.9	741	9.61E+17
150	17/5/2010	59:09.0	1.857	96.972	34	4.1	Mb	4.5	747	2.97E+17

Table B1: (continued)

Order	dd/mm/yyyy	Time	Lat	Long	Depth (km)	Mag	Magt	Mw	Epic. Dis. (km)	Mo (dyne-cm)
151	2/6/2010	05:01.7	5.39	95.349	104.9	4.5	Mb	4.9	488	9.61E+17
152	2/6/2010	20:44.0	4.754	94.485	35	4	Mb	4.4	604	2.21E+17
153	3/6/2010	24:15.6	4.778	95.785	74	5.4	Mw	5.4	507	6.31E+18
154	6/6/2010	37:35.6	1.329	97.141	36	4.3	Mb	4.7	800	5.34E+17
155	6/6/2010	44:07.2	2.478	95.859	35	4.5	Mb	4.9	722	9.61E+17
156	10/6/2010	22:36.1	0.849	97.164	44.6	4.4	Mb	4.8	851	7.16E+17
157	12/6/2010	26:50.5	7.881	91.936	35	7.5	Mw	7.5	725	8.91E+21
158	12/6/2010	03:41.6	7.597	91.811	35	4.4	Mb	4.8	742	7.16E+17
159	12/6/2010	12:25.4	7.769	92.057	35	4.7	Mb	5.0	713	1.73E+18
160	12/6/2010	28:29.8	7.716	92.038	30.4	4.3	Mb	4.7	716	5.34E+17
161	12/6/2010	44:42.1	7.674	91.967	35	5.2	Mb	5.5	724	7.50E+18
162	12/6/2010	57:59.4	8.035	92.211	22.1	4.9	Mb	5.2	694	3.11E+18
163	13/6/2010	50:33.0	7.629	91.9	11.6	4.9	Mb	5.2	732	3.11E+18
164	13/6/2010	47:30.4	2.231	96.26	35	4.3	Mb	4.7	730	5.34E+17
165	13/6/2010	01:07.7	7.86	92.09	37.3	5	Mb	5.3	709	4.17E+18
166	13/6/2010	15:14.6	7.426	91.895	35	4.5	Mb	4.9	736	9.61E+17
167	13/6/2010	26:04.8	7.779	91.992	35	5.2	Mw	5.2	720	3.16E+18
168	13/6/2010	38:43.1	7.532	91.621	29.1	4.7	Mb	5.0	764	1.73E+18
169	13/6/2010	05:35.6	7.794	91.895	27.7	5.2	Mw	5.2	731	3.16E+18
170	13/6/2010	36:59.5	7.676	91.953	22.8	4.5	Mb	4.9	726	9.61E+17
171	13/6/2010	37:35.7	7.649	91.956	35	4.7	Mb	5.0	726	1.73E+18
172	13/6/2010	44:11.4	7.726	91.835	35	4.2	Mb	4.6	738	3.98E+17
173	13/6/2010	57:38.1	7.779	91.959	35	4.4	Mb	4.8	724	7.16E+17
174	13/6/2010	38:13.9	7.774	91.957	31.1	4.3	Mb	4.7	724	5.34E+17
175	14/6/2010	48:49.5	2.064	97.691	35	4	Mb	4.4	710	2.21E+17
176	14/6/2010	04:32.7	1.401	96.872	12.7	4.6	Mb	4.9	798	1.29E+18
177	14/6/2010	34:20.7	7.666	91.909	35	4.3	Mb	4.7	731	5.34E+17
178	14/6/2010	15:02.2	7.673	91.853	27.9	4	Mb	4.4	737	2.21E+17
179	15/6/2010	43:07.6	7.944	91.816	35	4.1	Mb	4.5	738	2.97E+17
180	15/6/2010	55:11.9	7.693	92.03	35.8	4.1	Mb	4.5	717	2.97E+17
181	15/6/2010	14:31.1	7.268	91.615	35	4.3	Mb	4.7	769	5.34E+17
182	15/6/2010	42:49.3	1.92	96.653	35	4.4	Mb	4.8	749	7.16E+17
183	15/6/2010	24:27.7	7.404	91.823	35	5	Mw	5.0	744	1.58E+18
184	16/6/2010	29:42.8	7.455	91.847	18.6	4.6	Mb	4.9	741	1.29E+18
185	16/6/2010	57:32.8	7.605	91.849	35	4.5	Mb	4.9	738	9.61E+17
186	16/6/2010	10:45.4	7.714	91.85	26.5	4.8	Mb	5.1	736	2.32E+18
187	16/6/2010	37:03.7	7.588	91.783	25.6	4.5	Mb	4.9	745	9.61E+17
188	18/6/2010	42:48.2	7.743	91.885	35	4.6	Mb	4.9	732	1.29E+18
189	18/6/2010	44:49.2	7.645	91.825	35	4.2	Mb	4.6	740	3.98E+17
190	18/6/2010	48:01.2	2.206	96.238	28.6	4.3	Mb	4.7	734	5.34E+17
191	20/6/2010	07:01.5	7.482	91.669	35	4.5	Mb	4.9	759	9.61E+17
192	20/6/2010	10:31.8	7.787	91.924	13.7	4.5	Mb	4.9	727	9.61E+17
193	21/6/2010	35:38.8	2.655	95.628	44.2	4.6	Mb	4.9	715	1.29E+18
194	21/6/2010	08:37.0	4.594	94.969	53.8	4.7	Mb	5.0	579	1.73E+18
195	22/6/2010	45:06.8	7.563	91.879	27.8	5	Mb	5.3	735	4.17E+18
196	24/6/2010	08:35.1	7.696	91.958	20.5	5.5	Mw	5.5	725	8.91E+18
197	24/6/2010	39:56.7	7.552	91.931	35	4.6	Mb	4.9	730	1.29E+18
198	24/6/2010	10:30.5	1.647	97.078	35	4.3	Mb	4.7	767	5.34E+17
199	24/6/2010	05:59.1	7.641	91.95	25.3	4.6	Mb	4.9	727	1.29E+18
200	24/6/2010	06:22.1	7.761	92.047	30	4.9	Mw	4.9	714	1.12E+18

Table B1:   (continued)

Order	dd/mm/yyyy	Time	Lat	Long	Depth (km)	Mag	Magt	Mw	Epic. Dis. (km)	Mo (dyne-cm)
201	24/6/2010	07:46.8	7.622	91.979	26.1	5	Mb	5.3	724	4.17E+18
202	25/6/2010	29:00.7	7.588	91.856	35	5.2	Mw	5.2	738	3.16E+18
203	25/6/2010	48:15.3	7.444	91.884	20.8	4.8	Mb	5.1	737	2.32E+18
204	25/6/2010	21:30.8	6.8	91.607	35	4.3	Mb	4.7	781	5.34E+17
205	25/6/2010	43:22.3	7.545	91.861	35	4.6	Mb	4.9	738	1.29E+18
206	25/6/2010	22:25.5	7.53	91.871	19.7	4.3	Mb	4.7	737	5.34E+17
207	25/6/2010	09:16.0	2.065	96.762	40	4.8	Mb	5.1	731	2.32E+18
208	27/6/2010	13:25.0	7.558	91.889	35	4.3	Mb	4.7	734	5.34E+17
209	29/6/2010	54:45.9	1.244	97.111	40.9	4.4	Mb	4.8	810	7.16E+17
210	29/6/2010	57:38.9	2.067	96.755	42.1	4.5	Mb	4.9	731	9.61E+17

APPENDIX C
THE METEOROLOGY DATA

APPENDIX C1

THE EFFECT OF METEOROLOGICAL VARIABLE OF RADON

Table C1:   The meteorological parameters; Air pressure (mbar), Temperature (˚C) and Rainfall (mm) for the period July 1, 2009 to June 30, 2010.

Order	dd/mm/yyyy	Air Pressure (mbar)	Temperature (°C)	Rainfall (mm)
1	1/7/2009	1009.82	27.60	0.00
2	2/7/2009	1009.27	27.50	0.00
3	3/7/2009	1008.41	27.80	0.00
4	4/7/2009	1008.05	28.40	0.00
5	5/7/2009	1008.27	27.20	15.80
6	6/7/2009	1009.39	27.20	0.70
7	7/7/2009	1009.03	28.00	0.00
8	8/7/2009	1009.18	28.20	0.20
9	9/7/2009	1009.16	28.10	1.50
10	10/7/2009	1008.79	28.00	9.90
11	11/7/2009	1008.13	25.00	150.40
12	12/7/2009	1007.94	25.50	126.80
13	13/7/2009	1006.91	28.40	0.00
14	14/7/2009	1008.10	28.70	0.30
15	15/7/2009	1008.43	29.00	6.00
16	16/7/2009	1008.11	28.30	2.00
17	17/7/2009	1006.88	27.90	1.00
18	18/7/2009	1008.34	29.00	0.00
19	19/7/2009	1008.80	28.80	1.90
20	20/7/2009	1008.78	29.20	0.00
21	21/7/2009	1009.57	28.30	3.90
22	22/7/2009	1008.91	26.40	78.70
23	23/7/2009	1009.15	25.00	52.30
24	24/7/2009	1009.88	27.20	7.70
25	25/7/2009	1009.41	26.60	13.80
26	26/7/2009	1009.37	27.90	0.20
27	27/7/2009	1009.72	28.30	0.30
28	28/7/2009	1010.49	28.30	0.00
29	29/7/2009	1011.36	28.50	0.00
30	30/7/2009	1010.78	28.60	0.00
31	31/7/2009	1009.43	28.80	0.00
32	1/8/2009	1008.38	28.70	0.00
33	2/8/2009	1008.20	29.10	3.20
34	3/8/2009	1007.93	28.80	1.20
35	4/8/2009	1007.93	28.30	9.70
36	5/8/2009	1008.26	28.80	0.00
37	6/8/2009	1007.55	28.80	8.90
38	7/8/2009	1008.04	27.40	11.00
39	8/8/2009	1007.85	27.10	16.60
40	9/8/2009	1007.19	28.10	0.20
41	10/8/2009	1007.83	28.30	16.70
42	11/8/2009	1009.06	28.10	12.00
43	12/8/2009	1008.08	27.40	0.00
44	13/8/2009	1007.49	27.70	0.00
45	14/8/2009	1008.53	27.60	11.40
46	15/8/2009	1009.17	27.90	1.50
47	16/8/2009	1009.03	28.30	4.90
48	17/8/2009	1009.13	27.80	0.10
49	18/8/2009	1009.31	27.10	6.50
50	19/8/2009	1010.69	26.30	3.30

Table C1:   (continued)

Order	dd/mm/yyyy	Air Pressure (mbar)	Temperature (°C)	Rainfall (mm)
51	20/8/2009	1010.99	27.30	0.00
52	21/8/2009	1010.17	28.00	14.30
53	22/8/2009	1009.11	26.30	57.20
54	23/8/2009	1009.15	24.80	143.80
55	24/8/2009	1010.03	26.00	18.70
56	25/8/2009	1009.67	26.10	1.50
57	26/8/2009	1009.73	25.60	38.80
58	27/8/2009	1009.04	25.60	86.10
59	28/8/2009	1008.67	24.90	154.60
60	29/8/2009	1008.55	25.30	29.80
61	30/8/2009	1009.49	26.70	7.60
62	31/8/2009	1010.74	25.60	60.10
63	1/9/2009	1010.36	25.40	10.50
64	2/9/2009	1009.15	27.20	10.20
65	3/9/2009	1008.95	27.20	0.00
66	4/9/2009	1009.40	26.90	41.10
67	5/9/2009	1009.61	25.60	69.40
68	6/9/2009	1008.51	28.20	8.00
69	7/9/2009	1008.69	27.50	0.00
70	8/9/2009	1009.99	27.70	2.00
71	9/9/2009	1010.26	25.80	37.50
72	10/9/2009	1009.34	25.00	68.10
73	11/9/2009	1009.09	26.60	2.70
74	12/9/2009	1009.49	26.10	23.80
75	13/9/2009	1010.17	26.70	16.60
76	14/9/2009	1009.96	27.00	24.60
77	15/9/2009	1008.20	26.40	47.20
78	16/9/2009	1008.94	25.30	25.40
79	17/9/2009	1009.73	26.30	0.20
80	18/9/2009	1011.52	26.70	6.80
81	19/9/2009	1011.79	26.90	0.30
82	20/9/2009	1011.59	27.00	0.00
83	21/9/2009	1010.96	27.40	0.00
84	22/9/2009	1010.80	27.30	1.70
85	23/9/2009	1010.08	25.50	31.70
86	24/9/2009	1009.79	24.90	45.30
87	25/9/2009	1009.34	25.70	87.00
88	26/9/2009	1008.61	26.20	22.90
89	27/9/2009	1008.01	28.20	9.00
90	28/9/2009	1007.90	27.80	1.30
91	29/9/2009	1007.84	28.30	6.60
92	30/9/2009	1008.19	27.60	17.30
93	1/10/2009	1008.13	27.70	13.80
94	2/10/2009	1009.05	28.20	42.80
95	3/10/2009	1009.89	26.60	5.40
96	4/10/2009	1011.05	27.10	23.80
97	5/10/2009	1010.09	26.10	41.40
98	6/10/2009	1010.14	24.90	27.70
99	7/10/2009	1009.63	25.10	58.20
100	8/10/2009	1009.12	24.40	69.40

Table C1: (continued)

Order	dd/mm/yyyy	Air Pressure (mbar)	Temperature (°C)	Rainfall (mm)
101	9/10/2009	1008.98	25.00	25.00
102	10/10/2009	1010.59	24.70	33.90
103	11/10/2009	1010.79	24.90	47.50
104	12/10/2009	1010.65	25.70	0.50
105	13/10/2009	1011.04	26.70	5.30
106	14/10/2009	1010.66	27.00	0.00
107	15/10/2009	1010.87	27.20	0.00
108	16/10/2009	1010.76	26.90	2.50
109	17/10/2009	1009.32	27.10	23.50
110	18/10/2009	1009.74	25.90	16.70
111	19/10/2009	1010.21	26.10	1.40
112	20/10/2009	1010.15	26.20	2.50
113	21/10/2009	1009.95	26.60	0.20
114	22/10/2009	1010.81	27.10	8.90
115	23/10/2009	1010.64	27.30	0.00
116	24/10/2009	1010.03	27.20	4.70
117	25/10/2009	1010.10	25.90	12.80
118	26/10/2009	1009.85	26.50	0.70
119	27/10/2009	1009.13	25.50	29.10
120	28/10/2009	1009.73	25.60	12.70
121	29/10/2009	1009.57	26.60	0.00
122	30/10/2009	1009.80	26.80	0.00
123	31/10/2009	1008.90	26.90	0.00
124	1/11/2009	1008.74	27.50	0.00
125	2/11/2009	1008.46	27.70	0.00
126	3/11/2009	1008.43	26.70	0.00
127	4/11/2009	1008.94	26.50	2.00
128	5/11/2009	1008.20	27.90	0.60
129	6/11/2009	1007.61	27.60	0.00
130	7/11/2009	1006.99	27.60	0.00
131	8/11/2009	1007.18	27.50	16.00
132	9/11/2009	1007.11	27.50	0.00
133	10/11/2009	1005.57	27.70	0.00
134	11/11/2009	1005.78	27.30	1.60
135	12/11/2009	1007.76	27.90	0.00
136	13/11/2009	1009.58	27.60	4.90
137	14/11/2009	1009.17	27.40	0.00
138	15/11/2009	1008.78	27.30	20.40
139	16/11/2009	1009.47	25.90	13.60
140	17/11/2009	1009.60	25.70	9.70
141	18/11/2009	1010.33	25.50	40.90
142	19/11/2009	1010.82	26.80	0.00
143	20/11/2009	1011.47	26.30	0.00
144	21/11/2009	1011.47	26.90	0.00
145	22/11/2009	1011.38	26.50	0.00
146	23/11/2009	1011.21	25.90	0.00
147	24/11/2009	1011.09	25.70	0.00
148	25/11/2009	1010.52	26.00	0.00
149	26/11/2009	1009.72	26.70	0.00
150	27/11/2009	1010.27	27.60	0.00

Table C1:   (continued)

Order	dd/mm/yyyy	Air Pressure (mbar)	Temperature (°C)	Rainfall (mm)
151	28/11/2009	1010.79	27.50	0.00
152	29/11/2009	1011.26	26.40	2.80
153	30/11/2009	1011.00	26.80	0.00
154	1/12/2009	1011.37	26.40	3.20
155	2/12/2009	1011.28	26.80	0.00
156	3/12/2009	1010.60	27.30	0.00
157	4/12/2009	1010.44	26.80	10.20
158	5/12/2009	1010.14	27.20	0.00
159	6/12/2009	1009.82	27.60	0.00
160	7/12/2009	1010.40	26.20	9.20
161	8/12/2009	1010.12	26.90	0.00
162	9/12/2009	1009.77	26.70	0.00
163	10/12/2009	1009.24	26.60	0.00
164	11/12/2009	1009.32	26.80	0.00
165	12/12/2009	1008.51	25.90	0.00
166	13/12/2009	1010.51	26.30	0.00
167	14/12/2009	1010.93	27.30	0.00
168	15/12/2009	1011.47	26.60	0.00
169	16/12/2009	1011.24	27.60	0.00
170	17/12/2009	1011.93	26.90	13.50
171	18/12/2009	1012.81	27.20	0.00
172	19/12/2009	1013.01	27.50	20.30
173	20/12/2009	1013.35	27.40	0.00
174	21/12/2009	1012.42	26.80	0.00
175	22/12/2009	1011.00	27.40	0.00
176	23/12/2009	1010.61	28.00	0.00
177	24/12/2009	1010.32	28.10	0.00
178	25/12/2009	1009.60	27.40	0.00
179	26/12/2009	1009.39	27.70	0.00
180	27/12/2009	1008.92	27.50	0.00
181	28/12/2009	1008.94	26.80	7.10
182	29/12/2009	1009.06	26.90	0.00
183	30/12/2009	1008.87	26.90	0.00
184	31/12/2009	1008.76	26.10	0.00
185	1/1/2010	1009.03	26.00	0.00
186	2/1/2010	1009.09	26.80	0.00
187	3/1/2010	1009.18	26.60	14.00
188	4/1/2010	1008.57	26.70	27.00
189	5/1/2010	1007.49	26.90	2.10
190	6/1/2010	1008.30	27.00	0.20
191	7/1/2010	1010.58	25.60	2.40
192	8/1/2010	1010.98	26.80	10.50
193	9/1/2010	1011.03	26.70	0.00
194	10/1/2010	1011.06	26.70	20.60
195	11/1/2010	1011.68	26.80	0.30
196	12/1/2010	1011.98	26.70	0.00
197	13/1/2010	1013.13	26.80	2.40
198	14/1/2010	1013.83	27.20	0.00
199	15/1/2010	1013.88	27.50	0.00
200	16/1/2010	1014.54	27.00	0.00

Table C1:   (continued)

Order	dd/mm/yyyy	Air Pressure (mbar)	Temperature (°C)	Rainfall (mm)
201	17/1/2010	1014.01	26.10	0.00
202	18/1/2010	1013.24	26.70	0.00
203	19/1/2010	1011.54	26.90	0.00
204	20/1/2010	1011.47	26.50	0.00
205	21/1/2010	1011.39	26.90	0.00
206	22/1/2010	1011.70	27.20	0.00
207	23/1/2010	1011.46	27.70	0.00
208	24/1/2010	1011.58	27.30	0.00
209	25/1/2010	1012.05	26.90	0.00
210	26/1/2010	1011.69	27.00	0.00
211	27/1/2010	1011.81	27.10	1.30
212	28/1/2010	1011.97	27.10	4.10
213	29/1/2010	1011.78	27.00	0.00
214	30/1/2010	1011.91	26.90	0.00
215	31/1/2010	1012.02	27.40	0.00
216	1/2/2010	1011.22	27.50	0.00
217	2/2/2010	1010.79	27.00	0.00
218	3/2/2010	1010.75	27.60	0.00
219	4/2/2010	1010.67	28.30	0.00
220	5/2/2010	1011.22	28.20	0.00
221	6/2/2010	1011.63	27.60	0.00
222	7/2/2010	1011.66	27.70	0.00
223	8/2/2010	1010.58	27.90	0.00
224	9/2/2010	1010.33	27.70	0.00
225	10/2/2010	1009.94	28.20	0.00
226	11/2/2010	1011.12	28.00	0.00
227	12/2/2010	1011.58	27.90	0.00
228	13/2/2010	1010.22	28.40	0.00
229	14/2/2010	1009.88	27.20	0.00
230	15/2/2010	1010.92	27.50	0.00
231	16/2/2010	1010.81	27.50	0.00
232	17/2/2010	1011.03	28.20	0.00
233	18/2/2010	1011.08	28.00	0.00
234	19/2/2010	1012.13	27.60	0.00
235	20/2/2010	1012.42	28.20	0.00
236	21/2/2010	1012.11	28.00	0.00
237	22/2/2010	1011.09	28.80	0.00
238	23/2/2010	1010.05	28.90	0.00
239	24/2/2010	1009.95	28.80	0.00
240	25/2/2010	1010.42	27.30	2.50
241	26/2/2010	1010.04	27.60	0.00
242	27/2/2010	1009.69	28.10	0.00
243	28/2/2010	1010.02	28.30	0.00
244	1/3/2010	1011.02	28.40	0.00
245	2/3/2010	1010.64	29.00	0.00
246	3/3/2010	1009.79	28.80	0.00
247	4/3/2010	1010.12	28.80	0.00
248	5/3/2010	1010.90	28.60	0.00
249	6/3/2010	1011.31	27.60	0.00
250	7/3/2010	1011.53	27.60	0.00

Table C1:   (continued)

Order	dd/mm/yyyy	Air Pressure (mbar)	Temperature (°C)	Rainfall (mm)
251	8/3/2010	1011.01	28.10	0.00
252	9/3/2010	1012.37	28.40	0.00
253	10/3/2010	1012.92	28.30	0.00
254	11/3/2010	1013.84	28.50	0.00
255	12/3/2010	1013.94	27.90	0.00
256	13/3/2010	1012.29	28.30	0.00
257	14/3/2010	1010.29	28.50	0.00
258	15/3/2010	1009.96	29.00	0.00
259	16/3/2010	1010.50	28.70	0.00
260	17/3/2010	1012.02	29.10	0.00
261	18/3/2010	1011.96	28.40	0.00
262	19/3/2010	1010.49	29.00	0.00
263	20/3/2010	1009.60	28.60	0.00
264	21/3/2010	1008.90	28.80	1.10
265	22/3/2010	1007.72	28.90	0.00
266	23/3/2010	1007.24	29.20	3.70
267	24/3/2010	1007.64	29.00	0.00
268	25/3/2010	1008.01	29.50	0.00
269	26/3/2010	1008.81	29.80	0.00
270	27/3/2010	1010.28	27.70	25.80
271	28/3/2010	1010.62	27.40	0.00
272	29/3/2010	1011.25	27.80	15.60
273	30/3/2010	1011.11	27.70	0.70
274	31/3/2010	1010.89	26.80	85.20
275	1/4/2010	1010.33	26.70	7.50
276	2/4/2010	1009.44	28.10	6.50
277	3/4/2010	1009.84	27.60	21.50
278	4/4/2010	1010.24	28.60	0.00
279	5/4/2010	1009.02	29.10	0.00
280	6/4/2010	1009.16	29.80	0.00
281	7/4/2010	1010.04	30.20	0.00
282	8/4/2010	1010.88	29.60	0.00
283	9/4/2010	1009.65	29.40	0.00
284	10/4/2010	1008.35	29.50	0.00
285	11/4/2010	1007.91	29.50	0.00
286	12/4/2010	1008.22	29.30	0.00
287	13/4/2010	1009.06	29.90	0.00
288	14/4/2010	1008.77	28.60	0.00
289	15/4/2010	1009.75	29.40	0.00
290	16/4/2010	1010.02	28.70	11.80
291	17/4/2010	1010.87	28.80	0.00
292	18/4/2010	1010.31	29.20	9.90
293	19/4/2010	1009.52	28.80	0.00
294	20/4/2010	1009.02	29.00	0.00
295	21/4/2010	1008.95	29.40	0.00
296	22/4/2010	1009.19	29.40	0.00
297	23/4/2010	1009.82	29.30	27.40
298	24/4/2010	1009.57	29.10	2.80
299	25/4/2010	1009.07	29.00	0.00
300	26/4/2010	1011.09	28.60	26.40

Table C1:   (continued)

Order	dd/mm/yyyy	Air Pressure (mbar)	Temperature (°C)	Rainfall (mm)
301	27/4/2010	1012.01	28.10	0.40
302	28/4/2010	1011.06	28.60	0.10
303	29/4/2010	1009.76	28.90	0.00
304	30/4/2010	1009.90	28.00	34.50
305	1/5/2010	1009.94	28.60	0.00
306	2/5/2010	1008.50	29.80	0.00
307	3/5/2010	1007.27	29.60	0.00
308	4/5/2010	1007.15	28.80	2.50
309	5/5/2010	1006.65	29.60	0.00
310	6/5/2010	1006.49	30.00	0.00
311	7/5/2010	1006.33	30.30	0.10
312	8/5/2010	1005.88	30.00	1.70
313	9/5/2010	1005.63	29.70	29.60
314	10/5/2010	1005.70	29.50	18.80
315	11/5/2010	1006.19	28.40	7.80
316	12/5/2010	1006.81	29.60	0.00
317	13/5/2010	1006.41	29.40	11.30
318	14/5/2010	1006.24	29.00	4.10
319	15/5/2010	1006.33	27.90	14.30
320	16/5/2010	1005.99	28.70	0.00
321	17/5/2010	1007.09	28.80	7.20
322	18/5/2010	1009.18	28.10	7.10
323	19/5/2010	1008.86	28.90	1.00
324	20/5/2010	1008.54	29.70	0.00
325	21/5/2010	1009.24	29.20	1.20
326	22/5/2010	1010.03	26.50	9.50
327	23/5/2010	1009.08	27.80	0.00
328	24/5/2010	1008.25	28.80	3.90
329	25/5/2010	1007.83	29.10	16.10
330	26/5/2010	1008.20	29.30	0.10
331	27/5/2010	1008.57	30.00	49.40
332	28/5/2010	1009.58	27.00	33.90
333	29/5/2010	1009.56	26.60	5.90
334	30/5/2010	1009.39	27.40	0.00
335	31/5/2010	1009.19	28.60	0.00
336	1/6/2010	1009.43	28.60	26.80
337	2/6/2010	1009.74	28.60	4.90
338	3/6/2010	1010.24	28.60	34.70
339	4/6/2010	1010.68	26.10	39.80
340	5/6/2010	1008.91	25.90	52.50
341	6/6/2010	1008.15	26.10	23.10
342	7/6/2010	1008.57	27.70	32.40
343	8/6/2010	1008.86	28.20	2.60
344	9/6/2010	1008.41	29.10	3.90
345	10/6/2010	1008.84	28.30	0.00
346	11/6/2010	1009.21	28.50	0.00
347	12/6/2010	1009.14	28.60	0.90
348	13/6/2010	1009.31	27.90	2.80
349	14/6/2010	1009.67	27.40	77.00
350	15/6/2010	1010.33	26.40	29.60

Table C1:   (continued)

Order	dd/mm/yyyy	Air Pressure (mbar)	Temperature (°C)	Rainfall (mm)
351	16/6/2010	1010.10	27.00	19.30
352	17/6/2010	1011.05	25.40	17.10
353	18/6/2010	1010.46	27.90	0.00
354	19/6/2010	1010.12	28.60	0.90
355	20/6/2010	1008.78	28.00	32.30
356	21/6/2010	1008.06	25.40	35.00
357	22/6/2010	1007.92	26.70	24.60
358	23/6/2010	1009.07	28.10	4.90
359	24/6/2010	1007.97	28.20	2.00
360	25/6/2010	1007.90	27.80	1.40
361	26/6/2010	1007.89	28.40	0.00
362	27/6/2010	1008.63	28.30	42.40
363	28/6/2010	1008.87	25.70	57.10
364	29/6/2010	1008.11	26.90	4.00
365	30/6/2010	1007.18	26.10	72.30

APPENDIX D
PUBLICATION

APPENDIX D1

ABSTRACT OF PARER

Abstract of paper 1: (Published)

CrossMark

Correlation between radon and radium concentrations in soil and estimation of natural radiation hazards in Namom district, Songkhla province (Southern Thailand)

Pattama Pisapak[1] · Natasa Todorovic[2] · Tripob Bhongsuwan[1]

Abstract The purpose of this work was to investigate the correlation between concentrations of radon (^{222}Rn) and radium (^{226}Ra) in soil and to estimate the potential natural radiation hazard indices in Southern Thailand, Songkhla province, Namom district. In this study, the concentration of radon was measured by RTM1688-2 radon monitor and radium content was made using a high-resolution gamma spectrometer. A positive correlation coefficient between exhaled radon in soil gas and radium concentrations has been observed. Average concentrations of ^{226}Ra, ^{232}Th and ^{40}K in soil samples were (108 ± 26), (114 ± 22) and (1081 ± 278) Bq kg^{-1}, respectively. These values were used to estimate the radiological health hazard indices using standard analytical methods. The estimated absorbed dose rate, annual effective dose equivalent, gamma radiation hazard index and excess lifetime cancer risk are higher than world permissible limit. These values show a significant health risk due to radiation pollution in Southern Thailand.

✉ Natasa Todorovic
natasa.todorovic@df.uns.ac.rs

[1] Department of Physics, Faculty of Science, Prince of Songkla University, Hat Yai 90112, Thailand

[2] Department of Physics, Faculty of Science, University of Novi Sad, Trg Dositeja Obradovica 4, Novi Sad, Serbia

Introduction

Radon (^{222}Rn) is a naturally occurring radioactive noble gas arising from the ^{238}U decay series. It is a direct progeny of ^{226}Ra through alpha decay, which is an invisible, odorless, tasteless and emits ionizing radiation (3.8 d half-life) as it decays (Fleischer 1997; Barbosa et al. 2010). Radium (^{226}Ra), being a member of uranium radioactive series, is ubiquitous in nature and can be found in trace amounts in most rock and soil. While radon is a noble gas, a large portion of it is free to migrate away from radium. A sufficient quantity of radon migrates out of rock and soil in the environment (indoor and outdoor), ground water, oil and gas deposits (Tanner 1992). The soil gas radon concentration and its exhalation rate depend on the geology of the area, soil porosity, structures (shears, faults and thrusts) and radium content in the surrounding soil and bedrock (Choubey et al. 1997; Ramola et al. 1988; Ramola and Choubey 2003). Emanation of radon atoms from mineral grain is controlled by the circumstance of radium atoms in the grain, texture, size of the grain, soil permeability, porosity and water content of the soil. Moreover, meteorological effects (rainfall, temperature, winds) induce pressure differences and changes in water saturation and therefore are also, though, to influence radon migration. (Sharma et al. 2003; Iskandar et al. 2004; Kumar et al. 2012). The permeability of the soil and rock is of decisive importance for transporting radon (Kumar et al. 2012). Higher values of ^{226}Ra in soil contribute significantly to the enhancement of indoor radon. The main contributors to indoor radon concentrations are soil gas emanating from the ground beneath a dwelling and the materials from which the dwelling is constructed (Khan et al. 2012). In order to evaluate the radon risk in a given atmosphere, it is necessary to check the relation between radium and radon

Abstract of paper 2: (Published)

CrossMark

Radon concentration in well water from Namom district (Southern Thailand): a factor influencing cancer risk

Pattama Pisapak[1] · Tripob Bhongsuwan[1]

Abstract The radon concentrations were determined in well water samples from Namom district, Southern Thailand, by using a RAD7 radon monitoring system. The measured values ranged from 0.1 to 483.0 Bq l^{-1}, while the average $\pm 1\sigma$ across all measured samples was 32.0 ± 9.2 Bq l^{-1}. Regarding the health risks from radon in household drinking water, some settlements had radon concentration exceeding 100 Bq l^{-1}, an upper limit set by the European Union Directive EC2013/51/EURATOM. It is of concern that the results indicate health risks, especially to those consumers who directly use well water with high radon concentration.

Keywords Radon in well water · Annual effective dose · Inhalation · Ingestion · Cancer risk

Introduction

Radon is a naturally occurring radioactive gas present in rocks and soil under the earth's crust, and it continually emanates from these sources by diffusion, causing its presence also in groundwater [1]. Radon is an alpha emitter with a half-life of 3.825 days. The disintegration of radionuclide ^{222}Rn results in short-lived radionuclides (^{218}Po, ^{214}Bi, ^{214}Pb and ^{214}Po), which are responsible for the high radiation health risks, in particular developing lung cancer [2, 3]. Dissolved radon gas is found accumulated in water from underground sources, such as well water. The dissolved radon gas escapes from the well water, entering indoor air, during dish washing, cooking, laundry and showering [4]. The inhalation of radon released from water has been estimated to contribute 89% of its cancer risks, while radon ingestion from drinking water only accounts for 11% [5]. Radon concentrations can reach high levels in an indoor environment, causing significant human health risks [6]. The accumulation depends on ventilation, heating, and water use [7, 8]. Inhalation of radon indoors increases the risk of lung cancer, which is much higher than the risk of stomach cancer from drinking water with a high radon concentration [9–12]. There are potential serious risks to public health from high radon concentrations in groundwater. Regulatory guidelines and international recommendations for radon in drinking water have been issued. In 1999, The United States Environmental Protection Agency (USEPA) has proposed the allowed maximum contaminant level (MCL) for radon in drinking water as 11 Bq l^{-1} [13]. On the other hand, The European Union Directive EC2013/51/EURATOM has proposed in 2013 a recommendation that sets the reference level of radon in drinking water at 100 Bq l^{-1} [14], while concentrations above this level permit the consideration of possible remedial actions. The Namom district of Songkhla province has the highest radon concentrations in air and in groundwater within the province [15], and the Songkhla granite is known to contain uranium at levels as high as 18 ppm eU [16, 17]. Radium has been found in shallow well waters, in the area with granitic rock. The radium concentrations observed range from 3.51 to 292.1 mBq l^{-1} [18]. The highest radium concentration obtained in this study area exceeds the maximum acceptable radium concentration in drinking water, which the United State Environmental Protection Agency sets at

✉ Tripob Bhongsuwan
tripop.b@psu.ac.th

[1] Department of Physics, Faculty of Science, Prince of Songkla University, Hat Yai, Thailand

Ⓐ Springer

APPENDIX D2

ABTRACT OF PROCEEDING

Abstract of proceeding 1

The Correlation between Radon Concentration in Soil Air and Radium Content in Soil Samples in Namom District, Songkhla Province

Pattama Pisapak[1] and Tripob Bhongsuwan[2]

Abstract

The purpose of this work was to investigate the radon (^{222}Rn) concentration in soil air and the radium content in the soil samples collected from Namom district of Songkhla province, Southern Thailand. The immediate parent of radon is radium (^{226}Ra). It was imperative that radium content was measured in the various matrices present in the environment. In this study, the concentration of radon in soil air was measured by RTM1688-2 radon monitor and radium content in soil samples was made using a high resolution gamma spectrometer (HPGe, Canberra, USA). The result shows that the radon concentration in soil air varies from 43 ± 31 Bq m^{-3} to $641,927 \pm 6,419$ Bq m^{-3} and radium content in soil samples varies from 54 ± 2 Bq kg^{-1} to 279 ± 5 Bq kg^{-1}. A good positive correlation coefficient ($R^2 = 0.82$) between exhaled radon in soil air and radium concentrations in soil samples has been observed in the present investigation.

Keywords : Radon concentration, Radium content, Gamma spectrometry, RTM1688-2 radon monitor; Correlation coefficient

Introduction

Radon (^{222}Rn) is a naturally occurring radioactive noble gas that is part of the ^{238}U decay chain, found within all soils, rocks, water, and air. It is a direct progeny of ^{226}Ra, and is the heaviest gaseous element with its half-life of 3.825 days. Two other isotopes of radon, ^{220}Rn (thoron) and ^{219}Rn (actinon) subsist in nature; they are members of the ^{232}Th and ^{235}U natural radioactive decay series, respectively. In soil, radon is formed and released into small air or water-containing pores between soil particles (Sharma et al., 2003). Radon can move from the solid grains into the air or water-filled pores of the media and further migrate via diffusion or advection or both to the atmosphere. The emanation of radon depends mainly on radium content and mineral grain size (Vaupotic et al., 2010). Its migration is linked with the presence of radium and its ultimate precursor uranium in the ground (Saad et al., 2013). Therefore the determination of radon concentration in soil air and radium content in soil is important in view of human health. Enhanced level of it causes the health hazards and may cause serious diseases like lung cancer

Abstract of proceeding 2

Correlation of radon in soil gas and radium concentration in soil sample and estimation of natural radiation hazard indices in Namom district, Songkhla province

Pattama Pisapak[1], Natasa Todorovic[2] & Tripob Bhongsuwan[1]

[1] Department of Physics, Faculty of Science, Prince of Songkla University

[2] Department of Physics, Faculty of Science, University of Novi Sad, Serbia

Correspondence: Tripob Bhongsuwan, Department of Physics, Faculty of Science, Prince of Songkla University, Hat Yai, Thailand, 90110. Tel: 667-428-8761 E-mail: tripop.b@psu.ac.th

Abstract

The purpose of this work was to investigate the correlation of radon (^{222}Rn) concentration in soil gas and radium (^{226}Ra) content in soil samples and to estimate the potential natural radiation hazard indices in the Namom district of Songkhla province, Southern Thailand. In this study, the concentration of radon was measured by RTM1688-2 radon monitor and radium content was made using a high resolution gamma spectrometer (HPGe, Canberra, USA). The result shows that a positive correlation coefficient (R^2=0.72) between exhaled radon in soil gas and radium concentrations has been observed. Results indicate that the mean concentrations of ^{226}Ra, ^{232}Th and ^{40}K in soil samples were 108 ± 26 Bq kg^{-1}, 114 ± 22 Bq kg^{-1} and 1081 ± 278 Bq kg^{-1}, respectively. These values were used to estimate the radiological health hazard indices using standard analytical methods. The results showed that the mean value of radium equivalent activity is 354 ± 72 Bq kg^{-1}, while the values of absorbed dose rate 164 ± 34 nGy h^{-1} and annual effective dose equivalent 201 ± 42 μSv y^{-1}. The values of external and internal health hazard indices are 0.96 and 1.25, respectively. The estimated absorbed dose rate, annual effective dose equivalent, gamma radiation hazard index and excess lifetime cancer risk are higher than world permissible limit of International Atomic Energy Agency (IAEA, 2007) & United Nations Scientific Committee on the Effect of Atomic Radiation (UNSCEAR, 2000; 2008) values for such environment. These values show a significant risk due to radiation pollution in the Namom district.

Keywords: radon concentration, radium content, gamma spectrometry, RTM1688-2 radon monitor, radiological parameters

1. Introduction

Radon (^{222}Rn) is a naturally occurring radioactive noble gas arising from the ^{238}U decay series. It is a direct progeny of ^{226}Ra through alpha decay, which is an invisible, odorless, tasteless and emits ionizing radiation (3.8 d half-life) as it decays (Babosa et al., 2010). Radon can move freely through the solid grains into the air or water-filled pores of the media and further migrate via diffusion or advection or both to the atmosphere. Radon emanates from all rocks, soils and tends to concentrate in enclosed spaces like underground mines or houses. The emanation of radon depends mainly on radium content, mineral grain size, the permeability of the grains, temperature and pressure (Kumar et al., 2012). Hence, the concentration of radium determines concentration of radon atoms. Therefore, measurements of radon thus, facilities the need for uranium and radium estimation in the parent source for public health risk assessments (Kumar & Narang, 2014; Mir & Rather, 2015). Enhanced level of it causes the health hazards and may cause serious diseases like lung cancer in human beings. It is well known that the radiations emitted from the primordial radionuclides originating from the Earth's crust are the major contributors to the total background exposures to the human populations. These include external gamma exposures and inhalation exposures, approximately in equal measure, the latter being due to radon, thoron and their progenies in the indoor environment. An assessment of these exposures in different parts of the country provides the basic input for obtaining national averages of background population exposures and their distributions across the country (Eappen and Mayya, 2004).

The district of Namom is located southeast of the Hat Yai district of Songkhla province in southern Thailand. The airborne radioactivity map of Namom area showed the concentration of equivalent uranium ranged 8-12 ppm at ground surface (DMR, 1989). Bhongsuwan et al. (2001) reported the result of indoor-radon study in the Songkhla Lake Basin and found the highest radon concentration in air and in ground water in Namom district. Ishihara et al. (1980), Sirijarukul (1994) reported that the Songkhla granite contained uranium of as high as 18 ppm

Abstract of proceeding 3

Todorovic, N., Stojkovic, I., Nikolov, J., and Pisapak, P. 2015. Difference techniques for ^{222}Rn Determination in Drinking Waters. Proceeding of the Conference on "Association for Radiation Protection Serbian and Montenegro". On September 30 - October 2, 2015, Belgrade, Serbia.pp.260-266.

ДРУШТВО ЗА ЗАШТИТУ ОД ЗРАЧЕЊА
СРБИЈЕ И ЦРНЕ ГОРЕ

ЗБОРНИК РАДОВА

XXVIII СИМПОЗИЈУМ ДЗЗСЦГ
Вршац
30. септембар - 2. октобар 2015. године

Београд
2015. године

Abstract proceeding 3   (continued)

DIFFERENT TECHNIQUES FOR ^{222}RN DETERMINATION IN DRINKING WATERS

Nataša TODOROVIĆ[1], Ivana STOJKOVIĆ[2], Jovana NIKOLOV[1] and Pattama PISPAK[3]

1) University of Novi Sad, Faculty of Sciences, Department of Physics, Novi Sad, Serbia
2) University of Novi Sad, Faculty of Technical Sciences, Novi Sad, Serbia
3) Department of Physics, Faculty of Science, Prince of Songkla University, Thailand
e-mail: natasa.todorovic@df.uns.ac.rs

A procedure for the determination of ^{222}Rn in environmental water samples using liquid scintillation counting (LSC) was applied and optimized. For radon determination in drinking water from groundwater and surface water sources by LSC, the EPA Method 913.0 was used. A minimum detectable activity of 0.029 Bq l^{-1} in a 20 ml glass vial (10 ml water sample mixed with 10 ml of liquid scintillation cocktail) has been achieved during 300 minutes of measurement time. The procedure was compared with RAD 7 radon detector measurements. Factors that affect the measurement accuracy and precision of RAD 7 radon detector are the sampling technique, sample concentration, sample size, counting time, temperature, relative humidity and background effects. The minimal detectable activity (MDA) for RAD 7 technique was found to be 0,1 Bql^{-1}.

From obtained results of ^{222}Rn measurements in 15 water samples with different ^{222}Rn activity, correlation between two techniques applied for measurements of ^{222}Rn in water samples ($A < 400$ Bql^{-1}) could be determined. There is reasonable agreement (within statistical uncertainties) between the various techniques in most cases, while disagreements most likely come from systematic uncertainties associated with sampling procedures. Discrepancy in determined activities between the two techniques becomes more evident with increased ^{222}Rn activities in water.

LSC technique gives in general higher activity concentrations for about 30% than RAD 7 spectrometer. The interpretation of shown results could be that RAD7 is not properly calibrated for higher activities measurements, since USA reference level of ^{222}Rn concentrations in water is only 11,1 Bql^{-1} (US EPA, Proposed Radon in Drinking Water Regulation).

Detected ^{222}Rn in drinking waters from public fountains could result from its ^{226}Ra water content, as concluded from the measured activity concentration of ^{226}Ra with HPGe gamma-spectrometer in those samples.All measured activity concentrations and annual doses are well under the legally defined limits, so the drinking water from Novi Sad and Kopaonik mountain water is safe for consumption from the radioactivity point of view.

Abstract poster section

Abstracts Session

classified into low to medium enthalpy, suitable for possible small scale geothermal power plants. In this study, concentrations of major chemical constituents in geothermal water were sampled from hot springs in Krabi. Exit temperatures of the hot springs range 38-45 °C and pH values 6.5-7.2. Geochemical data show that cations, Ca, K, Mg, and Na, occur in relatively high contents, while Fe shows very low concentrations. On the other hand, HCO_3 is present in relatively high concentration compared to other anions (SO_4 and Cl). Chemical compositions classified as bicarbonate and chloride according to their origin. Partially equilibrated and immature waters were found with reservoir temperatures between 120 and 200 °C based on cation geothermometers. The rate of change of concentration depends on the discharge volume of fresh meteoric water in the groundwater reservoir. Meteoric fresh groundwater from shallow aquifers and hot water from deep aquifers mix while emerging from several springs along faults. After the rainy season, when elevations of the groundwater table rise in the regional aquifers and discharge rates of all springs increase, solute concentrations decrease all hot springs, but interestingly, increased in the saline hot spring, apparently suggesting different salinization mechanisms. Results obtained for all hot springs show that mean temperature values in shallow geothermal reservoirs occur due to mixing of fresh meteoric water along the pathways. A regional forced convective-circulation model is suggested based on differences interpreted to reflect deep structural controls on fluid pathways in the field, which has limited the degree of mixing between them.

Keywords: hot springs, geothermal energy, geochemistry, Krabi

Poster – P05

Earthquake Prediction Studies Using Radon as a Precursor in Southern Thailand:

A Case Study

Pattama Pisapak, and Tripob Bhongsuwan*

Department of Physics, Faculty of Science, Prince of Songkla University, Hat Yai, Songkhla, Thailand

*E-mail: tripop.b@psu.ac.th

Many theoretical and empirical algorithms have been proposed in the literature for radon release; however, whilst its relation to earthquake occurrence has been developed on occasions, there have been no specific complete studies of this phenomenon. In this study, radon monitoring was carried out using the emanometry technique at the Maung district in Phang Nga Province, located at the Khlong Marui Fault (KMF), a major active fault of southern Thailand. Radon in soil gas was continuously measured at a single station, using a solid state nuclear track detector (SSNTD). The site was suitable for the radon monitoring on the basis of a pre-surveyed most highest radon concentration. The measurement was made for a daily coverage during the period of July 1, 2009 to June 30, 2010. Influences of ambient temperature, atmospheric air pressure and humidity on the temporal variation of radon concentration are investigated by a statistical test. Radon anomaly peaks are selected and as a possible prediction involved with the observed earthquakes (data collected from ANSS; Advanced National Seismic System, of NCEDC; Northern California Earthquake Data Center). Results indicate that 67.3 % of $M_w \geq 4$ have been successfully predicted.

Keywords: Earthquake prediction, Radon anomaly, Khlong Marui Fault (KMF), Solid state nuclear track detector (SSNTD)

Poster – P06

A Numerical Study for Tsunami Prediction using FUNWAVE

Pawin Sitsungnoen
*E-mail: sc_pawin@hotmail.com

In this work, we simulate the propagation of the December 2004 and the March 2005 Indian Ocean Tsunamis using the FUNWAVE program that is based on the dispersive Boussinesq equations. A resolution of bathymetry data, tsunami source function, and earthquake magnitude are experimental parameters in three numerical experiments to study their effects to computational time and tsunami predictions of maximum wave height, first arrival time at locations near shorelines, and directionality in the open sea. The performance of this program is tested, and its scalability is presented for the simulation in the Andaman Sea and the Bay of Bengal. Furthermore, we use 24 processors as the maximum number of processors in the performance test due to the limitation of our computing system. We found that the vertical alignment of a parallel partition required the lowest computational time. Then the 2004 Indian Ocean Tsunami was chosen for testing the effect of the resolution of bathymetry data. To vary this parameter, the tsunami source function is fixed as the five Okada (1985) dislocation segments for generating an initial tsunami wave in the simulation. The first experiment is a testing of resolution of bathymetry data parameter. Ioualalen (2007) used the 2-minute gridded global relief data or ETOPO2 while this work uses the 1-minute gridded global relief data or ETOPO1 that is finer-resolution bathymetry data in minute unit. Therefore, a result of the increment in resolution is presented and discussed for predicting tsunami maximum amplitude and first arrival time. In addition, the tsunami predictions are compared with tidal gauge data. After that, the 2005 tsunami was used to validate the simulation and testing the last two parameters. In the simulation, the ETOPO1 bathymetry data and the spherical coordinates are used. Then the tsunami source function parameter is tested in the second experiment. An Okada dislocation segment is used

VITAE

Name   Miss Pattama Pisapak

Student ID   5410230041

Educational Attainment

Degree	Name of Institution	Year of Graduation
M.Sc. (Geophysics)	Prince of Songkla University	2009
B.Edu. (Physics)	Phuket Rajabhat University	2003

Scholarship Awards during Enrolment

1. Strategic Scholarships Fellowships Frontier Research Networks (Spectific for Southern region), The Office of the Higher Education Commission: OHEC, Thailand

2. Prince of Songkla University Graduate School Financial Support for Thesis Scholarships

3. The grant of student exchange program between Prince of Songkla University and University of Novi Sad, Serbia

4. Teaching assistance in Department of Physics

List of Publication and Proceedings

Pisapak, P., and Bhongsuwan T. 2017. Radon concentration in well water from Namom district (Southern Thailand): a factor influencing cancer risk. Journal of Radioanalytical and Nuclear Chemistry. doi:10.1007/s10967-017-5272-4.

Pisapak, P., Todorovic, N., and Bhongsuwan T. 2017. Correlation between radon and radium concentrations in soil and estimation of natural radiation hazards in Namom district, Songkhla province (Southern Thailand). Environmental Earth Sciences. 76:139. doi:10.1007/s12665-017-6439-6.

Pisapak, P., and Bhongsuwan T. 2016. Earthquake Prediction Studies Using Radon as a Precursor in Southern Thailand: A Case Study. Abstract of the 7th International Conference on Applied Geophysics, On January 14-15, 2016. Bangkok.

Todorovic, N., Stojkovic, I., Nikolov, J., and Pisapak, P. 2015. Difference techniques for ^{222}Rn Determination in Drinking Waters. Proceeding of the Conference on "Association for Radiation Protection Serbian and Montenegro". On September 30 - October 2, 2015, Belgrade, Serbia.pp.260-266.

Pisapak, P., Todorovic, N., and Bhongsuwan T. 2015. Correlation of radon in soil gas and radium concentration in soil sample and estimation of natural radiation hazard indices in Namom district, Songkhla province. Proceeding of the Conference on "The 1st International Conference on Environment, Livelihood, and Services" (ICELS 2015). On November 2 – 5, 2015. The Centara Grand and Bangkok Convention Center at Central World. Bangkok, Thailand. pp.A 09002 – 1- A 09002 – 9.

Pisapak, P., and Bhongsuwan T. 2015. The correlation between radon concentration in soil air and radium content in soil samples in Namom District, Songkhla Province. Proceeding of the Conference on "The 8th Silpakorn University International Conference on Academic Research and Creative Arts: Integration of Art and Science". On February 12-13, 2015. The Art and Cultural Center Commemorating the 6th Cycle Birthday Anniversary of His Majesty The King. Silpakron University, Sanam Chandra Palace, Nakhon Pathom Province. pp.OE-47-OE-54.

Bhongsuwan, T., Pisapak, P., and Duerrast, H. 2011. Result of alpha track detection of radon in soil gas in the Khlong Marui Fault Zone, Southern Thailand: A possible earthquake precursor. Songklanakarin Journal of Science and Technology. 33(5): 609-616.

Pisapak, P., Duerrast, H., and Bhongsuwan, T. 2010. Soil-Gas Radon as a Possible Earthquake Precursor: A Case Study from the Khlong Marui Fault Zone, Southern Thailand. Kasetsart Journal: Natural Science. 44: 1079 – 1093.

Pisapak, P., Bhongsuwan, T., Lohawijarn, W., and Duerrast, H. 2008. Variation of radon concentration in soil gas: an earthquake precursor? A case study from the Khlong Marui Fault Zone, Southern Thailand. Proceeding of the Conference on "the 2nd Graduate Research Conference for developing the New Knowledges". Princess Maha Chakri Sirindhorn Anthropology Centre, Silpakorn University. September 19, 2008. pp.358-372.